Investigation of Vibration Characteristics of a Hand Tractor and Detection of Target Vibration Reference Points based on Transfer Path Analysis Technique

プン, ソバタナ

Investigation of Vibration Characteristics of a Hand Tractor and Detection of Target Vibration Reference Points based on Transfer Path Analysis Technique

Phon Sovatna

プン　ソヴァンタナ

2023

TABLE OF CONTENTS

TABLES

LIST OF ACRONYMS

CH	chassis
CPM	cycles-per-minute
CPS	cycles-per-second
CTS	carpal tunnel syndrome
DoF	degree of freedom
dps	degree per second
DSP	digital signal processing
EF	engine-right-side front
ER	engine-right-side rear
ET	engine-cover top
FFT	fast Fourier transform
FL	front-left plate
FR	front-right plate
GB	gearbox
Gbit	gigabit
HAV	hand-arm vibration
HAVS	hand–arm vibration syndrome
HG	handgrip
Hz	hertz
IMU	inertial measurement unit
kg	kilogram
kW	kilowatt
LTI	linear time-invariant
MB	megabyte
MH	mid-handle
MH	middle between handle base and handgrip
mm	millimeter
PSD	power spectrum density

RMS	root mean square
RMSE	root mean square error
rpm	revolution per minute
RSS	root sum square
SVD	singular value decomposition
TPA	transfer path analysis
VWF	vibration induced white finger
WBV	whole-body vibration

Abstract

Mechanization has extremely increased to substitute draft animal and human forces in Cambodia provided to not only facilitate timely completion of operations but also increase production, labor savings, energy efficiency, productivity, and profitability. The increment and multipurpose uses of the mechanization, especially hand tractor meant that the time operation became longer that induces to vibrated discomfort known as early fatigue. In this study, therefore, two case studies were conducted on hand tractors using different types such as Cambodian type, which was focused on the investigation of vibration characteristics of a hand tractor using MEMS sensor, and for Japanese type on the investigation of vibration characteristics of hand tractor based on frequency-domain and vibration intensity. Vibration magnitude and dominant frequencies were observed using root mean square (RMS) and power spectrum density (PSD), and finally effective interventions for vibration reduction were suggested. For Cambodian type, two conditions were setup in stationary and driving modes. Five wireless MEMS sensors were rigidly tapped on the different point locations of the hand tractor such as engine front, engine-cover top, chassis, gearbox, middle between handle-base and handgrip and handgrip. The engine idling was picked up in both conditions. Whereas, for Japanese type, seven wireless sensors were firmly tapped on different locations such as engine-right-side front (EF), engine-right-side rear (ER), engine-cover top (ET), chassis (CH), gearbox (GB), and middle between handle-base (MH) and handgrip (HG) to observe vibration transmission. Three engine throttles: 1266rpm, 2110rpm, and 2658rpm were determined, indicating by a laser tachometer.

An opensource Python Language was intensively and manually coded based on designed techniques: amplitude, RMS, fast-Fourier transform (FFT), PSD, and dominant frequencies. Graphical figures were visualized in a function of water 3D using Statgraphics_Centurion 19.1.1.

Result presented Cambodian type that under stationary mode largest vibration acceleration appeared at handgrip in vertical axis of about 8.5m/s^2 followed by engine-cover top, gearbox and chassis, respectively. In driving mode, the main vibration magnitude occurs in vertical axis at about 11.8m/s^2. Within 50Hz frequencies, predominant acceleration occurred in longitudinal axis at about 10Hz frequencies at first peak and about 18Hz frequencies at next peak at engine-cover top. Whereas, at handgrip predominant acceleration appeared hugely in vertical axis at

about 10Hz frequencies, and at the same frequency was found in pitch axis of rotational angular velocity under stationary mode. However, it appears clearly at about 9Hz frequencies in vertical axis in driving mode. Both conditions, vibration exposures are much higher than that in health risk limitation standard that operators should be prevented effectively; otherwise, to suffer from early fatigue.

In case of Japanese type, the results showed that the vibration magnitude was the greatest at the top of the engine-cover along the lateral axis at low frequencies, followed by the handgrip along the vertical axis at different frequencies corresponding to the engine speed. RMS of hand–arm vibration exposure was extremely higher than those stated in the health guidance zone at all engine speeds. Thus, anti-vibration measures should be introduced.

Vibration signals sourced from hand tractor are produced in a complex form; therefore, to achieve a comfortable condition, it is essential to reduce interior vibration at the handle of hand tractor. Transfer path analysis (TPA) technique was employed to estimate the best reference points to response point of a hand tractor. Six locations of the hand tractor, specifically, engine-right-side front, engine-right-side rear, engine-cover top, chassis, gearbox, and middle between handle-base and handgrip were considered as reference points; whereas, handgrip was regarded as a response point. For TPA analysis, PSD of the seven locations were populated into a 3-dimensional matrix. Results of high contribution locations were combined in pairs to enhance accurate relationships. Finally, the best contribution was determined using the RMS and the root mean square error (RMSE) methods. Result indicated that chassis-gearbox combination are the best target points for the response point.

Acknowledgements

This research thesis could not have been written without the encouragement, support and inspiration of professors, friends and in essence, family and all sentient beings. Especially, please allow me to dedicate my acknowledgement of gratitude toward the following significant advisors and contributors, who have been always kept eyes with me throughout the thesis processes:

First, I would like to send my profound appreciation to my beloved professors—Professor Eiji Inoue, Assistant Professor Muneshi Mitsuoka, Associate Professor Takashi Okayasu and Associate Professor Yasumaru Hirai, who have supervised, encouraged, and inspired me so much through experimental research and good opportunities in Japan. They kindly read my thesis-paper and offered valuable advice on grammar, organization, and the theme of the thesis-paper. They have always expressed their expert guidance and extraordinary patience, and sincerely suggested me to pursue a higher degree in Kyushu University. Such help and care for me has brought me a very powerful and mind-spirit to achieve my goal.

Second, my warm appreciation goes to all my friends within and across laboratories for their assistance and for sharing our knowledge and experience together. Honestly, they have always been friendly and critically explained the processes of study. I have gained many ideas from them.

Third, I thank to the Japan International Cooperation Agency (JICA) and Coordinators and Royal Government of Cambodia (RGC), who provided me a scholarship to pursue my higher study at the Laboratory of Bioproduction Engineering in the renown of Kyushu University. I also never forget to sincerely thank the JICA coordinators who have taken care and preceded all documentation for me. I am really appreciated their hard-working support me so far.

Finally, I would like to pay my sincerest gratitude to my parents, Phy Sithan and Sak Sony, my siblings, grandparents, relatives, and all friends who support and encourage me to reach this stage. Furthermore, I love and never forget to thank my Japanese host family, Ms. はし真由美, her husband, and beloved children: アイリ, チョクン and マイカ who had kindly invited me to visit their home and brought me to see many interesting places. They have spent a lot of

valuable time with me. All of them have always kept me cared for, loved, and brought me a very hope for future development.

I would ultimately say that without all of them a great experience in the laboratory as well as in Japan would not have been possible.

Date: 2023

PHON SOVATNA

1. INTODUCTION

1.1 Background

Agriculture, predominantly rice production, employs almost 80% of Cambodian rural labor forces. It is a primary economic mechanism, and it represents great potential for the country's development. Most important, agriculture is considered to strongly support Cambodian people in ensuring food security as most Cambodian people' consume rice as part of their diet (Ngo and Chan, 2010). It constitutes a main source of income to the producers on which 93% of rural people depend (Ros et al., 2011). It is the main driver of poverty reduction as 71% of the total population engage in agricultural production Ngo and Chan, (2010), and it has a 29% contribution to the GDP (Chao, 2009; Chan, 2013).

The enhancement of agricultural production through agricultural tools has attracted much attention from farmers, relevant institutions, and government. The use of traditional agricultural tools, which have been prevalent since ancient times, has gradually decreased with an increase of agricultural mechanization, specifically over the last decade (Chan, 2013). The unrealizable use of traditional tools to field operation was noticed by (Phon et al., 2012). In an era of industrialization, problems related to draft animals such as diseases and feeding problems, and effective agricultural mechanization were the main reasons for the decreasing number of draft animals in employment. Singh et al., (2011) stated that the steady drift of agricultural labor to the industrial sector added to the woes of rice farmers. Moreover, the high level of performance of mechanization negatively affected the retention of draft animals. Singh et al., (2011) showed that agricultural mechanization not only facilitated timely completion of operations but also increased production, labor

1

savings, energy efficiency, productivity, and profitability. Hence, many farmers sold animals to buy mechanized tools for field operations (Chao, 2009).

However, the application of high-technology mechanization was reportedly a limitation to agricultural production. Unfamiliarity with controls, insufficient operational experience, a lack of knowledge on operational protocol, lack of operational skills, and minimal encouragement from institutions and the government led to safety and comfort issues for machine operators (Chan, 2011). The difficulties posed by mechanization mean that traditional tools are still used throughout the nation, especially in Coastal and Mountain Zones (FAO et al., 2010).

Although traditional agricultural tools and traditional operators were considered, subsequent increase in agricultural mechanization had become remarkable, specifically the use of hand tractors, which were thought to offer much potential for Cambodian farmers (Chan, 2013).

The occupational health problems of agricultural workers have not received significant attention in low-income countries although hand tractors have become more population and much powerful for agricultural operations (Chan, 2013; Taghizadeh et al., 2007). Tiwari and Gite, (2006) explain that machine vibration was detrimental to the farm users.

Vibration transmissions of hand tractors had been much considered during the last decades within researchers in term of the huge increase the number (Salokhe et al., 1995; Ying et al., 1998; Tiwari et al., 2006; Sam et al., 2006; Goglia et al., 2006). It is indicated that the intensive vibration from the main sources, engine, can be transmitted to its support frame and hands-arm of operators (Taghizadeh et al., 2007). It is said to be high level of vibration from the hand tractor while the suspended particles vibrate without

attenuating designs to prevent from it (Taghizadeh et al., 2007; Mehta et al., 2000). The statistical increase of mechanization in Cambodia, the concern on its use should be considered. It is indicated that the level increase of mechanization has introduced additional sources of risk for operators and fatigue of hand tractors, for instance vibrations, thus affecting the sustainability of the sector (Aiello et al., 2012). Many researchers who have measured on hand tractors as well as tractors had proved that the ride vibrations are usually most severe in the vertical direction (Mehta et al., 2000; Taghizadeh et al., 2007; Ykä, 2010; Heidary et al., 2013). Mechanical vibrations have instantaneous and long-term effects upon the instruments and operators. Obviously, the shafts and operators depend upon different characteristics of vibration, for instance, amplitude, speed, acceleration, and/or the rate of change of acceleration. The effects are complex, non-linear and depend at least upon the vibration amplitude, direction, frequency, duration and to which part of the body it is directed (Rosegger et al., 1960). A major part of the studies has been about measuring and analyzing the vibration level concerning damage and health for various work environments, for example in transportation, rota-tilling, rota-puddling and stationary modes have been much more put in interest (Dewangan et al., 2008; Salokhe et al., 1995; Varun et al., 2012; Tewari et al., 2004). It has also considered the improvement the methods for evaluating and calculating the effects of vibration because there is a consensus that vibration exposure causes problems to both hand tractor itself and operators. Although many researchers have focused hugely on vibration fatigue, the different conditions of hand tractors such as locations and type of hand tractors have become more attractive to researchers. The vibration characteristics of hand tractors has not been figured out the significant of interest referring to mentioned conditions.

In addition to the vibration characteristics of hand tractors, vibration signals are produced in a complex form; therefore, a reduction of the interior vibration at the handle of the hand tractor should be paid much attention. Thus, sensors should be installed at desirable reference locations to obtain vibrational behaviors at the response point of the hand tractor to minimize the number of vibration sensor allocation uses (Junji et al., 2013).

Regarding to the increased use of hand tractors in Cambodia, the safety attention should be much paid to prevent both drivers and the whole hand tractor system away from fatigues. Recently, the focus on machinery safety is out of consideration, thus increasing the number of concerns of such problems. Current research was figured out the vehicle safety during transportation condition (Shridar et al., 2002; Ericson, 2010). It is observed that the safety concern on driving mode is specifically related to vehicle safety standards and limited road use knowledge and experience of drivers. It is indicated that most farmers have little road safety knowledge and experience with motorized vehicles, which is a particular problem when they first operate it. The problem resulted in poor brakes (front only), a narrow front-tyre spread, little or no rear-vision (the driver is seated low and in the centre of a vehicle without mirrors), and the driver was only able to steer to a very narrow angle due to the long-reach handlebars (to steer at a greater angle, the driver must alight from the vehicle and 'walk' the hand tractors through the turn). The carts were frequently wooden, and few had reflectors let alone lights.

The study on safety of hand tractors has only been focused on descriptive analysis, but experimental test (Matthew, 2009). It was also literally reported the agricultural functions of the machine, including occupational health and safety. Many reports found machine vibration induced early fatigue in the agricultural users and recommended an intervention

development to free drivers from health risk perspective (Tiwari et al., 2006).

However, the literatures on vibration safety of hand tractors have been little/not studied and documented in Cambodia. Therefore, this study is very important to be an indicator standard to operators. Furthermore, the study proposed and presented novel results to new researchers and readers to understand and continue their concentration on mechanization to widely spread information. Moreover, it is a good start to agricultural mechanization development contribution for Cambodian young researchers.

1.2 Objectives

The objectives in this study were to detect vibration characteristic of a hand tractor based on frequency domain and time series analyses through an investigation of vibration magnitudes and vibration transmissibility of translational acceleration, and measurement of hand-arm vibration exposure based on ISO standard (ANSI/ASA S2.70-2006) in stationary condition. This study observed various locations of a hand tractor such as front-right plate (FR), front-left plate (FL), engine top (ET), chassis (CH), gearbox (GB), mid-handle (MH), and handgrip (HG) with commercial sensors installed. Many factors were considered in this study including inclination angles of the sensors, sampling rate, operation duration, and translational acceleration outputs.

The vibration generated over the hand tractor is in a complex form; hence, interior vibration should be reduced and/or eliminated. This study extends the experiment to consider a dynamic condition where commonly practiced by operator. A suitable method to apply on this specific case, transfer path analysis (TPA) method was introduced to estimate the stimulation between reference points and response point. This method also

detects target reference points to response point. A reconstruction method defines a target point signals which were generate to the response point at the handgrip. This method reduces significant number of sensors required to install on the hand tractor to investigate vibration characteristics of that hand tractor.

1.3 Thesis organization

Chapter 2 studied the investigation of vibration characteristics of hand tractor using MEMS sensor under stationary and driving conditions. The experiment was conducted in Cambodia using a popular long-handle hand tractor, driving along a pathway, off the village. During driving condition, a villager was hired to operate the hand tractor, which is attached with a two-wheels trailer. MEMS sensor was employed to rigidly tapped on different point locations such as engine front, engine-cover top, chassis, gearbox, middle between handle base and handgrip and handgrip. The vibration characteristics of the hand tractor was calculated using power spectrum density (PSD), root mean square (RMS), vibration transmissibility and hand-arm vibration exposure. Finally, a suggestion was made to prevent operation from any health risky.

Chapter 3 presented the study on the investigation of vibration characteristics of hand tractor in stationary condition based on frequency-domain and vibration intensity. A fundamental knowledge of sensor was introduced, and the usefulness of vibration characteristics detection was evaluated in this chapter. Source of vibration was investigated, power spectrum density (PSD) and root mean square (RMS) were introduced to detect harm-arm vibration exposure in comparing with an international health-risk standard for operation.

Chapter 4 presented the observation and detection of target reference points of a hand tractor in a dynamic condition based on transfer path analysis (TPA) technique. A method of TPA was introduced to detect the reference point signals. This method as well reconstructed data obtained from initial analyses using fast Fourier transform (FFT), RMS and root mean square error (RMSE). This chapter clearly presented the processes of TPA, and a usefulness of this finding to a deduction of number of sensors to be installed on the hand tractor to ultimately characterize its vibration.

Chapter 5 summarized major results and implications of this study.

CHAPTER 2 INVESTIGATION OF VIBRATION CHARACTERISTICS OF A HAND TRACTOR USING MEMS INERTIAL SENSOR

2.1 Background

Agriculture employs almost 80% of Cambodian rural labor forces. It is considered to strongly support Cambodian people in ensuring food security (Ngo and Chan, 2010) and constitutes a main source of income (Ros et al., 2011). It is the main driver of poverty reduction (Ngo and Chan, 2010), and it has a 29% contribution to the GDP (Chao, 2009; Chan, 2013).

The enhancement of agricultural production through agricultural tools, the use of agricultural mechanization has gradually increased, specifically over the last decade (Chan, 2013). It is evident that the agricultural mechanization not only facilitated timely completion of operations but also increased production, labor savings, energy efficiency, productivity, and profitability (Singh et al., 2011). In Cambodia, therefore, many farmers sold animals to buy mechanized tools for field operations, especially hand tractors (Chao, 2009). Multipurpose uses of mechanization meant that time operation to hold handgrip became longer that induce to vibrated discomfort known as early fatigue. Tiwari et al., (2006) explained that machine vibration was detrimental to agricultural users. Many researchers also confirmed that vibration would be very harmful to health induced such as early fatigues that may cause physical, physiological, and musculoskeletal disorders after long-time exposure over months and years (Salokhe et al., 1995, Sam et al., 2006).

This study measures vibration magnitude and vibration transmissibility at various locations of hand tractors such as engine-cover top, chassis, gearbox and handgrip, hand-arm vibration exposure and suggests effective intervention for future development.

2.2 Research fundamental

2.2.1   Theoretical consideration

Hand tractor is an agricultural machine which is fitted with a small diesel engine. This machine has been capable of using small and medium farm sizes (Sam et al., 2006; Hassan-Beygi et al., 2005). This is corresponding to the small land size of each farmer's pocess in Cambodia as being graphically (FAO et al., 2010).

With the increment of hand tractors, its characteristics should be critically understood and analyzed. Hand tractor, using a single cylinder diesel engine, does not have a good balance component. The forces acting on the piston during compression and power strokes transmitted to the crankshaft and engine block (Bahareh et al., 2013; Francis et al., 1978). The processing induced by acting forces to support frame cause the engine to vibrate, thus the primary source of vibration at the stationary mode (Bahareh et al., 2013; Salokhe et al., 1995). Rahimi stated that there are many reasons, in the engine combustion, that may lead engine vibrate such as cetane number, flash point, viscosity, lubrication properties, chemical, and molecular structure of all fuel blends (Rahimi et al., 2009). Due to the lack of vibration dampers intervention between the engine and hand tractor chassis, the engine forces entering to the hand tractor chassis as shocks and then through the chassis transmitted to the whole part of hand tractors. Handle of hand tractors acts like a cantilever beam so that the relative transmission vibrates freely at one end, and another end vibrate corresponding to the chassis of hand tractors because this part is harnessed with hand tractor chassis (Bahareh et al., 2013; Varun et al., 2012). Long time running with unbalanced condition, the engine parts will be fatigued. Operators of the walking type hand tractors are also exposed to levels of vibration and [noise, another concern] because these machines are guided entirely by the operators' hand. Long time working

with such condition might cause damage to various organs of the body including bearing loss, spine and gastrointestinal disorders and even neurological disorders. All these mentioned issues lead to a decrease in work efficiency and quality. In order to attenuate and/or eliminate the risk of working environment with these machines, many interventions have been taken into account, for instance, the development of regulations recommended by international organization to limit working hours and duration of vibration exposure was put into affective (Salokhe et al., 1995; Dewangan et al., 2008; Dennis et al., 1994).

2.2.2 Vibration characteristics

Vibration is given to be as simply the cyclic or oscillating motion of a machine or machine components from its position of rest (Dennis et al., 1994). It is also given by Griffin, (1990) that vibration is reciprocating or oscillatory motion. Griffin, (1990) also stressed a concept definition that all the motions are not permanently constant during working. These motions are alternatively oscillated greater and/or lesser than the equilibrium values. It is illustrated that the extent of cyclic determines the magnitude of vibration, and the repetition rate of cyclic oscillation is said to be the determination the frequency of vibration.

The oscillation can be predictable knowledgeably. It is observed that a future oscillation may be assumed based on the previous oscillation (i.e., a deterministic motion) or may be characterized only as having some statistical properties (i.e., a stochastic motion, commonly called a random motion) (Griffin, 1990). Salokhe et al., (1995) concluded that the main vibrations may be obtained by primarily using two types: mainly, sinusoidal, and random. By definition, sinusoidal vibrations are regular in nature and predictable. Random vibrations are irregular and unpredictable. To understand and predict

the response to a single frequency of motion, the only with sinusoidal vibration is possible to study. The random vibration can be descriptively determined in such cases during work, travel and leisure (Griffin, 1996). Almost all hand tractors during field operation are subjected to three translational accelerations, specifically vertical, longitudinal and lateral and three rotational angular velocities; namely, roll, pitch and yaw.

2.2.3 Effect of vibration

It can be simply understood from the engine vibration magnitude or density that the low level of forces acting on machinery vibration system would result in improving machine lifespan, meaning to attenuate fatigue of machineries and operators. Therefore, it is necessary to manufactory quality products and operators from a dimensional tolerance and surface finish quality standpoint that the important considered focus should be undertaken on engine vibration to be mindful to strive for low levels of machinery vibration (Dennis et al., 1994).

The previous description demonstrated that engine part is the main source of vibration produced by acting forces. This kind of vibration may cause fatigue in all parts of hand tractor base frame. It is given an example that vibration causes many problems to engine or parts attached with its engine. Thus, carelessness on vibration lead to loosening or stretching of mounting bolts, a broken weld, a crack in the foundation, deterioration of the grouting, increased bearing clearance through wear or a rotor loose on its shaft, resulting in reduced stiffness to control even normal dynamic forces, thus causes cautiously to an increase in machine vibration (Dennis et al., 1994).

2.2.4 Methods to evaluate vibration

To evaluate vibration characteristics, three parameters are involved such as vibration frequency, vibration amplitude (vibration displacement, vibration velocity and vibration

acceleration) and phase angle. All the parameters are employed to evaluate the characteristics of machinery. It is also noticed that all these parameters were engaged in this study, except vibration displacement and phase angle. The following descriptions explain each parameter based upon theory (Dennis et al., 1994).

2.2.4.1 Vibration frequency

Considering vibration characteristics, it is recommended to understand vibration frequency. Period of vibration is the simplest of complete cycles that occur in a specified period which is denoted as "cycles-per-second" (CPS) or "cycles-per-minute" (CPM) or Hertz (Hz).

To detect, analyze and obtain the vibration frequency, the method of inversion of the period of the vibration can be employed, and it is not necessary to observe the vibration time waveform. In recent time, many collectors instrument and/or vibration analyzers provide a very nice indicator to output automatically signals generated by machine. Furthermore, the modern machine equipped with new technology devices can be used to record data fast and more accuracy to be reliable. Moreover, the outcome of data generator can be calculated easily (Dennis et al., 1994).

2.2.4.2 Vibration amplitude

The vibration frequencies are not essential when the engine runs desirably, vibration amplitude can be expressed to obtain the magnitude of vibration, to identify how rough or smooth the machine vibrates. It also detects the fatigue of all engine components. The vibration amplitude can be measured and expressed as ① displacement, ②velocity and ③acceleration. As to focus on the vibration amplitude, some parameters should be kept into account the significance and application such as vibration displacement, vibration velocity, and vibration acceleration). These are used to detect and diagnose vibration

signal of engine's components.

a. Vibration displacement

Severity of vibration that caused fatigue problems can be detected and/or analyzed not only using frequency vibration, but vibration displacement method as well. The vibration displacement measures a piece of wire which is repeatedly bent back and forth. This repeated bending eventually causes the wire to break due to fatigue in the bend. In many respects, this is exactly the way a machine component fails - from the repeated cycles of flexing caused by excessive vibratory forces (Dennis et al., 1994).

The example of repeatedly bending a piece of wire, there are two ways to reduce the amount of time required to achieve fatigue failure. One is to increase the distance (displacement) that the wire is bent. The farther the wire is bent each time, the less time it will take to reach fatigue. The other is to increase the number of times per minute or second (frequency) the wire is bent. The more times per minute the wire is flexed, the less time it will take to reach fatigue failure. Thus, severity of vibration is dependent on both vibration displacement and frequency.

b. Vibration velocity

As earlier pointed out, the vast majority of machine failures caused by vibration problems are fatigue failures, thus both objects are applied to achieve measurement including deflected (displacement) and the rate of deflection (frequency). The vibration displacement is to measure the distance of wire bent and frequency is to measure how many times it bent. From these methods, speed or velocity can be generated. Thus, a measure of vibration velocity is a direct measure of fatigue.

The vibration velocity is a measurement of speed of movement of a machine or machine components as it oscillates the motion. The moving speed of components at

some speed is identified by vibration displacement or frequency (Dennis *et al.,* 1994). The significant indicators that benefit and advances of measuring velocity instead of vibration displacement are indicated in the following description:

1. Vibration velocity is a direct indicator of fatigue since vibration displacement and frequency are already parts of velocity.

2. Thus the severity of vibration can be evaluated using only vibration velocity.

3. Vibration velocity is a measurement of the overall condition of a machine whether the vibration is simple (one frequency) or complex (more than one frequency).

These indicators of vibration velocity have become the industry standard for evaluating machinery condition based on vibration (Dennis et al., 1994).

To measure fatigue failure using only vibration velocity is not possible to establish an absolute vibration tolerance level on machine. In other words, there is no absolute vibration level dividing continuous operation and immediate failure. The objective of a predictive maintenance program is simply to detect problems so that they can be identified and corrected before failure. The objective is not to see how much vibration a machine can tolerate before failure.

c. Vibration acceleration

The speed or vibration of a vibrated object is mechanically and constantly changing. When the velocity momentarily stops, the limit of travel velocity is zero. Acceleration pushes the speed up as it travels toward other extreme limits of travel. Vibration acceleration is another way used to obtain amplitude or magnitude of vibration. It is technically and simply the rate of change of velocity (Dennis *et al.,* 1994).

Acceleration is the reverse speed of velocity. It is simply said that when an object first speeds up, this picks up acceleration, and when the speed comes to its constant the

velocity is taking place. However, when the object stops there is neither vibration velocity nor vibration acceleration acting on the object. For a measurement, the highest or peak acceleration is recommended.

Since vibration acceleration is technically the rate of change of vibration velocity (in/sec-peak or mm/sec peak), it follows that the units of vibration acceleration could be expressed in in/sec/sec-peak or mm/sec/sec-peak (Dennis *et al.,* 1994).

d. Phase angle

The definitions of phase angle of machine vibration were undertaken as "the position of a vibrating part at a given instant with reference to a fixed point or another vibrating part". Another definition of phase is "that part of a vibration cycle where one part or object has moved relative to another part".

Repeatedly, two measurement devices; for instance, MEMS sensors, are needed to experiment with the phase angle. Both are mounted at different desirable locations with identical time recorded to check vibration transmissibility from reference point to a pick-up point.

It is important to be clear that the phase measurements are not undertaken during routine periodic check or the "detection" phase of a predictive maintenance program. However, when a developing problem is detected, comparative phase measurements can provide invaluable information as part of the analysis to aid in pinpointing the specific problem such as unbalance, bent shafts, misalignment of couplings, bearings and pulleys, looseness, distortion from soft feet and piping stains, resonance, reciprocating forces and eccentric pulleys and gears.

In this research, it is initially focused on the first stage of detecting problem of hand tractors; therefore, phase angle is not considered with this study. Moreover, to analyze the

phase angle, two sensors are needed to install simultaneously and the period and set-off are needed to be at the same length. It is obvious that this research used only one sensor to check various locations at different time set-off (Dennis *et al.,* 1994).

e. Power spectrum density (PSD)

The rotation of components of the engine produces vibration. To analyze the vibration of the engine components, many parameters are needed to calculate the magnitude of vibration such as frequency, displacement, velocity, acceleration, and phase angle (Shreve, 1994).

Another parameter which is useful to process and analyze the rotating machine vibration is Fourier spectrum known as power spectrum density (PSD). Power Spectrum Density of vibrations measured on rotating machine contains a lot of peaks at many different frequencies (Docekal *et al.,*). The PSD is also used to define the magnitude of strength of a signal which is distributed in the frequency domain, relative to the strengths of other ambient signals, and it is central to the design of any linear time-invariant (LTI) filter intended to extract or suppress the signal (Verghese, 2010). Recognition of peaks produced by an analyzed part of the machine is necessary for machine monitoring. This could be accomplished by theoretical estimation of frequencies characteristic for the analyzed part. These theoretical estimations are unknown for new designs of a selected part or even these estimations are often uncertain. Frequencies or bands important for the solved task have to be estimated directly from the measured data too (Docekal *et al.,*).

Another important point resulting from PSD measurement is to check the revolution per minute by each rotation of components.

f. Root mean squares (RMS)

The motion of the engine is complex that may result in severity to its shaft as well the

operators. The major severity that may be caused by vibration is evaluated by difference frequency and amplitude. The severity determination of vibration is not representative by one peak; however, the average measure is carried out—specifically root-mean-square (RMS) value. The root-mean-square of translation acceleration and rotational angular velocities is used to quantify the severity of human vibration exposure as well as shaft fatigue. It is experimentally said that the RMS measure is more accurately predicted than those peak-to-peak, peak or another measure and it is very convenience and harmonization analyze to many fields of engineering (Ykä, 2010).

Through the laboratory experiment, all root-mean-square, peak-to-peak and peak of accelerations have the same trend even though there is different in numerical value. The acceleration RMS aids many communities by unifying methods of measurement. Root-mean-square measures are obviously as reasonable as other alternatives so long as they and the alternatives yield similar conclusions (Ykä, 2010).

The root mean square is not universally accepted, and peak velocity is preferred by many. Many similar methods can also be used to quantify the magnitude of vibration response and vibration severity of human response (Ykä, 2010). It is suggested by Griffin and Whitham (1977) that to evaluate the discomfort of vibration magnitude at multiple axes the summed combination of all axes should be effectively done by using new method—mainly root sum square (RSS) (Parsons and Griffin 1978b).

2.2.5 Operation of a hand tractor

Vibrations are a well-known potential cause of health diseases and therefore constitute a main concern for the safety of workers in a large number of daily activities. In order to prevent health hazards, national and international institutions have issued laws and directives which establish recommended limits to operator's exposure to vibrations

17

during operation (Aiello *et al.,* 2012).

If the vibrations occurred from the sources exceed the limitable daily limits, the operators must stop working; otherwise, it would be harmful to health induced. It is important to understand the hand-arm vibration (HAV) and whole-body vibration (WBV) because the transmission of vibration from the source, handle of hand tractors, are straightly to operators' whole-body through hand that grasp the grip. The effect of vibration causes discomfort to the operators and results in early fatigue. Such fatigue stretched over a period of months and years may cause physical, physiological, and musculoskeletal disorders (Waersted *et al.,* 1991; Buckle, 1997). It is also confirmed by many researchers that long-time exposure to vibration causes discomfort and hurt to different part of body such as ear, spine and digestion disorders, and vascular disease (Sam *et al.,* 2006; Salokhe *et al.,* 1995, Tiwari and Gite, 2002).

The detrimental effects of the prolonged exposure to hand–arm vibration on the operators have been clinically known for a long time and the occupational health disorders are referred to as 'vibration induced white finger (VWF)' or 'hand–arm vibration syndrome (HAVS)' (Taylor *et al.,* 1975; Hellstrom *et al.,* 1972; Griffin, 1996). The disorder vibration can be also known as "Dead man's hand" or Raynaud's disease of occupational origin (Mansfield, 2005).

Vibration can typically cause blurred vision, loss of balance, loss of concentration (Sayed *et al.,* 2012). Aiello *et al.,* (2012) also stated that the exposure to vibrations was a potential cause of muscular/skeletal pains in hand-arm system, and specific pathologies such as VWF and carpal tunnel syndrome (CTS), HAVS. The detrimental effects of hand–arm vibration depend on the vibration energy transmitted to and absorbed by the hand–arm system (Cundiff, 1976; Lidstro¨m, 1977; Burstro¨m, 1990; Lenzuni *et al.,* 2001). The

detrimental effects of hand–arm vibration depend on the vibration energy transmitted to and absorbed by the hand–arm system (Cundiff, 1976; Lidstro¨m, 1997; Burstro¨m, 1990; Burstro¨m *et al.,* 1994; Lenzuni *et al.,* 2001). It is also concluded by Manal *et al.,* (2012) that in several years after daily exposure, it would result in several health disorders affecting such as permanent harm to internal organs, muscles, joints and bone structure. It is clearly indicated by researchers that exposed to vibration is more prevalent and severe versus non-exposed.

Manal *et al.,* (2012) cited from (Whole Body Vibration, 2005) that with the short-term exposure in frequency range 2-20 Hz at m/sec^2 the operators feel several different symptoms, for instance abdominal pain, general feeling of discomfort such as headaches, chest pain, loss of equilibrium (balance), muscle contractions with decreased performance in precise manipulation tasks, shortness of breath, and influence on speech. In long-term exposure, operators suffer serious health problems, particularly with the spine such as disc displacement, degenerative spinal changes, lumbar scoliosis, intervertebral discs, degenerative disorders of the spine, herniated discs, disorders of the gastrointestinal system, and urogenital systems.

Many researches that have conducted on the hand-arm transmission had used Strain Gauges Type putting on different parts of operators' body such as metacarpal, wrist, elbow and acromion (Dewangan *et al.,* 2008).

Methods proposed for the evaluation of human vibration exposures have usually assumed that the motion is in stationary and that a representative average value can be used to indicate the severity of the motion over the full period of exposure. In practice, of course, the vibration conditions often change from moment to moment. Restricting the evaluation of vibration to periods when the motion is stationary may exclude the periods

of greatest interest. A rigid body may oscillate so that all its parts undergo the same motion. This will occur if the motion is in under stationary condition. If a rigid body rotates, not all its parts undergo the same motion. Both translational and rotational vibration influence human responses (Griffin, 1990). It is also said that the effect to operators induced to decrease efficiency and work quality (Tewari *et al.,* 2004).

2.2.6 Vibration exposure

Inattention to the effect of mechanization vibrations on the operators has been a big concern among researchers and relevant stakeholders. The natural problems occurred from the source have been figured out that it is important to understand the whole-body vibration, because thousands of farmers in Cambodia have engaged with mechanizations, specifically hand tractors. Vibrations expose many pictures of problems to operators such as ability to carry out some tasks, eating, reading, and writing (Oborne, 1977). Under more extreme conditions, vibrations will have psychological and physiological effects such as motion sickness, headaches, and even chronic health effects (Oborne, 1977). Size effect from vibrations costs a lot of money. It is observed by Hostens, (2004) that direct medical costs related to low back pain, which can be caused by vibration exposure, are in billions of dollars.

As being viewed above, the vibration exposure to operators can be understood from HAV and WBV, it is clear that the focus on WBV should be figured out. The Whole-body vibration is defined as a motion transmitted to the human body as a whole through supporting surfaces, as opposed to vibration directed more locally, such as hand-arm vibration (Oborne, 1977). The term "whole-body vibration" is applied to standing, seated and recumbent persons (ISO, 2631-1 1997). Among these three postures, standing person tends to use legs to attenuate vibration. Recumbent also has less association with low

back pain (Magnusson *et al.,* 1998).

Many indications from researchers had pointed out the big difficulty of vibrations from engine, though, there is less/no researchers pay attention on such a viewpoint.

2.3. Methodology and research structure

2.3.1 Theoretical consideration

Vibration from engine source under stationary and driving conditions is very complex. Vibration occurs in three translational acceleration axes: longitudinal ($\dot{x}$), lateral ($\dot{y}$), vertical ($\dot{z}$) axes and three rotational angular velocity axes: roll ($\ddot{\varphi}$), pitch ($\ddot{\theta}$), yaw ($\ddot{\Psi}$) axes. Frequencies extend over a wide range in the experiments. The vibration magnitude of the source and transmission to a hand tractor depended on conditions, i.e., excitation stroke (Griffin, 1996; Ykä, 2010).

2.3.2 Vibration detection

The experiments were carried out in two conditions: under stationary and driving modes. Under stationary mode, the main source of vibration signal is only produced from the engine. However, in driving mode, many sources induced vibration such as engine, uneven road condition and so on (Salokhe et al., 1995). Therefore, investigations were undertaken to observe if there is any relation between the engine power stroke and the dominant frequencies of vibration of the hand tractor. Three axes of translational accelerations ($\dot{x}$, $\dot{y}$, $\dot{z}$), and three axes of rotational angular velocities ($\ddot{\varphi}$, $\ddot{\theta}$, $\ddot{\Psi}$) were detected by placing a single MEMS sensor at various locations, for instance engine-cover top, engine front, chassis, gearbox, middle between handle base and handgrip and handgrip as depicted in Fig. 1.
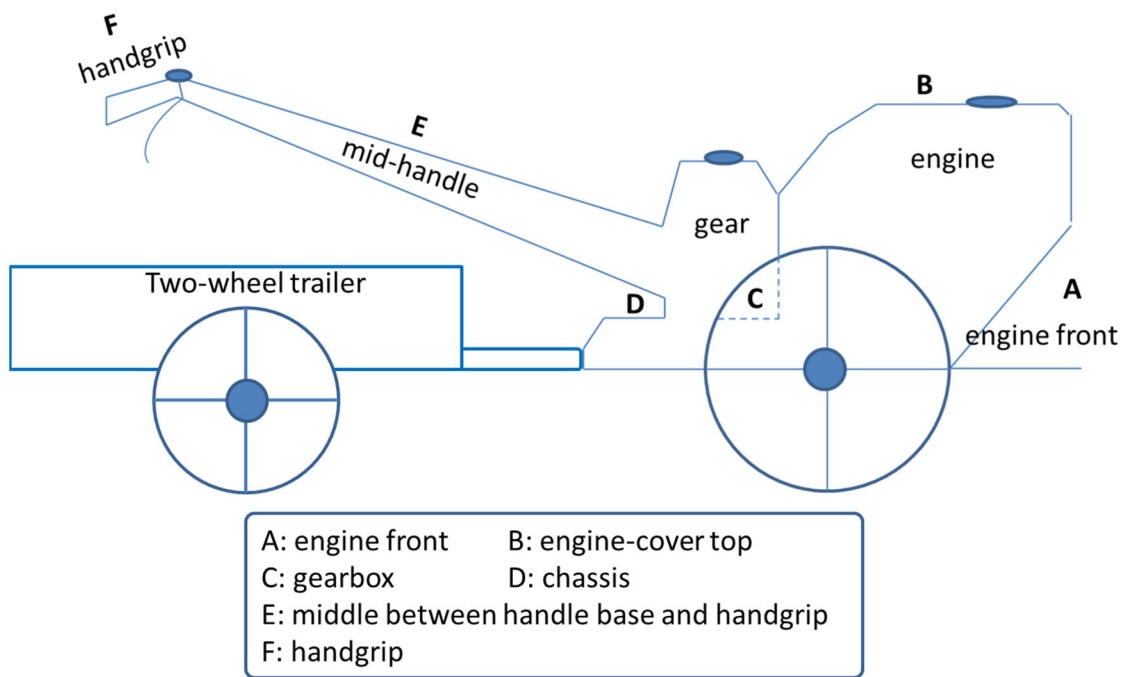
Fig. 1 Experimental hand tractor and sensor allocations

2.3.3 Techniques of measurement

Vibration transmission measurement on a hand tractor had been done by many researchers on specific locations, i.e., at the front of the engine foundation, on engine-cover top, chassis, gearbox, middle between handle base and handgrip, handgrip, human's body (metacarpal, wrist, elbow and acromion and chest (Salokhe et al., 1995; Taghizadeh et al., 2007; Dewangan et al., 2008; Heidary, 2013). On the other hand, the researchers used strain-gage accelerometer to sense magnitude of vibration signals. This device is heavy and complicate in manipulation such as strain amplifier, channel-data-tape recorder, autonomous data acquisition unit and microcomputer. Furthermore, distance of measurement depends upon connected cord.

In modern society; however, MEMS sensor is very compact, light, total weight of 35g including a battery, easy in use, and requires minimal installation space to pick up vibration signal. It is a wireless sensor which can detect signal within 50 meters as described in table 1. The output vibration signal is easy to convert and calculate. Moreover, this MEMS sensor only costs 1/10 of the conventional system, allowing for inexpensive measurement of translational acceleration and rotational angular velocity (Choe, 2013).

Table 1 Main specifications of 9-axis wireless motion sensor

Modulation type	DS-SS
Radio frequency	2405 MHz~2480 MHz, 5 MHz interval
Battery	AAA battery x 1
Power consumption	Maximum 230 mV
External dimensions	40 mm x 20 mm x 55 mm
Weight	Approximately 35 g

2.3.4 Experimental hand tractor

In this experiment, A diesel hand tractor with a power of 12 Hp was used for the experiment under stationary and dynamic conditions on an uneven road, as shown in Fig. 2. Typically, a hand tractor is designed to be equipped without an engine speed gauge; therefore, throttle measurement has been introduced to measure the engine throttle instead of the engine speed. the experiment was conducted within a duration of 30 seconds with the idling speed (5 km/h). the vibration signal was recorded using MEMS sensor.

Fig. 2 Vibration experiment in Cambodia under stationary and driving modes

2.3.5 Experimental Instrumentation

Vibration transmission measurement at various locations of hand tractor had been carried out by many researchers, and strain gage were mostly employed for the experiments (Salokhe et al., 1995, Taghizadeh et al., 2007). However, strain gage was complicated in manipulation such as Strain Amplifier, Chanel-Data-Tape Recorder, Autonomous Data Acquisition Unit and Microcomputer with a limited connected cord. In modern society, however, a MEMS sensor is very compact, light, and easy to use. So, it was chosen for this study. The wireless sensor can detect signals within 50 meters, and the output is easy to convert and calculate (Choe et al., 2013).

2.3.6 MEMS sensor processing

The Micro-electro-mechanical system (MEMS) as presented in figure 3 and figure 4 was designed and fabricated to wirelessly measure translational accelerations, rotational angular velocities, and geomagnetic orientation in three directions for each measure. With this study, only translational acceleration and rotational angular velocity axes were generated by using MEMS sensor (Choe, 2013).

The MEMS sensor, a wireless 9-axis motion sensor which is used in this study, was manufactured by Logical Product with a capacity of 5G/300dps. It can receive and transfer data from sources to a personal computer. It is also capable to wirelessly measure translational acceleration, rotational angular velocities, and geomagnetic orientation in three directions for each measurement (Choe, 2013).
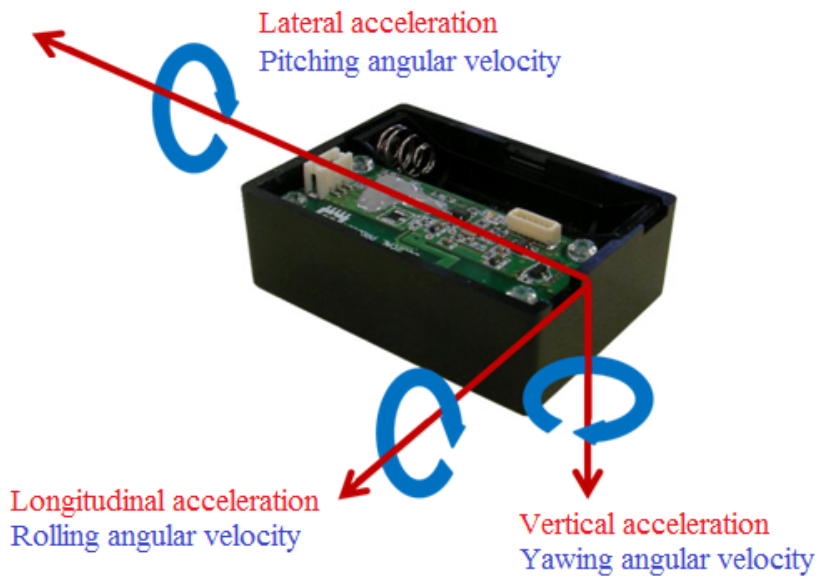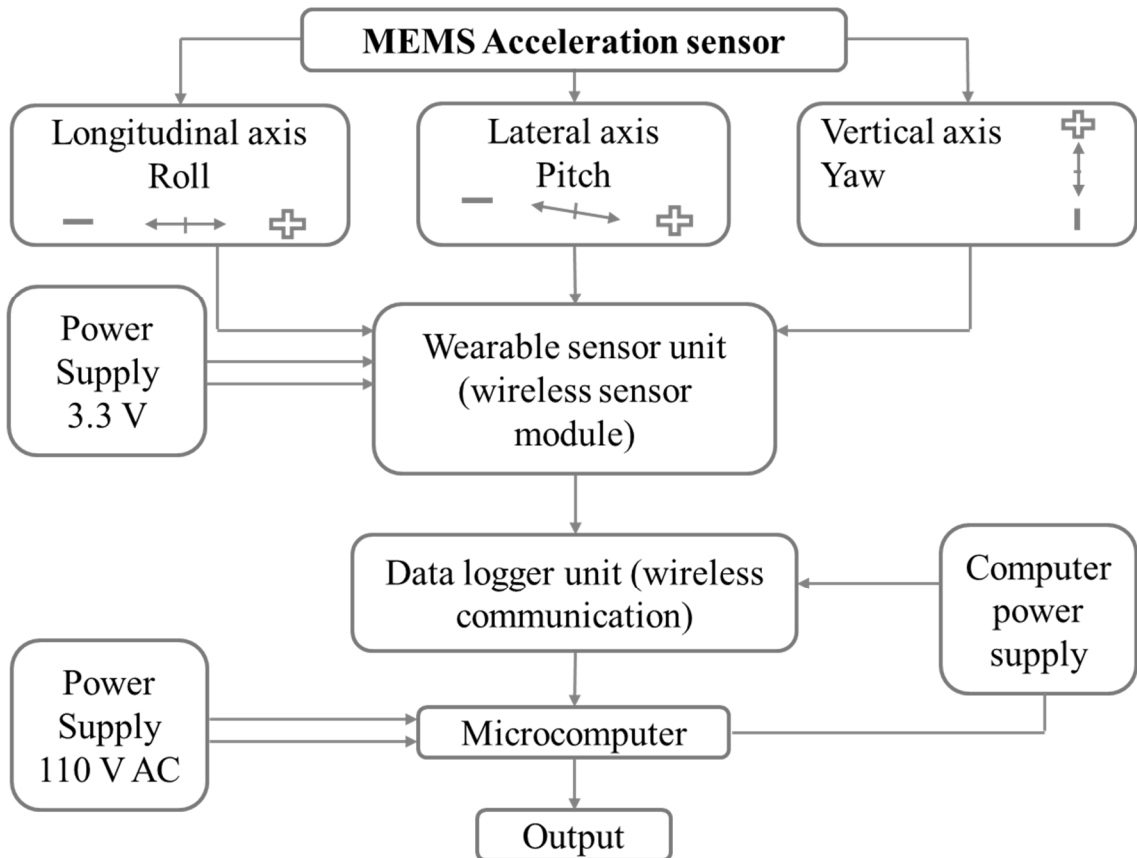
Fig. 31 Micro-electro-mechanical system (MEMS)

Fig. 4 Schematic of instrumentation and data transfer of MEMS sensor

2.3.7 Acceleration sensor

Validation of voltage supplied for acceleration sensor in the MEMS sensor is 3.3V. Output of the sensor at 0 G is 1.65V, and the sensor sensitivity is 190.0mV/g. The output voltage of the acceleration sensor is Analog-to-Digital (AD) which is converted into 12 bits, and full scale is 3.3V. Therefore, when the output voltage is V, AD converted value X_{acc} is expressed in equation 1.

$$X_{acc} = \frac{4095 \times V}{3.3} \tag{1}$$

When acceleration is **G**, the conversion equation is expressed in equation 2.

Note: at actual output 0G, some offsets are included due to factors such as temperature.

$$G = \frac{(V - 1.65) \times 9.8}{0.19} \tag{2}$$

This study, MEMS sensor was set vertically at **1G**, thus generating new equation in equation 3.

$$G = \frac{(V - 1.65 + 0.19) \times 9.8}{0.19} \tag{3}$$

Where:

- V: voltage output,

- G: translational acceleration (Choe et al., 2013).

2.3.8 Angular velocity sensor

Output from angular velocity sensor is filtered by a low pass filter with cutoff frequency of approximately 190Hz which is amplified by 5.6 times using an Operational Amplifier (op-amp) and is converted by an AD converter. The op-amp operates in according with the reference voltage of gyro sensor (V_{ref} = 1.35V). Based on the reference voltage, the sensor output is multiplied by 5.6 times, and converted using AD converter. The sensor output at 0 deg/sec (deg/sec is hereafter referred to as dps) is 1.35V

and sensor sensitivity is 0.67mV/dps.

When output voltage of the sensor is V, AD-converted value X_{gyro} is expressed as in equation 4.

$$X_{gyro} = \frac{4095 \times V}{3.3}$$ (4)

When translational angular velocity is W, conversion is given in the following equation 5.

$$W = \frac{V - 1.35}{5.6 \times 0.00067}$$ (5)

Where:

- V: voltage output,

- W: rotational angular velocity (Choe et al., 2013).

2.3.9   Angle consideration

It is important to consider the angle of each location when applying MEMS and strain gage sensors. The directions of each sensor are based comparatively on gravity; therefore, the straight perpendicular to gravity (longitudinal and vertical directions) is considered when oriented axes are directed, i.e., longitudinal axis is a forward direction. In this case, angle in lateral direction is considered because it runs straightly in side-by-side direction.

The following figure 4 clearly represented the signal obtained based on each location angle. Generally, the hand-made experiment with these sensors cannot be installed properly; therefore, angle should be considered, otherwise results would be completely wrong.
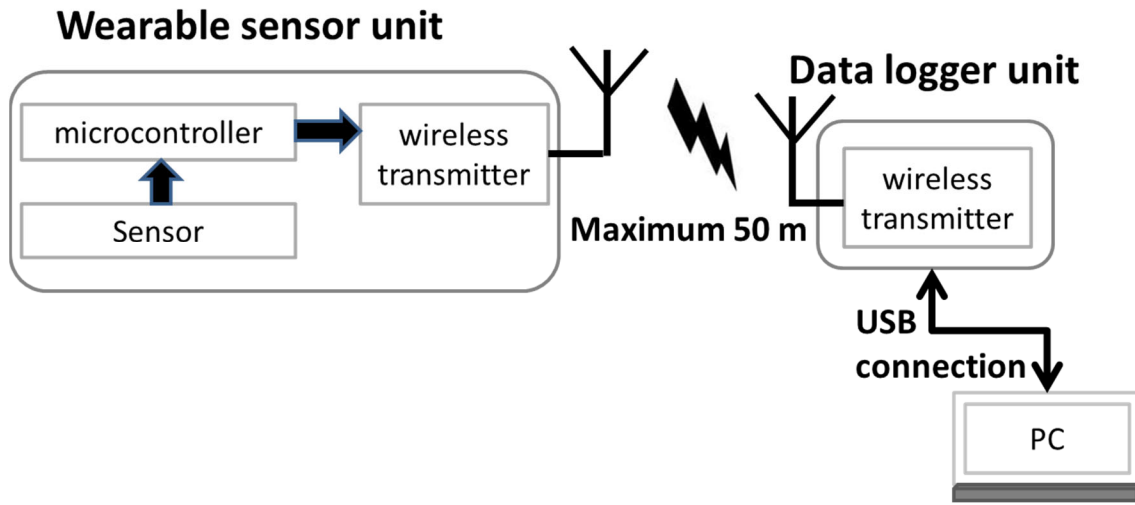
Fig. 5 Data collection tools and its processing

2.3.10 Root mean square

Root mean square for translational accelerations is expressed in equation 6.

$$RMS_{translational\ acc} = \sqrt{\frac{1}{n}\sum_{i=1}^{n}(G_i)^2} \tag{6}$$

Where G_i is translational acceleration value, obtained from the MEMS sensor.

Root mean square for rotational angular velocities is expressed in equation 7.

$$RMS_{rotational\ ang.\ v} = \sqrt{\frac{1}{n}\sum_{i=1}^{n}(W_i)^2} \tag{7}$$

Where:

- $n:$ number of sampling data in each experimental test,

- W_i is rotational angular velocity value, obtained from the MEMS sensor.

Special note: if average value of individual translational acceleration and rotational angular velocity for an experimental test is exceeding **0.85**, it is recommended that new equations for root mean square (RMS) be determined as in following equations 8.

$$RMS_{translational\ acc} = \sqrt{\frac{1}{n}\sum_{i=1}^{n}(G_i - \overline{G_i})^2} \qquad (8)$$

$$RMS_{rotational\ ang.v} = \sqrt{\frac{1}{n}\sum_{i=1}^{n}(W_i - \overline{W_i})^2} \qquad (9)$$

Where:

- *n:* number of sampling data in each experimental test,

- $\overline{G_i}$ *and* $\overline{W_i}$ are means of translational acceleration and rotational angular velocity values, respectively.

2.3.11 Magnitude of vibration

Mechanical vibrations in a machine are caused by the moving components of the machine. Since a machine may consist of many such moving components, overall vibrations from engine transmitted to all parts in contact with the machine are made up of vibration of different frequencies occurring simultaneously. The vibration from the hand tractor is highly dependent on the frequencies, translational acceleration, rotational angular velocity, and power spectrum density (PSD) of vibration. It is recommended that the magnitude output of vibration from engine measured using MEMS is described in RMS (Dewangan et al., 2008).

Even in stationary case, the vibration signals were very complex in nature. It was not possible to find the frequencies by observing them in the time domain. Thus, fast Fourier transform (FFT) technique, obtained from computer package, DADiSP/PRO 4.1, Japanese Version, was employed to transfer these signals from the time domain to the frequency domain, and the PSD, a measure of the engine at various frequencies, at different frequencies was obtained using a computer software package for mathematical

computations and signal processing. The power spectrum was plotted against the frequencies of the signal and the dominant frequencies of vibration were obtained from the plot (Salokhe et al., 1995).

Finally, hand tractor vibration transmissibility is defined as ratio of the vibration measured between the vibration intensity on the engine-cover top on which is the main source under stationary mode and connecting parts to engine such as chassis, gearbox, middle between handle base and handgrip, and handgrip. Transmissibility was measured at the same axis and expressed in the following equation 10. (Dewangan et al., 2008; Taghizadeh et al., 2007; Stikeleather, 1991; Salokhe et al., 1995).

$$Vibration\ transmissiblity = \frac{a_{rms\ main\ source}}{a_{rms\ absorbed\ parts}} \qquad (10)$$

Where:

- $a_{rms\ mainsource}$ is acceleration at engine top-cover/engine front,

- and $a_{rms\ absorbed\ parts}$ are acceleration at chassis, gearbox, middle between handle base and handgrip, and handgrips, and i is axis of orientation.

Vibration transmissibility was calculated for six monitored vibration axes; namely, three translational accelerations and three rotational angular velocities. In addition, to evaluate vibration assessments, individual measurement made in orthogonal axes should be combined (Mansfield, 2005). The separated three translational accelerations and three rotational angular velocities and therefore the measurements should be performed in two different combinations, namely, longitudinal, lateral, vertical for translational accelerations and roll, pitch, and yaw for rotational angular velocities are derived expressed by (Griffin, 1996; ISO, 2001; Tiwari et al., 2002; Tewari et al., 2004; Goglia et al., 2006; Heidary et al., 2013). A quantity of three combination axes was recommended by ANSI S2.70-2006 to evaluate hand-arm vibration exposures as expressed in equation.

(11) – (12).

$$a_{hw(rms)} = \sqrt{\sum_i (W_{hi} a_{hi(rms)})^2} \tag{11}$$

$$a_{hv} = \sqrt{(a_{hwx})^2 + (a_{hwy})^2 + (a_{hwz})^2} \tag{12}$$

Where:

- $a_{hw(rms)}$: vibration in each direction,

- a_{hv}: vibration combined value,

- W_{hi}: correction coefficient as presented in table 2,

- $a_{hwx}, a_{hwy}, a_{hwz}$: each direction value.

Table 2 Strength of 1-1 / 3 octave band table ISO

The strength of 1-1 / 3 octave band table ISO to convert the strength frequency correction for hand-arm vibration ISO frequency correction coefficient W_{hi}.

Frequency band No. I	Band frequency Hz	Correction coefficient W_{hi}
Six	Four	0.375
Seven	Five	0.545
Eight	6.3	0.727
Nine	Eight	0.838
Ten	Ten	0.951
Eleven	12.5	0.958
Twelve	Sixteen	0.896
13	Twenty	0.782
14	25	0.647
Fifteen	31.5	0.519
Sixteen	Forty	0.411
17	Fifty	0.324
Eighteen	63	0.256
19	80	0.202
Twenty	Hundred	0.160
21	125	0.127
22	160	0.101
23	200	0.0634
24	250	0.0634
25	315	0.0503

26	400	0.0398
27	500	0.0314
28	630	0.0248
29	800	0.0186
Thirty	1,000	0.0135
31	1,250	0.00894
32	1,600	0.00536
33	2,000	0.00295

Cited from ANSI, S2.70-2006

2.4. Results

2.4.1. RMS of stationary hand tractor

Vibration magnitudes of the 12Hp hand tractor using MEMS sensor are described in Fig. 6. It can be seen that RMS values at handgrip in vertical axis was the biggest followed by those at gearbox, engine top and chassis, respectively. The high vibration magnitude at handgrip in vertical axis was given that handle acts like a cantilever beam (Salokhe et al., 1995, Bahareh et al., 2013). At engine top, magnitude is observed higher in longitudinal axis given that it responses to the corresponding of engine power stroke. The excitation of power stroke induces the rotating engines to vibrate in the same direction (Mehta et al., 2000). At the same location, extreme vibration signals predominantly in roll axis. It would be reasonable that engine is the main source of vibration excitation that vibration is movably parallel to the displacement of piston. As the engine is a main source of vibration, the relationship between engine top and other connecting parts was observed. It revealed that the engine transmitted vibration slightly to chassis of 0.4 m/s^2, and gearbox of about 0.4 m/s^2, but largely to handgrip 1.1 m/s^2.
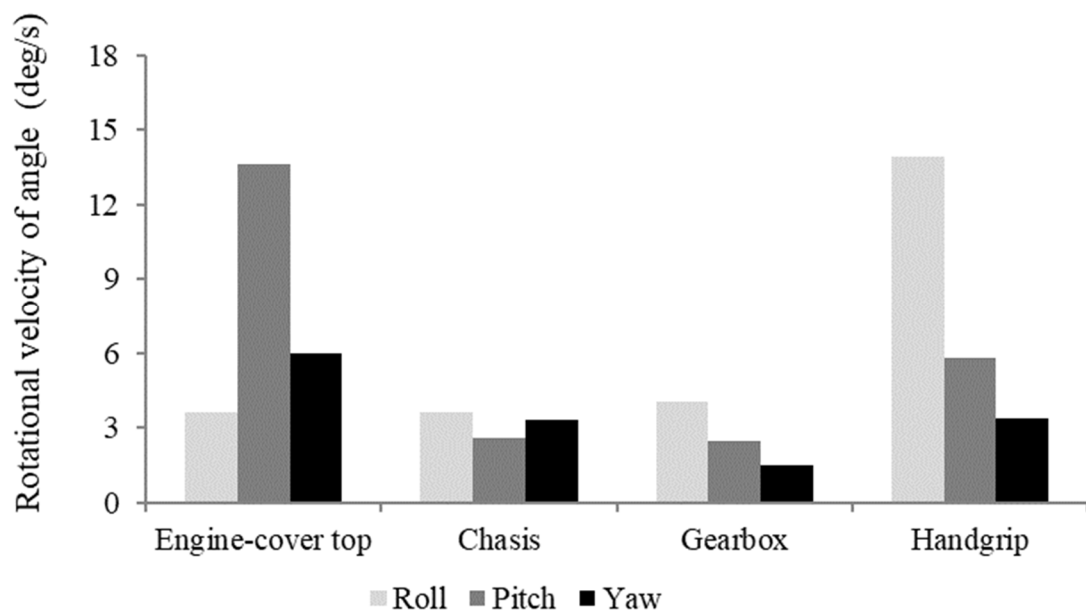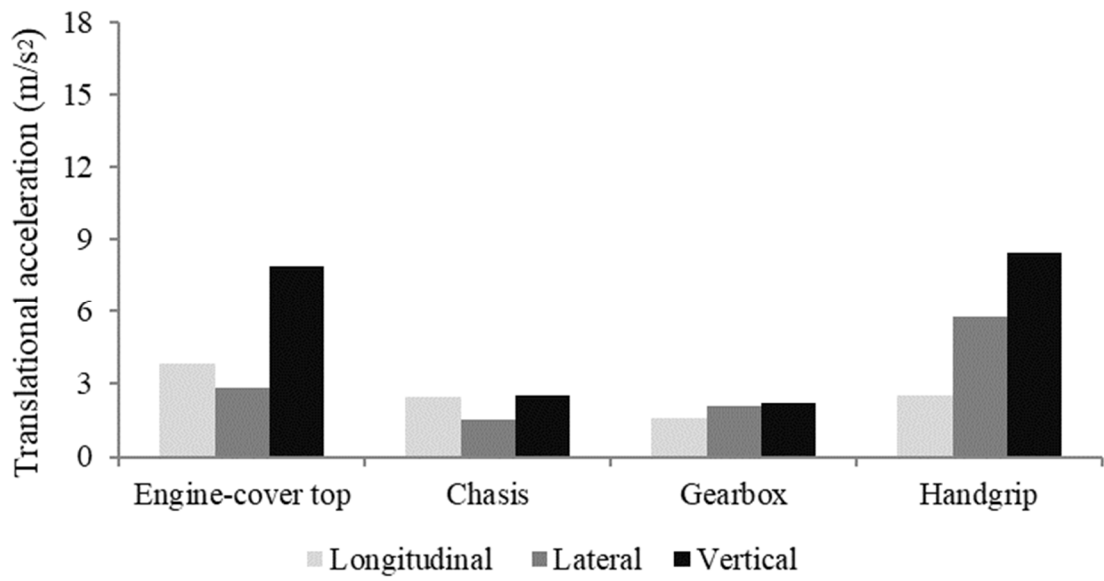
Fig.6 RMS of translational acceleration and rotational angular velocity (stationary)

2.4.2. RMS of driving hand tractor

Figure 7 represents the RMS of translational acceleration and rotational angular velocity at idling speed. As for the translational acceleration, peak magnitude appears in vertical axis of around 12m/s^2, and it as well occurred hugely at roll axis of about 11m/s^2. The predominant vibration may be caused by cantilever beam the hand tractor acts (Salokhe et al., 1995, Bahareh et al., 2013).
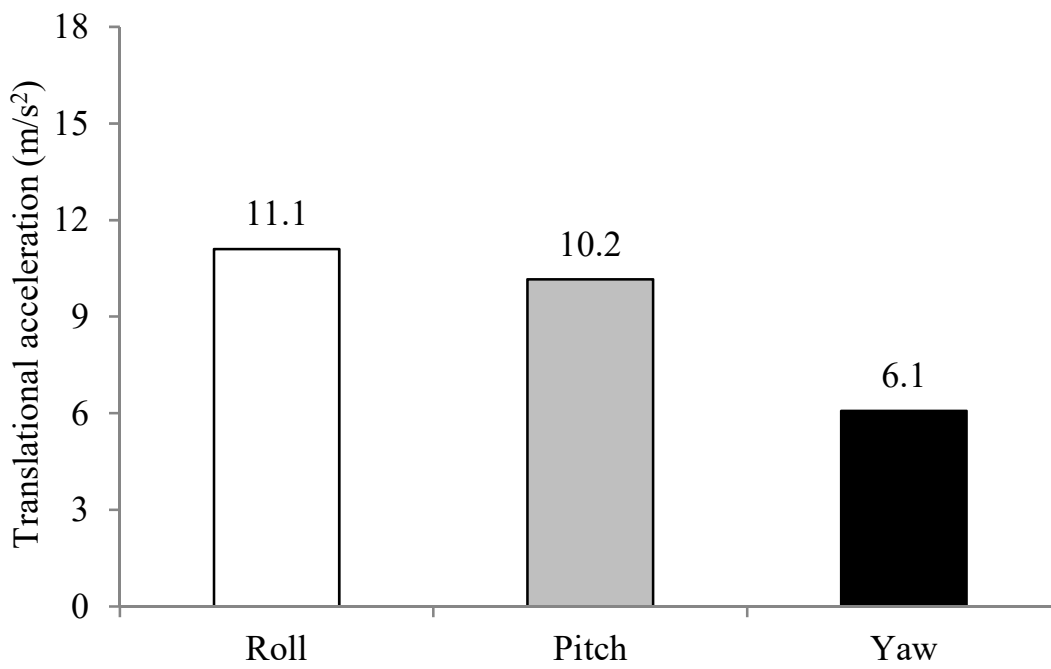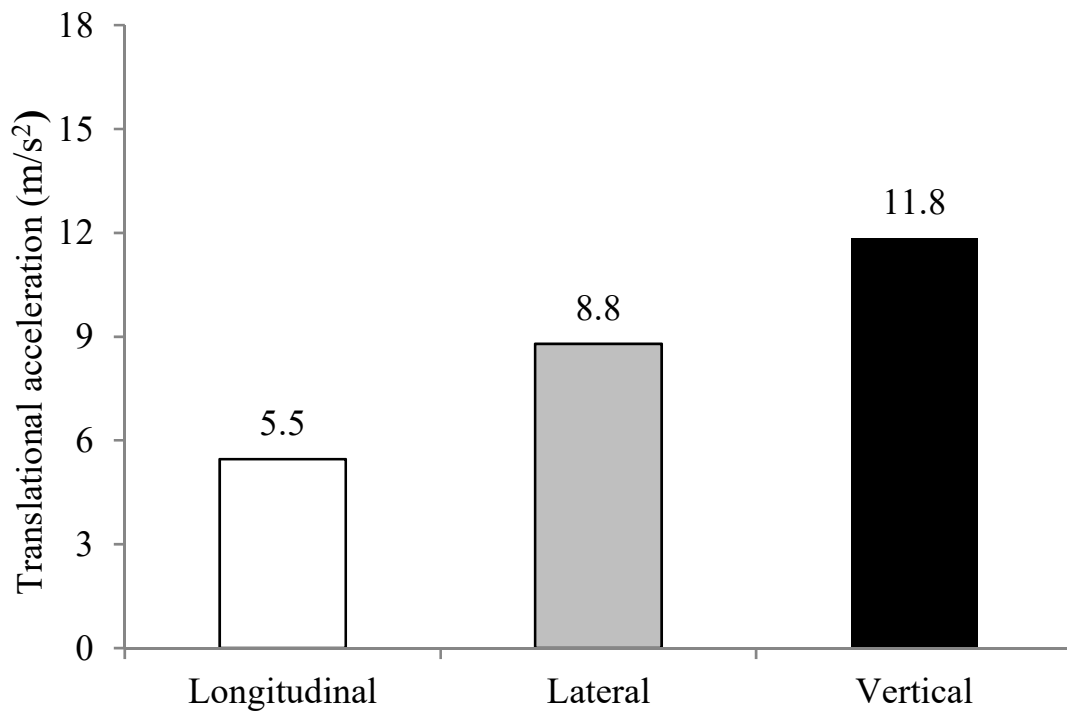
Fig.7 RMS of driving hand tractor at handgrip

2.4.3 Power spectrum density at stationary and driving modes

The results of PSD on the engine top and handgrip were partly represented in Fig. 8 and Fig. 9. The sensitivity vibration at 2, 5 or 20Hz may cause severe discomfort or injury but will not produce nausea, vomiting and color changes so characteristic of motion sickness (M. J. Griffin, 1990). It is seen in stationary condition that predominant magnitude at the engine top occurred largely at about 10Hz frequencies in longitudinal axis while at about 11Hz frequencies dominantly emerged at handgrip in vertical axis. These may be due to the corresponding to the movement of engine piston and movement of cantilever beam that the handle acts (Salokhe et al., 1995).
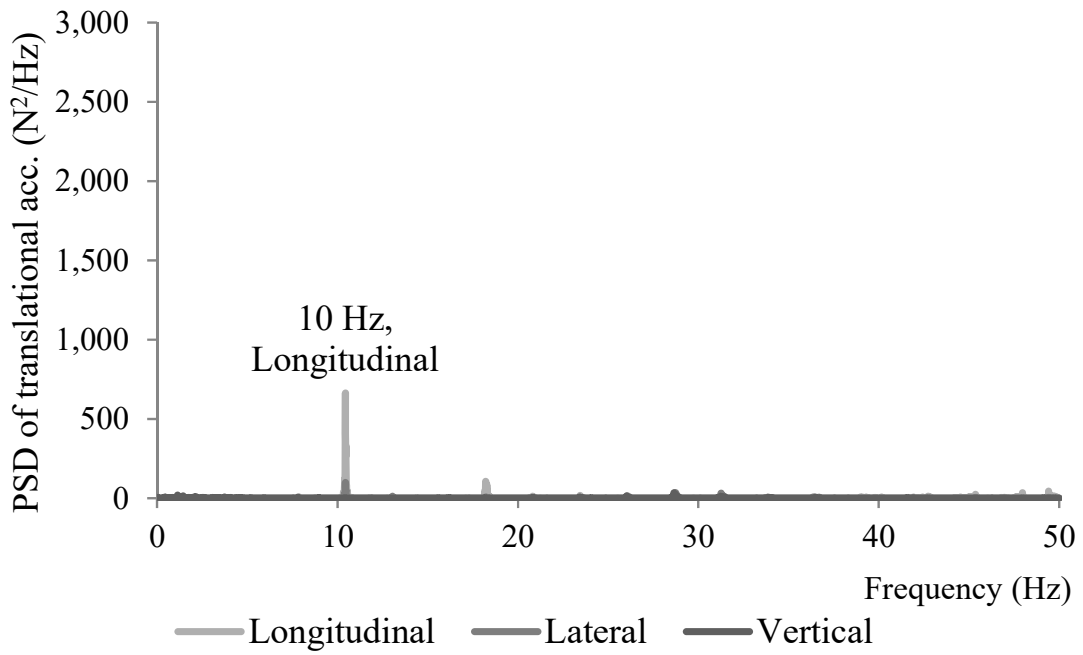
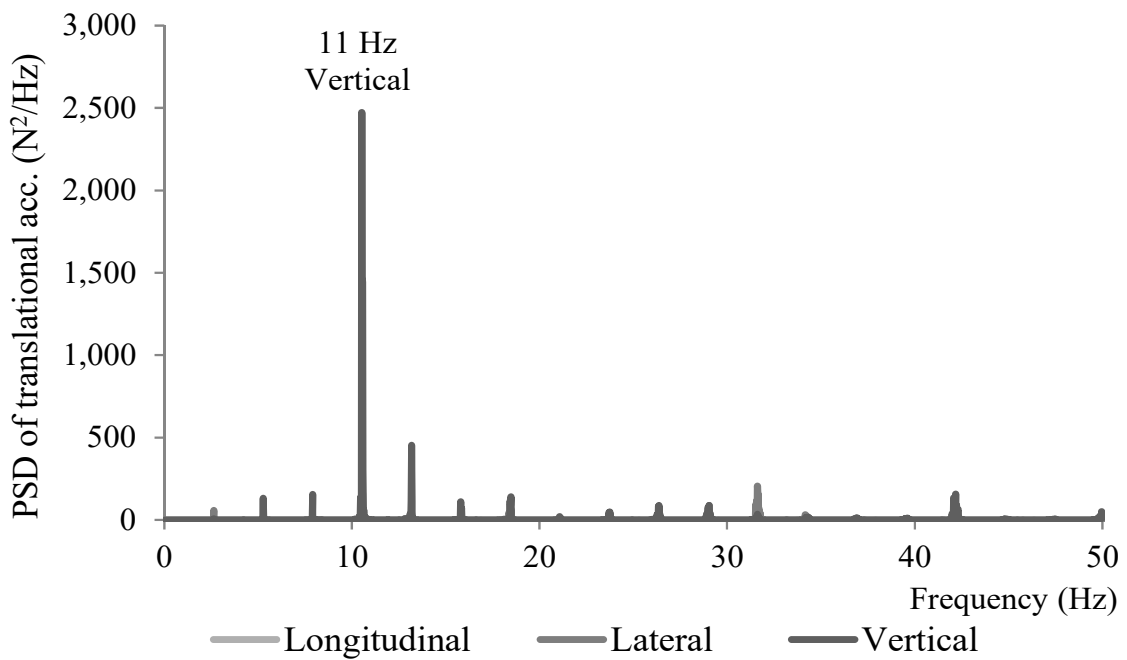Fig. 8 PSD at engine top (stationary)

Fig. 9 PSD at handgrip (stationary)

In driving mode, dominant frequency is found at about 3Hz frequencies first in longitudinal axis and about 9Hz frequencies next in vertical axis as presented in Fig. 10. The first frequencies would cause by movement of engine piston and the second peak would cause by cantilever beam that these results also confirmed by Salokhe (1995) and Bahareh et al., (2013).
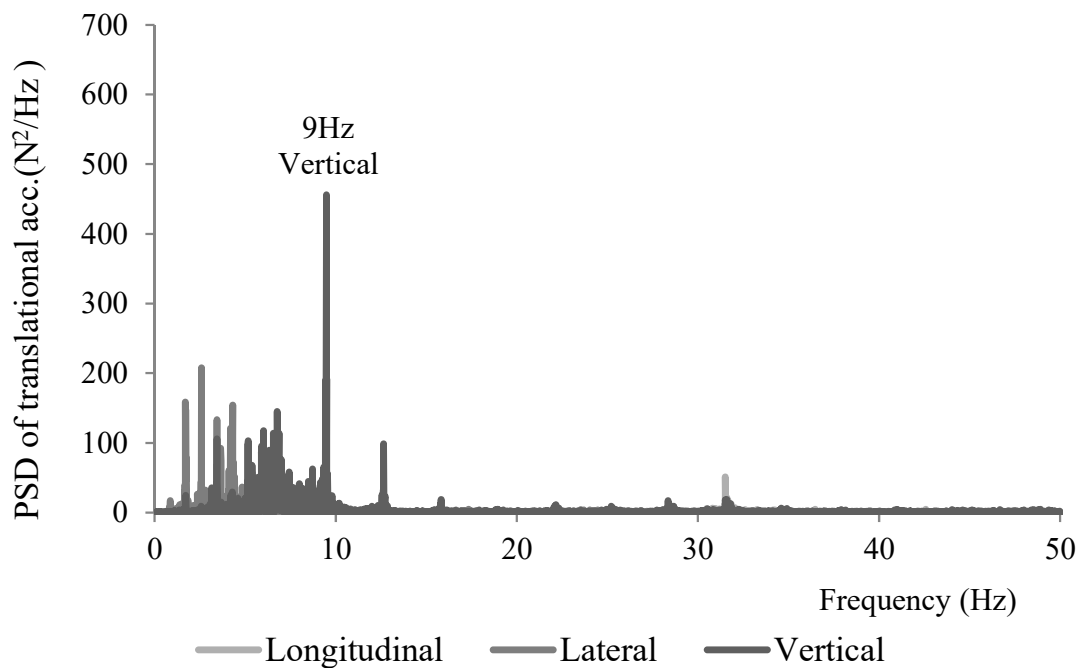
Fig. 10 PSD at handgrip (driving)

2.4.4 Hand-arm vibration exposures

The hand-arm vibration exposures were conducted based on RMS of engine vibration magnitude under hand-gripped modes to observe the severity of vibration from hand tractor to the operators, and a picked-up frequencies were experimentally needed to compute exposure.

Results appeared that in stationary and driving modes the RMS of hand-arm vibration exposures were extremely higher than those stated in health guidance zone as presented in Fig. 11 and Fig. 12. This means that operators shall be technically advised to stop their

operation; otherwise, it would be longer-sooner risky to health.

Fig. 11 RMS of hand-arm vibration exposure in stationary and driving modes
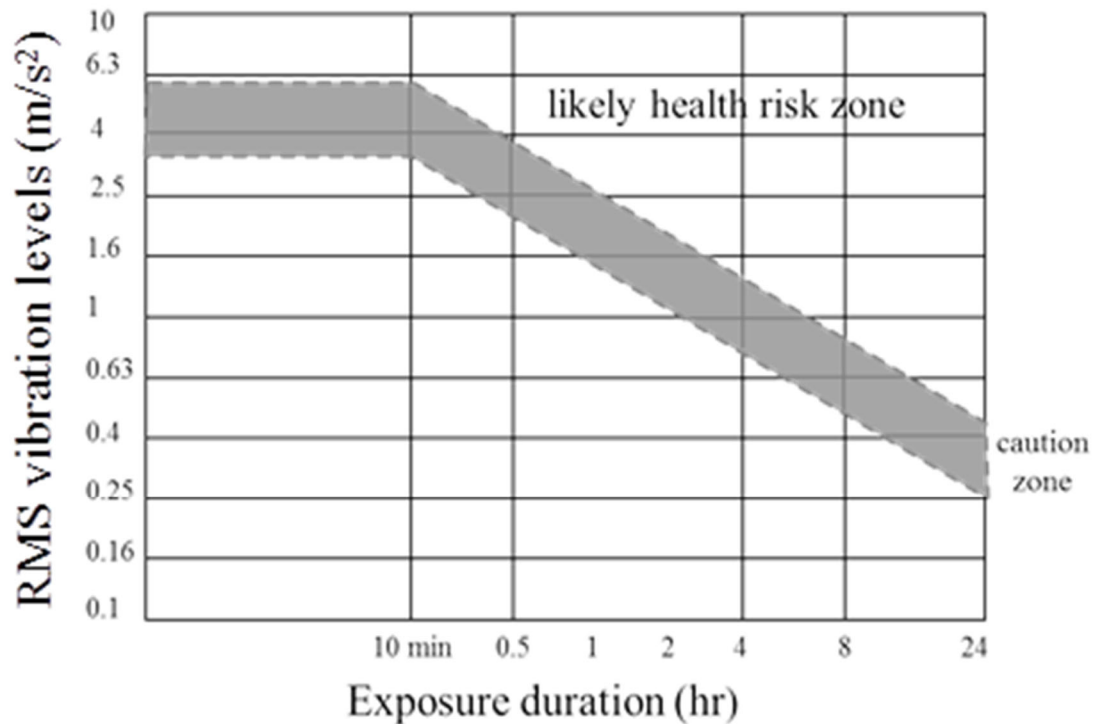
Fig. 12 Health Guidance Zones (Sayed M.E. *et al., 2012*)

2.4.5 Future development

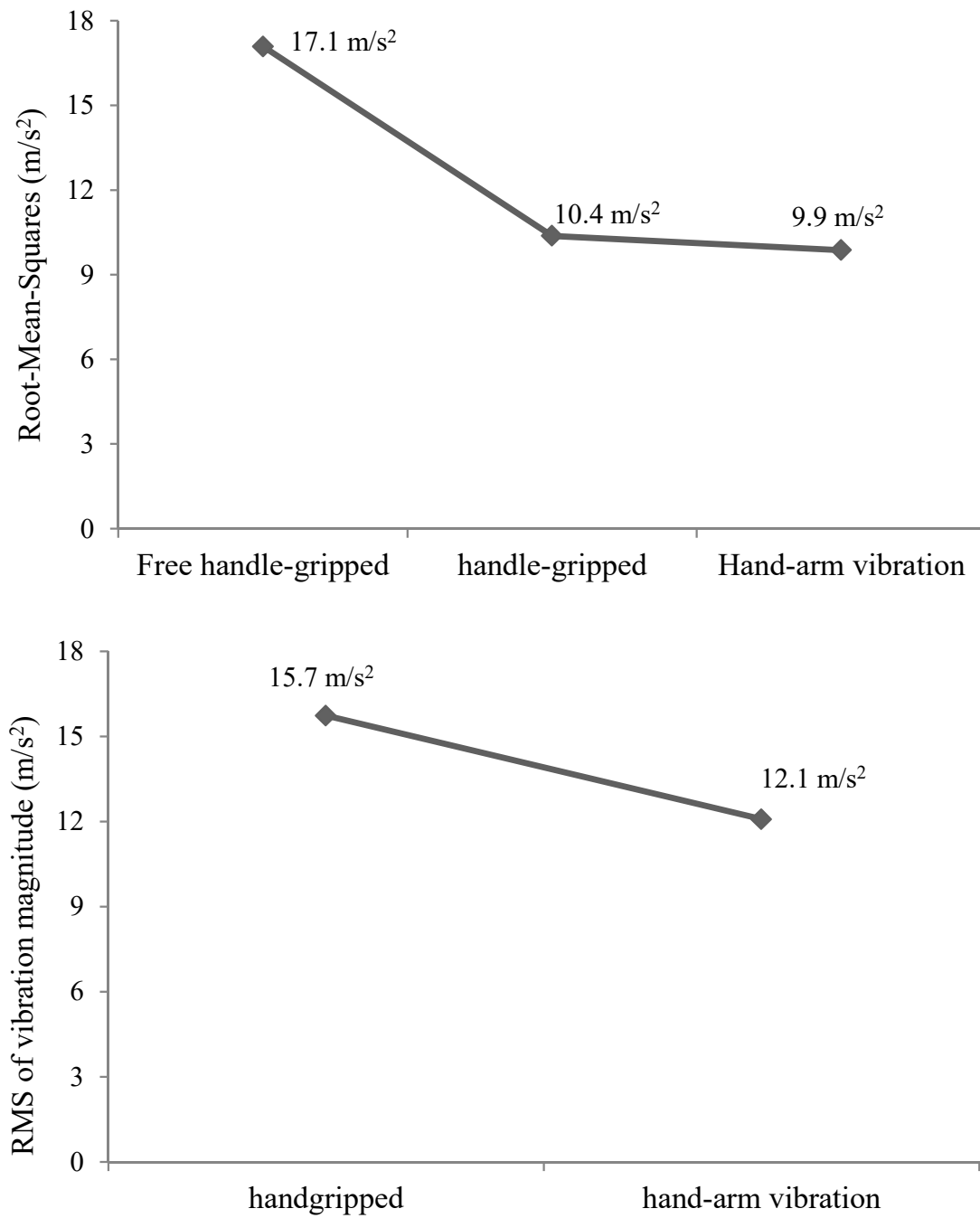To prevent health risks, an effective intervention such as isolator dampening sleeves, splitting handle arm installed on some locations in between engine and base frame and between handle and gearbox. Some researchers applied successfully with isolators dampening sleeves, splitting handle arm on some locations (Chavan et al., 2013, Charturvedi et al., 2012).

2.5 Conclusion

The demand to improve agricultural production through enhancing agricultural mechanization was important for country development, Cambodia. However, with multipurpose uses of mechanization, especially hand tractors, long-time operation would cause discomfort to operator through handgrip vibration. Experiment results showed that the large vibration occurred at the handgrips in vertical axes. The RMS of hand-arm

vibrations exposure at the handgrip of the 12Hp hand tractor were much higher than that in health risk limitation standard. Therefore, effective intervention should be developed to protect operator's health.

CHAPTER 3 INVESTIGATION OF VIBRATION CHARACTERISTICS OF HAND TRACTOR BASED ON FREQUENCY-DOMAIN AND VIBRATION INTENSITY

3.1 Background

Employment in the Cambodian agricultural sector has sharply decreased from 80% in 1993 to 40% in 2015 and is anticipated to decline to 35% by 2020 (OpenDevelopment Cambodia, 2015). In this regard, agricultural mechanization, particularly the use of hand tractors, has been adopted as a substitute for the labor of human workers and draft animals. This has not only facilitated the timely completion of operations but also increased production, labor savings, energy efficiency, productivity, and profitability (Singh et al., 2011). In addition, the hand tractor is suited to the sizes and scattered locations of farms, can be used under dry and wet conditions, has a low cost, and has multiple uses (FAO, 2013; Chan, 2013).

However, the numerous applications of hand tractors have resulted in operators holding the handles for longer periods, which has produced the vibration discomfort known as early fatigue. Tiwari and Gite (2006) explained that machine vibration is detrimental to agricultural workers. Many studies have confirmed the adverse health effects of vibration; for example, early fatigue may cause physical, physiological, and musculoskeletal disorders over months and years (Salokhe et al., 1995; Sam and Kathivel., 2006; Dewangan and Tewari., 2009).

In industrial production, the machine components of the hand tractor must operate according to manufacturer-designed specifications and have an assembled capacity that allows optimum productivity. However, a lack of knowledge and experience regarding machine operations and maintenance reduces the overall performance of the machine

through unscheduled shutdowns, economic loss, industrial casualties, and adverse health effects on the operator. The in-time detection of machine failure and performance loss can ensure the reliability and security of the machinery, as well as personal security and safety (Koenigsberger and Tobias, 1972). It is thus important to investigate the vibration characteristics and its mechanism of transmission from the engine to the connecting parts to reduce this machine vibration and detect faults.

The present study measured the vibration magnitudes and transmissibility at various points on a hand tractor and analyzed the hand–arm vibration exposure. Effective intervention methods for future applications can be developed based on the results.

3.2 Research fundamental

3.2.1 Research experiment

The experiment was carried out under stationery condition, where the main source of vibration signal is only produced from the engine. The investigation was undertaken to observe if there is any relation between the engine power stroke and the dominant frequencies of vibration of the hand tractors. Three axes of translational accelerations, and three axes of rotational angular velocities were detected by placing a single DSP sensor on different locations of the hand tractor as shown in Fig. 13. The specifications of the hand tractor are listed in Table 3.

Fig. 13 Experimental hand tractor and sensor allocations

Table 3 Specifications of the experimental hand tractor

Specification	
Length (mm)	2210
Width (at handles) (mm)	720
Height (mm)	1250
Weight (kg)	288
Cooling system	Horizontal water-cooled fan
Output (kW)	5.5
Rated speed (rpm)	2500
Implement width (mm)	600
Implement diameter (mm)	400

3.2.2 Measurement methods

Vibration transmission measurement on hand tractors had been done by many researchers on specific locations, i.e., at the front of the engine foundation, on engine top, chassis, gearbox, and handgrip, human's body (metacarpal, wrist, elbow and acromion and chest (Salokhe et al., 1995; Taghizadeh et al., 2007; Dewangan et al., 2008; Heidary, 2013). On the other hand, the researchers used strain-gage accelerometer to sense magnitude of vibration signals. This device is heavy and complicated with arrangements such as strain amplifier, channel-data-tape recorder, autonomous data acquisition unit and microcomputer. Furthermore, distance of measurement depends upon connected cord.

In modern society, however, wireless inertial measurement unit (IMU) sensors (SS-MS-SMA200G60, Sports Sensing Inc, Japan) sensor is very compact, light including a battery, easy in use, and requires minimal installation space to pick up vibration signal. It is a wireless sensor which can detect signal within 50 meters as described in Fig. 14, and specification of the sensor is presented in Table 4. The output vibration signal is easy to convert and calculate. Moreover, this MEMS sensor is cheaper than the conventional system, allowing for inexpensive measurement of translational acceleration and rotational angular velocity (Choe, 2013).
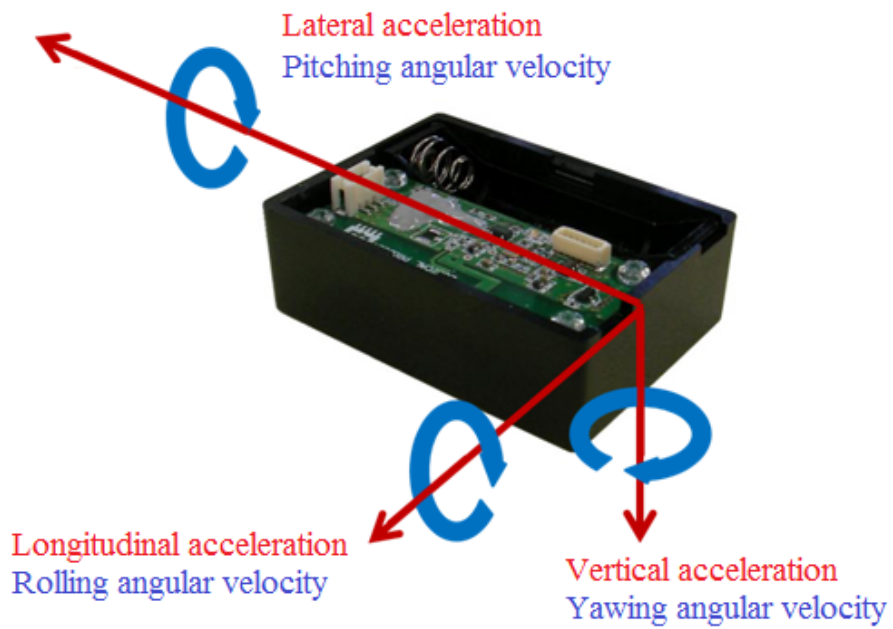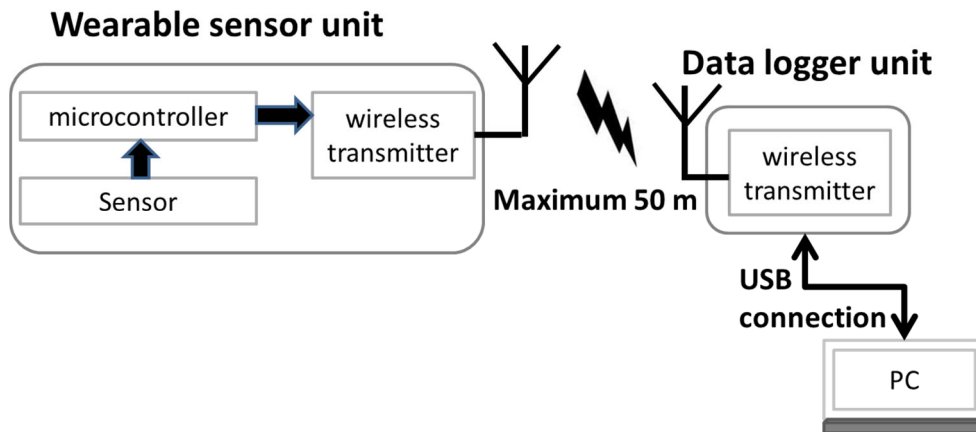
Fig 14. SS-MS-SMA200G60 detection features and its operation

Table 4 Specification of the experimental wireless sensor

Specification	
Model number	SS-MS-SMA200G60
Acceleration	±200G
Angular velocity	±6000dps
Built-in memory	128MB (1Gbit)
Sampling rate	1Hz～1000Hz (9 DoF)
Comm. Method	Either wireless or wired
Weight	24g (waterproof type 32g)
Dimension	38mm(W) x 53mm(D) x 11mm(H)

3.2.3　Data acquisition and setup

To obtain the vibration data, seven wireless sensors (SS-MS-SMA200G60, Sports Sensing Inc, Japan), which are mentioned in Table 4 and Fig 14, were firmly taped to different points on the hand tractor, specifically , engine-right-side front (EF), engine-right-side rear (ER), engine-cover top (ET), chassis (CH), gearbox (GB), and middle between handle-base (MH) and handgrip (HG), as shown in Fig. 13.

This type of sensors directly communicated with a digital signal processing (DSP) analog voltage data logger that was plugged into a personal computer. Commercial package software (ss_wSensor, Sports Sensing Inc, Japan) was installed on the computer to initially setup conditions before recording data such as recording length, sampling rate, and number of sensors to be attached.

Before starting operation, it is important consideration in calibration the sensors. Five steps were adopted (1) sensors were calibrated on the plate plan before taping sensors on to the hand tractor, (2) the sensors were equipped tightly on the designed positions of the hand tractor, and angles of each sensor were directly measured and recorded, (3) setup sensor conditions including 200 Hz of sampling rate, stringently runs for 30s with frequency resolution of 100Hz, (4) national vibration at each location were recorded during engine idling and (5) start the engine and record vibration signals.

3.2.4　Data analyses

Three engine speeds were adopted in the experiment such as minimum, middle, and maximum based on opening throttle positions of the hand tractor. The three revolution speeds of the engine measured by a laser tachometer were 1266, 2110, and 2658 rpm, respectively.

The wireless sensors output 3-translational accelerations, 3-rotational angular

velocities, and 3-magnetometer results in the CSV file format. The recorded data was instantly stored in sensor memory before backing up on the computer wirelessly for analysis.

An opensource programming language Python under an Anaconda Jupyter Notebook, which provides powerful tools and handy NumPy, Pandas, Matplotlib and OS libraries were hired, as presented in Fig. 15. This platform allowed intensive and manual programming using defined techniques based on the amplitude, fast Fourier transform (FFT), power spectrum density (PSD), dominant frequency, root mean square (RMS) value of acceleration, and vibration transmission ratio. The hand–arm vibration exposure was then calculated using an ISO standard (ANSI/ASA S2.70-2006 (R2016)).
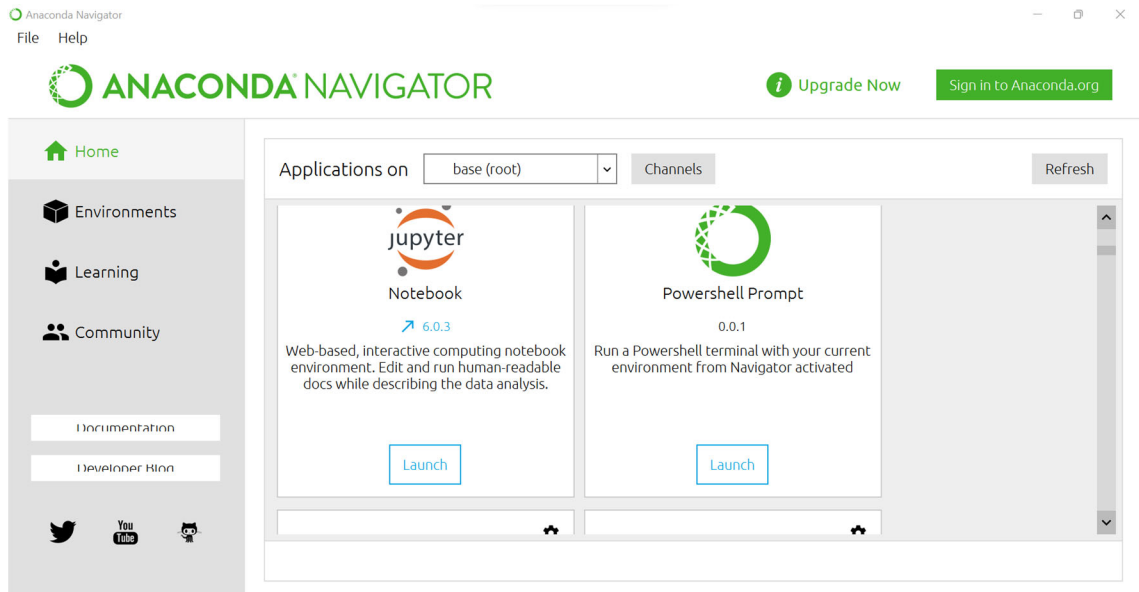
Fig. 15 An opensource platform Anaconda Jupyter Notebook

The RMS value of acceleration was used to obtain the vibration magnitudes, while the PSD was adopted using the FFT to obtain the signals in the frequency domain (Salokhe et al., 1995). In the theoretical analysis, the PSD was plotted against the frequency of the signal, and the dominant frequency of vibration was obtained.

3.2.4.1 Data calibration

Vibration may occur naturally, and that is considered as white noise. Therefore, to obtain actual vibration it is better to remove noise through sensor calibration. Equation 13 was presented to split white noise from the actual vibration.

$$A_i = A_{total} - \frac{\sum_{i=1}^{n} x_i}{n} \tag{13}$$

$$A_{actual} = A_i * \cos(\theta_{sensor} * pi * 180^{-1}) \tag{14}$$

Where:

- A_i is acceleration data obtained after removing the white noise,

- A_{total} is acceleration data in combination with white noise,

- $\frac{\sum_{i=1}^{n} x_i}{n}$ is an average of acceleration data during engine idling.

The data recorded is susceptible to changes of sensor angle. Hence, the attitude angle was calculated as expressed in the following equation (14) to stabilize the translational acceleration, where:

- A_{actual} is actual translational acceleration data,

- θ_{sensor} is angle at sensor positions,

- $(pi * 180^{-1})$ is used to convert translational acceleration from radiant to degree.

3.2.4.2 Root mean square (RMS)

Mechanical vibrations in a machine are caused by the moving components of the machine. Since a machine may consist of many such moving components, overall vibrations from engine transmitted to all parts in contact with the machine are made up of vibration of different frequencies occurring simultaneously. The vibration from the hand tractor is highly dependent on the frequencies, translational acceleration, rotational angular velocity, and power spectrum density of vibration. It is recommended that the magnitude output of vibration from engine measured using sensor is described in RMS (Dewangan et al., 2008).

The RMS value of the acceleration was calculated using equation (15). Meanwhile, the vibration transmission ratio was the acceleration ratio between the connecting parts and the source of vibration, as expressed by equation (16).

$$a_{rms} = \sqrt{\frac{\sum_{i=1}^{n} x_i^2}{n}} \tag{15}$$

$$Vibration\ Transmission\ Ratio = \frac{a_{Connecting\ Parts}}{a_{Source\ of\ Vibration}} \tag{16}$$

- a_{rms} is the root mean square,
- x is the time-series data,
- n is the length of the data,
- i denotes a data point,
- $a_{Connecting\ Parts}$ denotes the accelerations at different points on the hand tractor, and
- $a_{Source\ of\ Vibration}$ is the acceleration at the engine top.

The RMS values of acceleration along the three axes were combined as recommended by ANSI/ASA S2.70-2006 (R2016) to evaluate the hand–arm vibration exposure, as

expressed in equations (17) and (18). Vibration transmissibility was calculated for six monitored vibration axes; namely, three translational accelerations and three rotational angular velocities. In addition, to evaluate vibration assessments, and compare the vibration transmissibility among the three hand tractors, individual measurement made in orthogonal axes should be combined (Mansfield, 2005). The separated three translational accelerations and three rotational angular velocities and therefore the measurements should be performed in two different combinations, namely, longitudinal, lateral, vertical for translational accelerations and roll, pitch, and yaw for rotational angular velocities. The original equation is derived expressed by (Griffin, 1996; ISO, 2001; Tiwari et al., 2002; Tewari et al., 2004; Goglia et al., 2006; Heidary et al., 2013).

$$a_{hw} = \sqrt{\sum_{i=1}^{n}(w_{hi}a_{rms})^2} \qquad (17)$$

$$a_{hv(rms)} = \sqrt{a_{rms_x}^2 + a_{rms_y}^2 + a_{rms_z}^2} \qquad (18)$$

3.2.4.3 Power spectrum density (PSD)

Even though in stationary case, the vibration signals were very complex in nature. It was not possible to find the frequencies by observing them in the time domain. Thus, Fast Fourier transform (FFT) technique was employed to transfer these signals from the time domain to the frequency domain, and the PSD, a measure of the engine at various frequencies, at different frequencies was obtained using Python language.
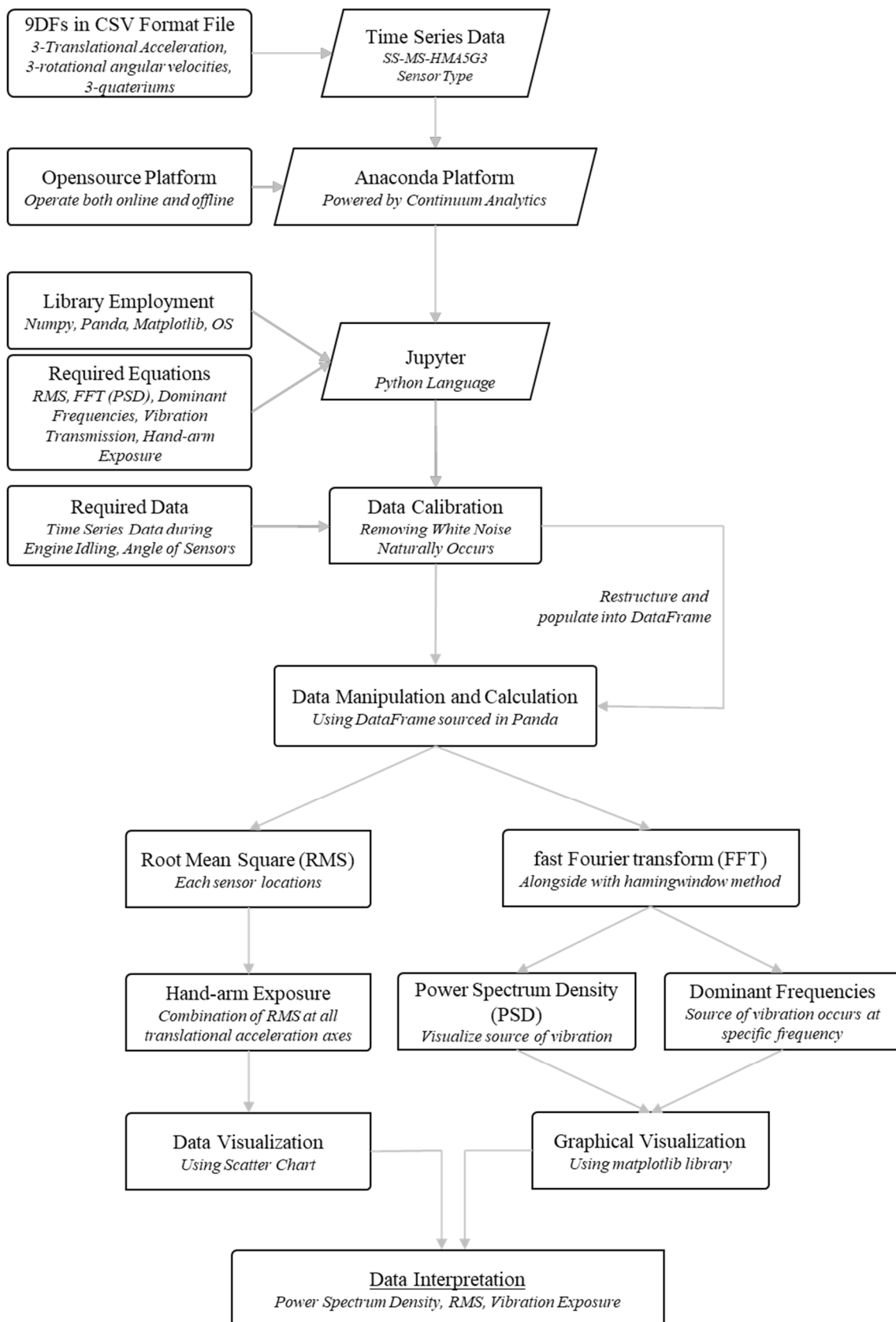
Fig. 16 Experimental process flow for vibration acquisition in stationary condition

Figure 16 presents the flow of experiments alongside wireless sensors using a commercial built-in function to detect vibration at the designed point locations. The data obtained from the sensor described by time series were manipulated and populated as a matrix and fed into Python Language to analyze RMS, PSD, dominant frequencies, and hand-arm vibration exposure using numpy, pandas, matplotlib and os libraries. The results of the analyses were visualized using a function of waterfall 3D in Statgraphics_Centurion 19.1.1 software for report.

3.3 Results and discussion

The experiment was conducted for a hand tractor with a single-piston diesel engine under stationary conditions for three engine speeds. Seven wireless sensors were installed at various points on the hand tractor. The results of the analysis are described below.

Figure 17 presents the vibration magnitudes at different locations on the hand tractor. It can be seen that RMS values of acceleration was the highest at the engine top for all engine speeds, followed by handgrip, chassis, middle between handle-base, engine-right-side front, engine-right-side rear, and gearbox. It was given that the engine was the main source of vibration, transmitting vibration directly to the connecting parts, and causing the whole body of the hand tractor to vibrate at different magnitudes and frequencies.
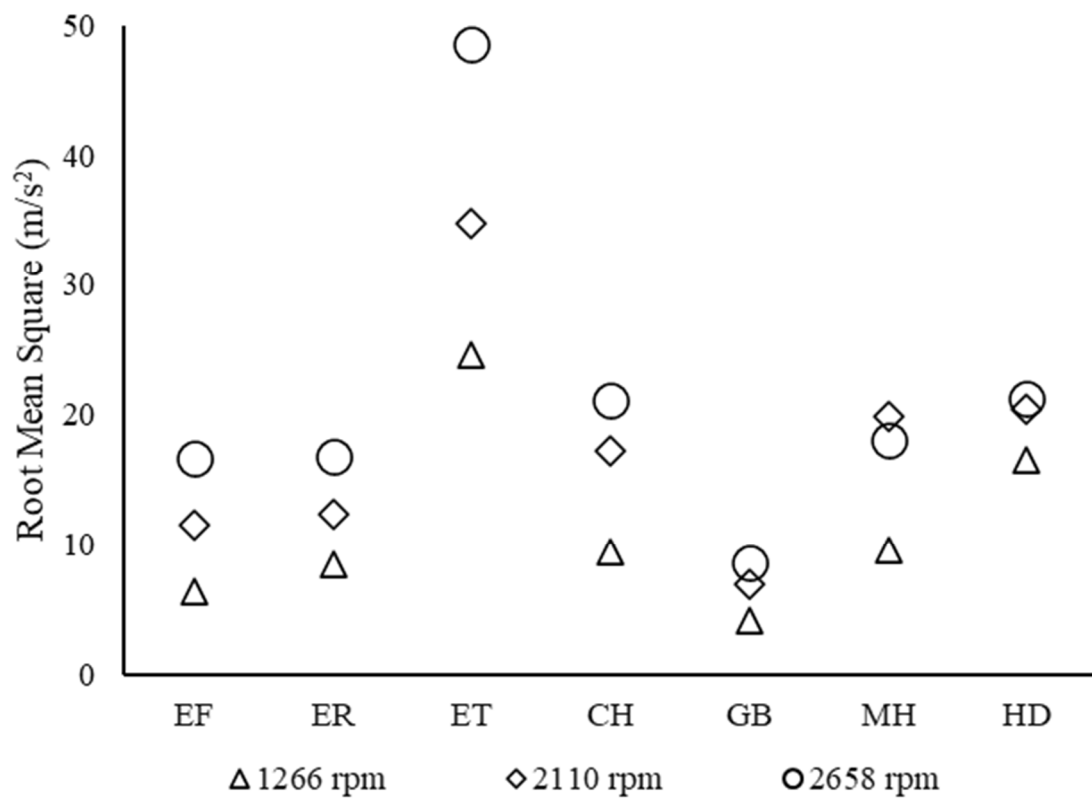
Fig. 17 RMS values of integrated three axes accelerations at different engine speeds

The engine top was the main source of vibration transmission as determined by the piston displacement, horizontal water-cooled fan, and oscillation of various engine parts. Therefore, it was important to investigate this location. The handgrip, which directly absorbs vibration from the engine source and responds to the operator's actions during operation, was also characterized.

The vibration magnitudes were thus measured at the engine top and handgrip, which are the areas of most concern to the structural frame and human operator, respectively.

3.3.1 Magnitude of vibration

3.3.1.1 Vibration characteristics at engine top

Table 5 shows that RMS values of the three translational accelerations at the engine top, were dominated by lateral acceleration followed by longitudinal and vertical axes, subsequently. This dominance was due to the structural frame of the hand tractor being equipped with a horizontal water-cooled fan that took air from one side and exhausted it to the other side in the lateral direction. Additionally, the design was such that the system tended to oscillate and exhibit typical pitching movement.

Table 5 RMS values of the three directions at the engine top

Engine revolution speed (rpm)	Longitudinal (m/s^2)	Lateral (m/s^2)	Vertical (m/s^2)
1266	14.54	18.03	8.10
2110	19.85	25.07	13.65
2658	27.19	33.69	21.96

The observed large vibrations along the lateral axis are represented by the PSD in Fig. 18. It is seen that the PSD had the highest peaks along the lateral axis, followed by the longitudinal and vertical axes. It can also be noted that a higher engine speed resulted in a higher PSD. There was a remarkable peak at 44 Hz for the highest engine revolution speed of 2658 rpm.
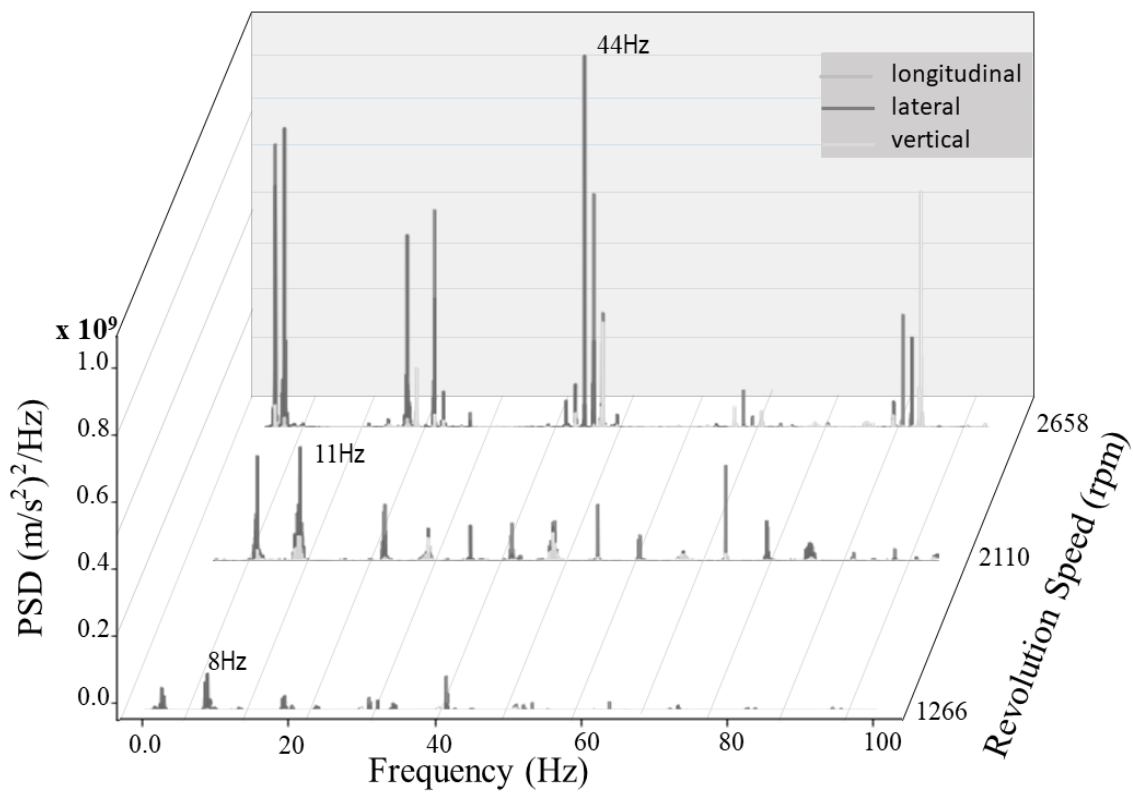

Fig. 18 PSDs in three directions at the engine top

Two findings were obtained from the above PSD results.

(1) There were several peaks in the PSD visible for all engine speeds at different dominant frequencies. This phenomenon might have been due to an imbalance between engine components oscillating at different frequencies. The highest peak was obtained for the lateral axis.

(2) All the dominant peaks in the PSD along the lateral axis were at low frequencies, while those along the longitudinal and vertical axes were scattered from low to high frequencies.

The low-frequency vibration might have been the vibration generated by the displacement of the piston and components, while the high-frequency vibration was associated with noise and the natural vibration frequencies.

3.3.1.2 Vibration characteristics of handgrip

Among the component parts of the hand tractor, the handgrip absorbs vibration directly from the engine source and transmits that vibration to the operator, causing early fatigue. Measurements were thus made to obtain the vibration characteristics at the handgrip for the development of anti-vibration measures.

Table 6 presents RMS values of the three translational accelerations at the handgrip. It is seen that the RMS values of acceleration of the handgrip were greatest along the vertical axes of 13.12 m/s^2, 15.80 m/s^2, 15.27 m/s^2 followed by the lateral axes of 8.84 m/s^2, 11.53 m/s^2, 13.16 m/s^2, and longitudinal axes of 4.79 m/s^2, 5.60 m/s^2, 6.88 m/s^2, with respect to the three engine speeds. It is reasonable that the handgrip acted as a cantilever beam, resulting in the handle vibrating vertically and freely.

Table 6 RMS values of the three directions at the handgrip

Engine revolution speed (rpm)	Longitudinal (m/s^2)	Lateral (m/s^2)	Vertical (m/s^2)
1266	4.79	8.84	13.12
2110	5.60	11.53	15.80
2658	6.88	13.16	15.27

Figure 19 shows that the PSD had high peaks predominantly on the vertical axis of 88 Hz, 70 Hz, 21 Hz, followed by the lateral of 44 Hz, 53 Hz, 53 Hz, and longitudinal axes of 44 Hz, 41 Hz, 21 Hz at all engine speeds. The figure also shows that high peaks appeared largely at low frequencies for low engine speeds but at high frequencies for high engine speeds.
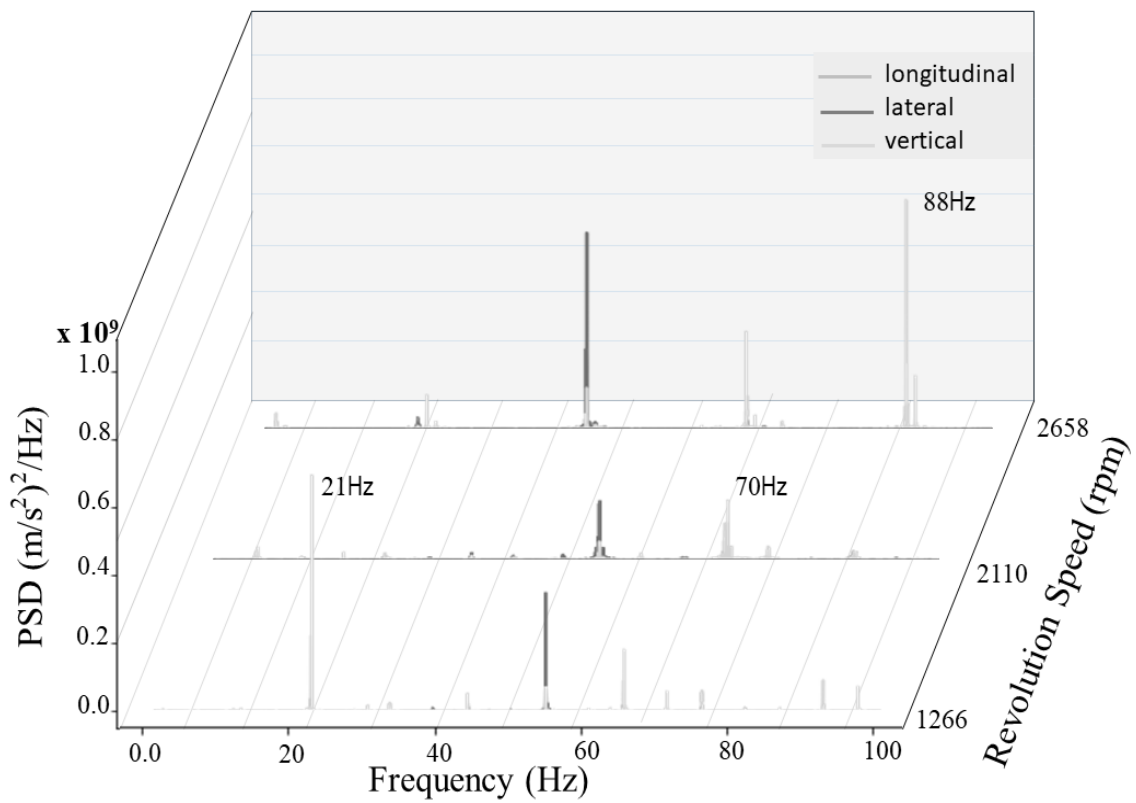

Fig. 19 PSDs in three directions at the handgrip

The peaks at different frequencies for different engine speeds may have been due to the oscillation of the handgrip being excited by the transmission of vibration from the engine source (i.e., high-frequency vibration from the engine produced high-frequency vibration in the connecting parts, especially the handgrip).

3.3.2 Vibration transmission ratio

The vibration transmissibility is defined as the ratio of the measured vibration at connecting parts such as the engine-right-side front, engine-right-side rear, chassis, gearbox, middle between handle-base, and handgrip to the measured vibration at the engine top. The transmissibility was measured at orientations suggested in the literature (Stikeleather, 1991; Salokhe et al., 1995; Taghizadeh et al., 2007; Dewangan and Tewari, 2008).
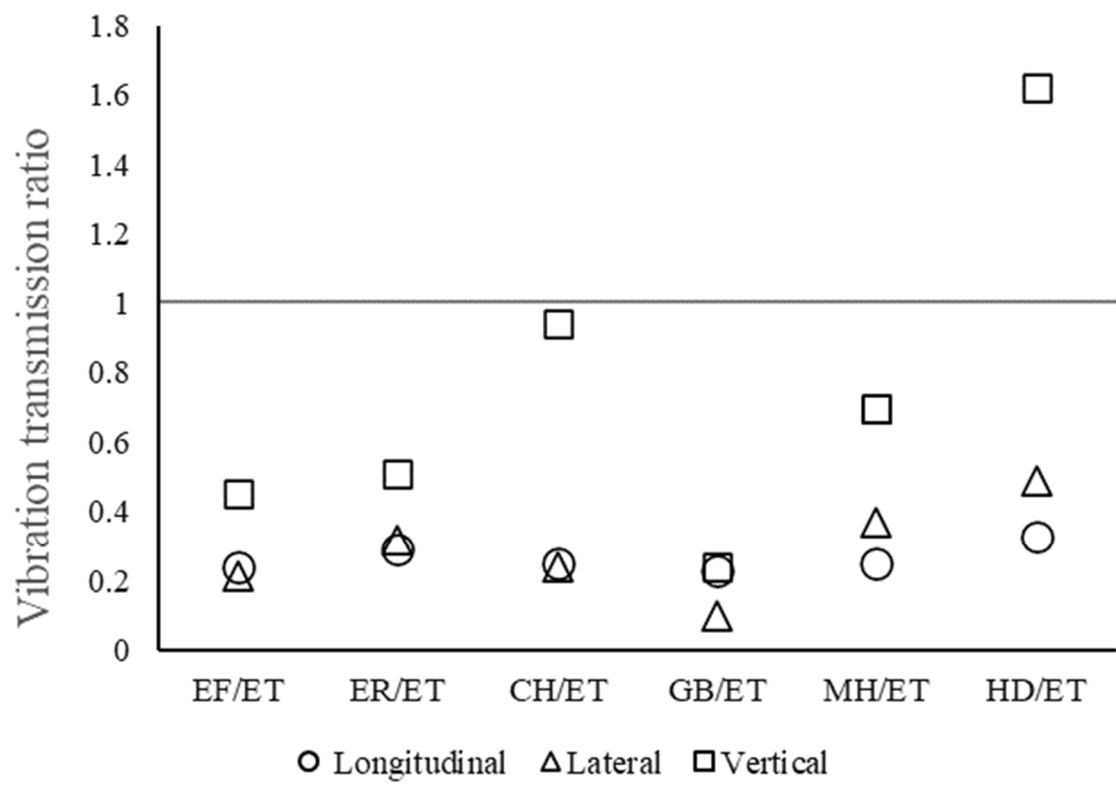
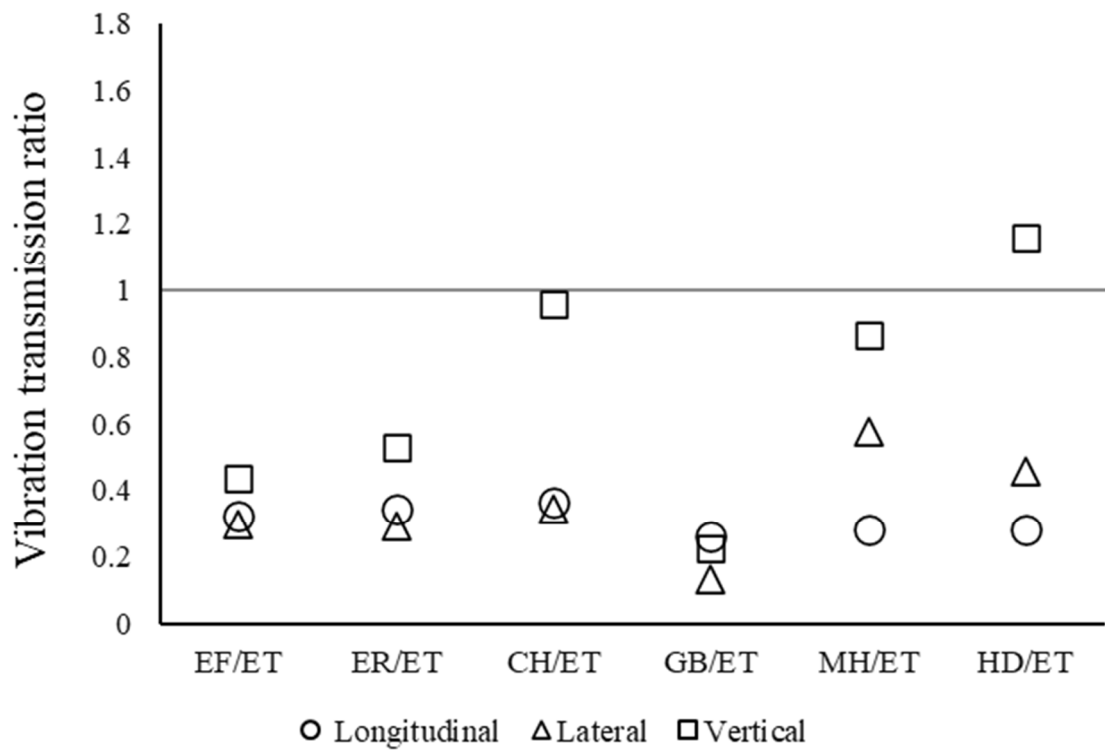Fig. 20 Vibration transmission ratio at 1266 rpm

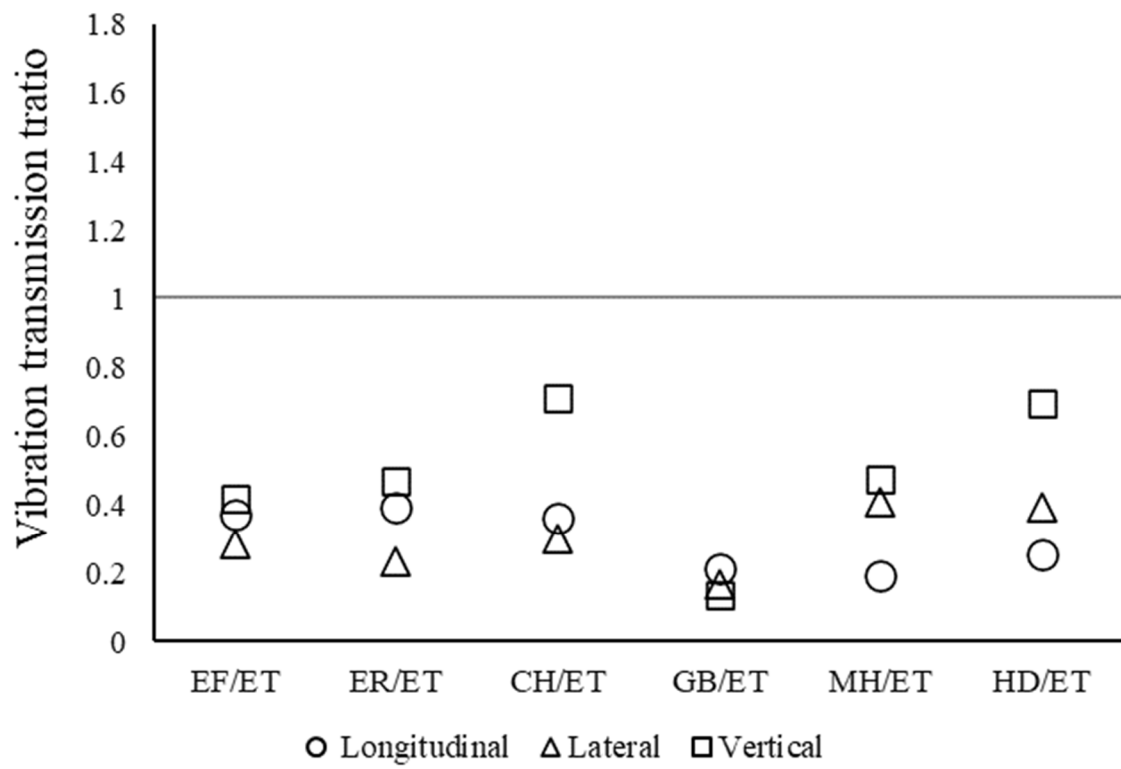Fig. 21 Vibration transmission ratio at 2110 rpm

Fig. 22 Vibration transmission ratio at 2658 rpm

Figures 20, 21, and 22 show that vibrations were transmitted slightly to the engine-right-side front, engine-right-side rear, chassis, gearbox, middle between handle-base, and handgrip at all the engine revolution speeds. It was reasonable for these locations to be sources of vibration. Because they were connected to the frame of the hand tractor, they therefore acted as vibration dampeners. However, the transmission ratio at the handgrip was high on the vertical axis of 1.61, 1.15 at minimum and middle engine speeds, respectively. Nevertheless, transmission ratio was observed in low value in vertical axis of 0.69 at maximum engine speeds. The high transmission ratio in vertical axis can be also found at chassis of 0.93, 0.95, 0.70 in respect of all engine revolution speeds.

It should be noted that the vibration transmission ratio was the greatest on the vertical axis at the handgrip because the handle acted as a cantilever beam. However, the ratio gradually decreased with an increase in engine speed. This indicates that external excitation frequency tends to equal to the natural frequency of the handgrip in vertical axes at low engine speed and hence the system resonates with higher amplitudes at low engine speed.

3.3.3 Hand–arm vibration exposure

The hand–arm vibration exposure was analyzed using the RMS of the engine vibration magnitude under the stationary condition. The experiment was conducted to clarify the severity of the vibration transmitted from the engine source to the handgrip, which is directly used by the operator to guide the tractor.

Figure 23 graphically shows the RMS acceleration of the hand–arm vibration exposure under the stationary mode. The vibration clearly increased with the engine speed.
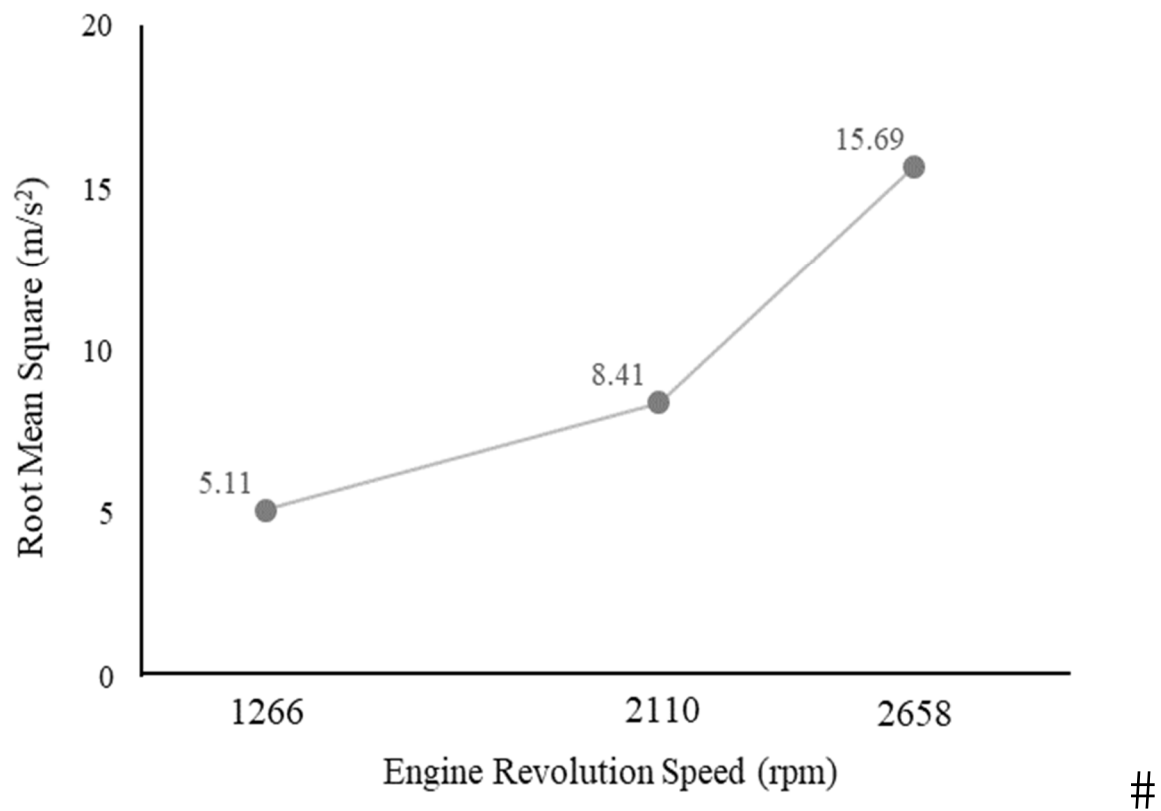
Fig. 23 RMS of hand–arm vibration exposure

#

A comparison with the health guidelines in Fig. 24 shows that the RMS acceleration exceeded the healthy limits at all engine speeds. Therefore, a vibration absorber should be introduced to reduce vibration. Otherwise, the operator should not be allowed to guide the tractor by holding the handles because of the health risk.
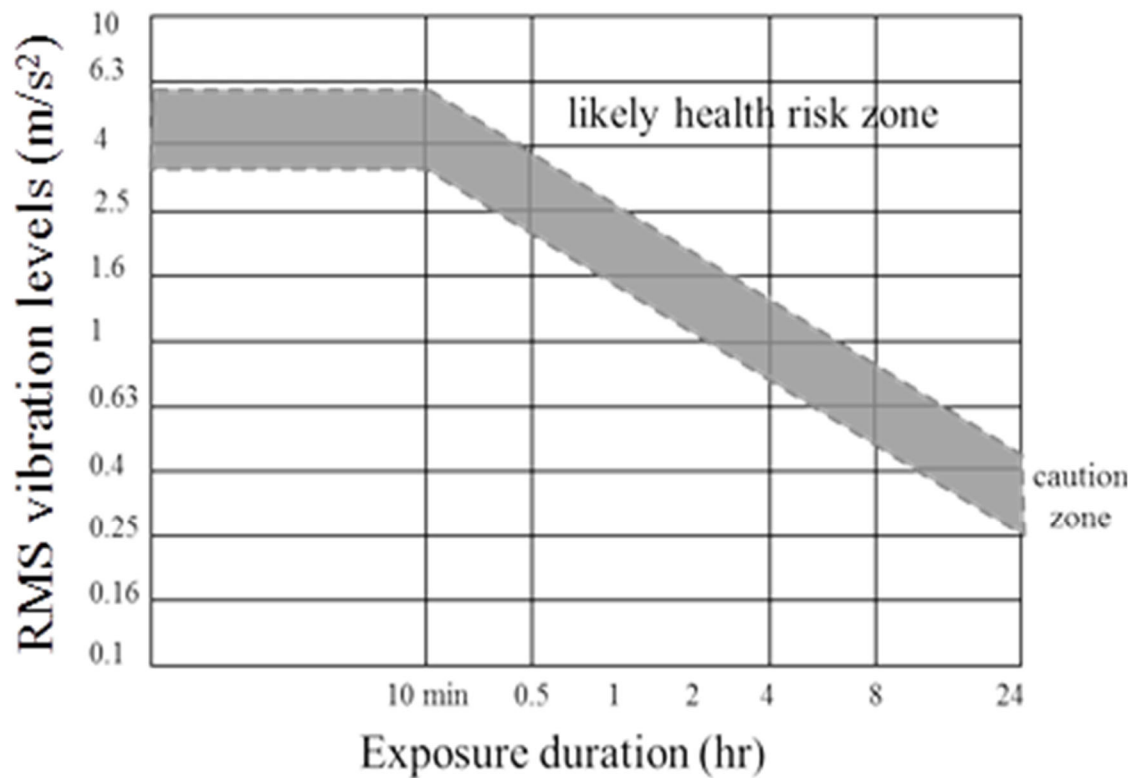

Fig. 24 Health guidelines (Sayed M.E. et al., 2012)

3.4 Discussion

The experimental results showed that the vibration of the engine top was transmitted to all the measurement points of the hand tractor. The measurements were analyzed by visualizing the RMS acceleration. Previous research likewise found that the piston displacement of an engine was the main source of vibration (Mehta et al., 2000; Taghizadeh et al., 2007; Marjanen, 2010; Heidary et al., 2013). It was reasonable for the vibration to be the greatest along the lateral axis followed by the longitudinal and vertical axes considering the fact that the structural frame of the hand tractor was equipped with a horizontal water-cooled fan. This horizontally acting fan partly contributed to the lateral vibration. Furthermore, with this new design, the system tended to oscillate and exhibit a typical pitching movement (Gialamas et al., 2016). At the same measurement point, the vibration along the longitudinal axis was the greatest after the vibration along the lateral axis, revealing that the excitation of the power stroke induced the vibration of the rotating engine in the same direction (Mehta et al., 2000; Taghizadeh et al., 2007; Ykä, 2010; Heidary et al., 2013). Meanwhile, the vibration at the handgrip of the hand tractor was the largest along the vertical axis, followed by the lateral and longitudinal axes, because the handle acted as a cantilever beam. The same trend has been confirmed in other studies (Francis et al., 1978; Salokhe et al., 1995; Heidary et al., 2013).

3.5 Conclusions

The vibration magnitude of a new type of hand tractor was found to be the greatest at the engine top along the lateral axis, followed by that at the handgrip along the vertical axis. There was severe hand–arm vibration exposure for the operator. Therefore, anti-vibration measures should be introduced. Many researchers have successfully applied vibration absorbers (Yibin et al., 1998; Charturvedi et al., 2012; Chavan et al., 2013).

CHAPTER 4 DETECTION OF TARGET REFERENCE POINTS OF A HAND TRACTOR BASED ON TRANSFER PATH ANALYSIS TECHNIQUE

4.1 Background

The adoption of hand tractors as substitutes for human workers and draft animals has become an extremely significant matter for field operations in Cambodia. The hand tractor not only facilitates the timely completion of operations but also increases production, labor savings, energy efficiency, productivity, and profitability (Singh et al., 2011). In addition, the hand tractor is suited to the sizes and scattered locations of farms, can be used in dry and wet conditions, has low cost, and multiple uses (FAO, 2013; Chan, 2013).

Numerous applications of hand tractors have resulted in workers holding handles for longer, resulting in early fatigue caused by vibrational discomfort. Tiwari et al. (2006) explained that machine vibrations are detrimental to agricultural workers. Many studies have confirmed the adverse health effects of vibration. For example, early fatigue may cause physical, physiological, and musculoskeletal disorders over months and years (Salokhe et al., 1995; Sam et al., 2006; Dewangan et al., 2009).

Vibration signals are produced in a complex form; therefore, to achieve a comfortable condition, it is essential to reduce the interior vibration at the handle of the hand tractor. During this process, sensors should be installed at desirable reference locations to obtain vibrational behaviors at the response point of the hand tractor to minimize the number of vibration sensor allocation uses (YOSHIDA et al., 2013).

To visualize the contribution of a range of different factors to vibration levels and effectively measure the interior vibrations of the hand tractor, an ideal method to

determine the effective locations for vibration reduction, the TPA technique, was developed. The transmitted vibration from an engine overlap in a complex manner with various noises or vibrations; therefore, the TPA technique has proved to be an effective method (Noumura, 2011).

TPA can also be applied to characterize the sensitivity effect caused by noise and the strong relationship between the input signals of a control system and output signals; thus, in addition to performing contribution separation, it has been used to set the reference signal targets and suggest countermeasure guidelines (Cowell, 1969; Erdal et al., 2013). To implement the TPA, in this experiment, power spectral density (PSD), which were obtained from a calculation of time-series signals using the fast Fourier transform (FFT) technique at reference points and response points, were applied. This TPA method is a useful analytical tool for determining the main contributions to vibration in hand tractors and for developing effective countermeasures to maintain vibrations below the target levels. Therefore, in the present study, "reference points to the response point through vibration transmission using transfer path analysis" were studied to determine the best reference point location where it represents the vibration characteristics at the handgrip using transfer path analysis method (TPA). This reference point can be used as a source of vibration reduction instead of handgrip.

4.2 General condition

Hand tractor is an agricultural machine which is fitted with a small diesel engine. This machine is capable of capable with small and medium farm size. Hand tractor has been remarkably increased, therefore, their characteristics should be critically understood and analyzed.

Hand tractor, using a single cylinder diesel engine, does not have a good balance

component. The forces acting on the piston during compression and power strokes transmitted to the crankshaft and engine block. The processing induced by acting forces to support frame cause the engine to vibrate, thus the primary source of vibration at the stationary mode. There are many reasons, in the engine combustion, that may lead engine vibrate such as cetane number, flash point, viscosity, lubrication properties, chemical, and molecular structure of all fuel blends.

Due to the lack of vibration dampers intervention between the engine and hand tractor chassis, the engine forces entering to the hand tractor chassis as shocks and then through the chassis transmitted to the whole part of hand tractors.

The handle of hand tractors acts like a cantilever beam so that the relative transmission vibrates freely at one end, and another end vibrates corresponding to the chassis of hand tractors because this part is harnessed with hand tractor. Long time running with unbalanced condition, the engine parts will be fatigued. Operators of the walking type hand tractors are also exposed to levels of vibration because these machines are guided entirely by the operators' hand. Long time working with such condition might cause damage to various organs of the body including bearing loss, spine and gastrointestinal disorders and even neurological disorders.

Reducing vibration interior level provides essential solution to achieving vibration conform. In a dynamic case, vibration may influence from different sources such as road condition and wheel, and it is difficult to apply a model applied in the stationery condition directly into a dynamic case. The transfer path analysis (TPA) is a suitable technique applied on the dynamic case to determine different contributions from the sources of vibration to the response point, and it effectively measures the vibration.

4.2.1   Experimental setup

In this experiment, A diesel hand tractor was used for the experiment under dynamic conditions on an asphalt road, as shown in Fig. 25. The specifications of the hand tractor are listed in Table 7. Typically, a hand tractor is designed to be equipped without an engine speed gauge; therefore, throttle measurement has been introduced to measure the engine throttle instead of the engine speed. Five engine throttles were picked up at 650, 880, 1050, 1200, and 1300 revolution per minute (rpm), where 650 rpm was the lowest engine throttle, and 1300 rpm was the highest engine throttle using a laser tachometer.

Fig. 25 Experimental hand tractor and sensor allocations

Table 7 Specifications of the experimental hand tractor

Specification	
Length (mm)	2210
Width (at handles) (mm)	720
Height (mm)	1250
Weight (kg)	288
Cooling system	Horizontal water-cooled fan
Output (kW)	7.5
Rated speed (rpm)	2500
Implement width (mm)	600
Implement diameter (mm)	400

4.2.2 Sensor arrangement

Seven wireless sensors were firmly taped at different points on the hand tractor: the engine-right-side front (EF), engine-right-side rear (ER), engine-cover top (ET), chassis (CH), gearbox (GB), middle between handle base and handgrip (MH), and handgrip (HG), as shown in Fig. 25. Figure 26 presents a sensor feature, and the specifications of the sensor are shown in table 8. The performances of the sensors were recorded in 9 degrees of freedom such as 3 degrees of freedom of translational acceleration data, 3 rotational angular velocity data and 3 degrees of freedom of quaternion data at a sampling rate of 200 Hz. The data are instantly stored in memory and backed up on the computer through wireless communication using a DSP analog voltage data logger.
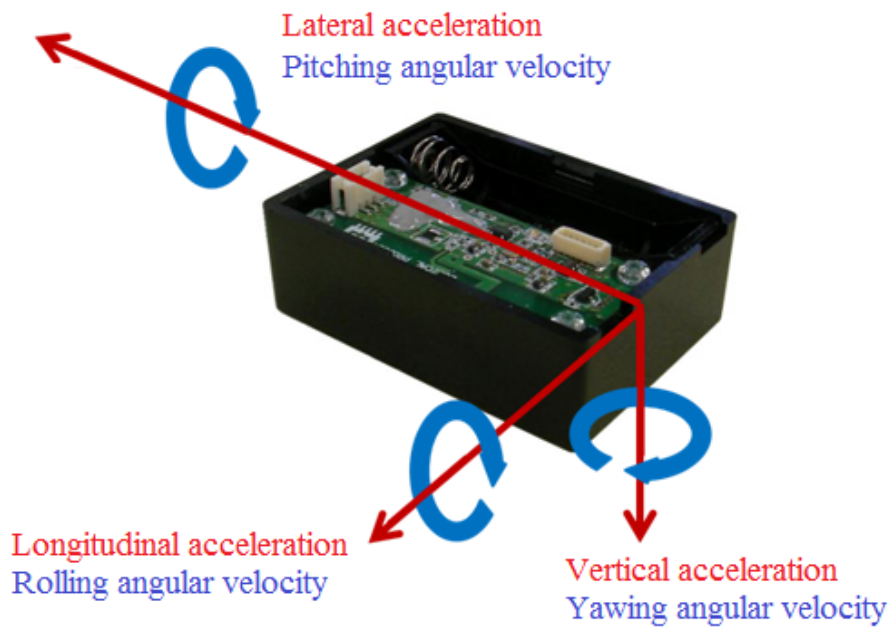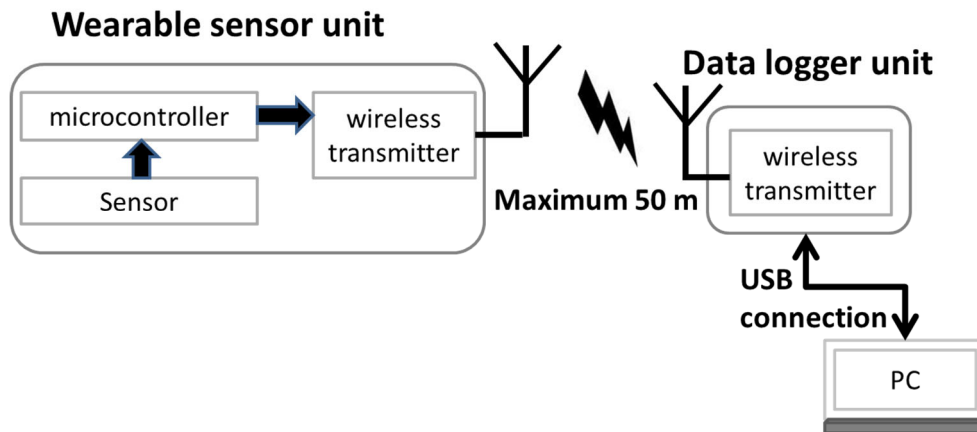
Wearable sensor unit

microcontroller → wireless transmitter

Sensor → microcontroller

Maximum 50 m

Data logger unit

wireless transmitter

USB connection

PC

Lateral acceleration
Pitching angular velocity

Longitudinal acceleration
Rolling angular velocity

Vertical acceleration
Yawing angular velocity

Fig. 26 SS-MS-SMA200G60 detection features and its operation

Table 8 Specification of DSP analog voltage data logger

Specification	
Name of sensor	SS-MS-HMA5G3
Translational acceleration range	±5G
Angular velocity range	±300dps
Sampling rate	1H~1000Hz (9 degrees of freedom)
Resolution	16bit

4.3 Feature extraction and analysis methods

4.3.1 Feature acquisition techniques

The instant data in the memory of the sensors were backed up on a computer, manipulated, and analyzed using the open-source programming language, Python 3.7.4, under the Anaconda 4.12.0, Jupyter Notebook 6.0.3. It provides powerful tools and handy libraries such as numpy 1.18.1, pandas 1.0.2, matplotlib.pyplot 3.1.3, matplotlib.ticker 3.1.3, scipy.linalg (svd) 0.16.2 and sklearn.preprocessing 0.16.2 to intensively and manually code the amplitude, FFT, PSD, dominant frequency, singular value decomposition (SVD), TPA technique, inverse time series from FFT, root-mean square (RMS), and root-mean-square error (RMSE). The data analysis process is illustrated in Fig. 27.
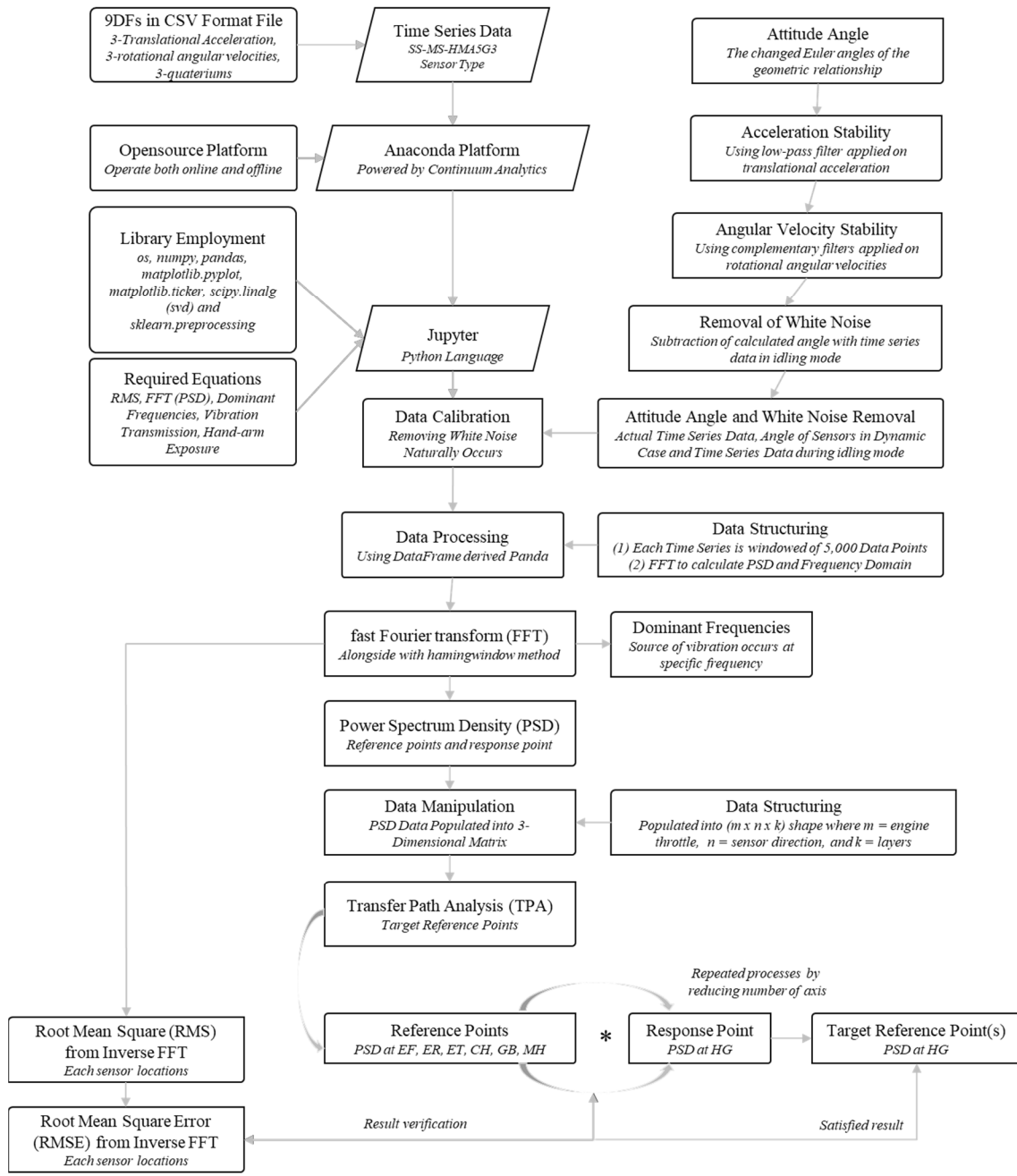
Fig. 27 Block-diagram for feature extraction and analysis

4.3.2 Feature extraction for TPA technique

In principle, few steps are followed for data or feature extraction. First, because the angle of each sensor frequently changes in a dynamic case, the actual angles of the acceleration in three dimensions were calculated based on the changed Euler angle of the geometric relationship, as mentioned in equations (19) – (21) (Zhou, et al., 2017). The angle generated from each sensor is susceptible to frequent changes during transportation. Hence, a low-pass filter was added to reduce high fluctuations, as presented in the following equations (22) – (24) to stabilize the acceleration angle. Next, the attitude angle was calculated using complementary filters as expressed in the following equations (25) – (27) to stabilize the rotational angular velocities. Finally, the angle in the radian was converted to degree using equations (28) – (30). Sensors are highly sensitive and require calibration. Thus, this calibration was calculated by subtracting the individual amplitude during operation from the mean amplitude during engine idling, as shown in equation (31). Finally, the power spectrum densities were plotted against the frequency of the signal and dominant frequency of vibration using an existing library in Python. These power spectrum densities were then used for TPA analysis.

$$A_{\theta_{P,i}} = \arctan \sqrt{\frac{A_x}{A_y^2 + A_z^2}} \tag{19}$$

$$A_{\theta_{R,i}} = \arctan \sqrt{\frac{A_y}{A_x^2 + A_z^2}} \tag{20}$$

$$A_{\theta_{Y,i}} = \arctan \sqrt{\frac{A_x^2 + A_y^2}{A_z}} \qquad (21)$$

Where A_{θ_P}, A_{θ_R}, and A_{θ_Y} are the output angles of acceleration, respectively, in the longitudinal axis (A_x), lateral axis (A_y), and vertical axis (A_z) directions.

The angle generated from each sensor is susceptible to frequent changes during transportation. Hence, a low-pass filter was also used to reduce high fluctuations, as presented in the following equations:

$$A_{\theta_{P,i}} = w_1 * \left(A_{\theta_{P,i-1}} + A_{x,i} * \Delta t\right) + w_2 * A_{\theta_{P,i}} \qquad (22)$$

$$A_{\theta_{R,i}} = w_1 * \left(A_{\theta_{R,i-1}} + A_{y,i} * \Delta t\right) + w_2 * A_{\theta_{R,i}} \qquad (23)$$

$$A_{\theta_{Y,i}} = w_1 * \left(A_{\theta_{Y,i-1}} + A_{z,i} * \Delta t\right) + w_2 * A_{\theta_{Y,i}} \qquad (24)$$

$$\theta_{P,i} = w_g * \left(\theta_{P,i-1} + G_{x,i} * \Delta t\right) + w_a * A_{\theta_{P,i}} \qquad (25)$$

$$\theta_{R,i} = w_g * \left(\theta_{R,i-1} + G_{y,i} * \Delta t\right) + w_a * A_{\theta_{R,i}} \qquad (26)$$

$$\theta_{Y,i} = w_g * \left(\theta_{Y,i-1} + G_{z,i} * \Delta t\right) + w_a * A_{\theta_{Y,i}} \qquad (27)$$

Where:

- w_1 and w_g is a weight value of 0.95,

- w_2 and w_a is a weight value of 0.05,

- i is the individual amplitude,

- Δt is the time interval,

- $\theta_{P,i}$, $\theta_{R,i}$, and $\theta_{Y,i}$ are the output angles of pitch, roll, and yaw, respectively, in the pitch axis (G_x), roll axis (G_y), and yaw axis (G_z).

The time-series data formats in radians were converted into degrees by default. Then, the actual values of the rotational angular velocity were obtained by multiplying the degree $\left(\theta_{P,i}, \theta_{R,i}, \theta_{Y,i}\right)$ by the individual amplitude, as expressed in equations (28) – (30) below:

$$G_{P,i_{angle}} = \cos\left(\theta_{P,i} * \frac{pi}{180}\right) \tag{28}$$

$$G_{R,i_{angle}} = \cos\left(\theta_{R,i} * \frac{pi}{180}\right) \tag{29}$$

$$G_{Y,i_{angle}} = \cos\left(\theta_{Y,i} * \frac{pi}{180}\right) \tag{30}$$

$$G_{actual} = G_{angle} - G_{idling_{mean}} \tag{31}$$

4.3.3   Transfer path analysis (TPA)

The TPA principal theorem involves a relationship between the input/reference point signals and the output/response point signal of a block control system. It is generally applied in dynamic cases, whereas in this experiment, a hand tractor moving on an asphalt road was observed. In a dynamic hand tractor, a location at the handgrip was considered as a response point, whereas locations at EF, ER, ET, CH, GB, and MH were regarded as reference points. YOSHIDA et al. (2018) stated that, for a large structure of mechanical analysis, a large number of reference points and response points are required to be introduced; otherwise, unreliable results would be produced.

Individual elements (PSD) from all the positions obtained from the above calculations were selected for transfer path analysis, as presented in Fig. 28.
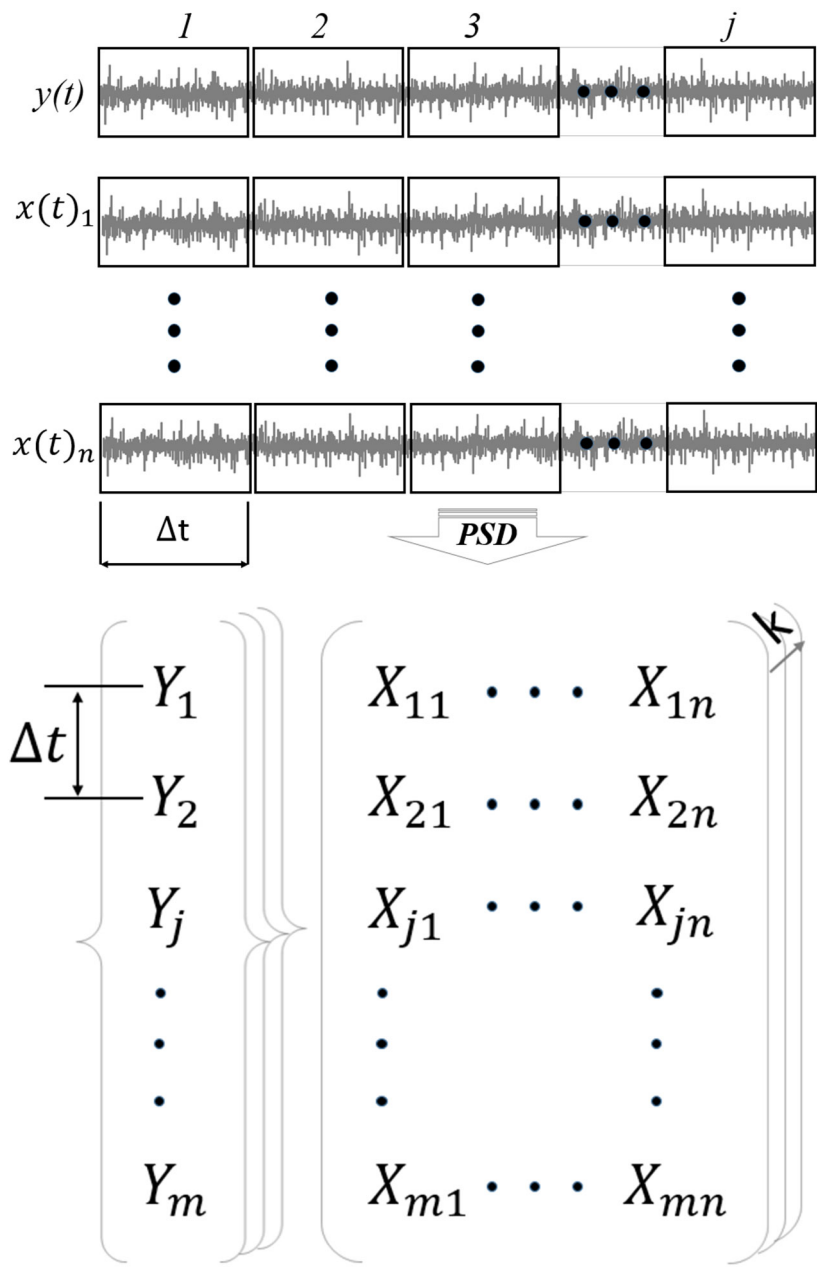
Fig. 28 Data population structure into a three-dimensional tensor flow matrix

Structurally, the PSDs were populated into a 3-dimensional matrix $m \times n \times k$, where m is the individual PSD of the engine throttle, n is the individual axis of all reference points, k is the layer of k_{PSD} based on the frequency domain, and Y is the individual axis of the response point (YOSHIDA et al., 2013).

In other words, the relationship between vector reference point signals $x(t)$ and vector response point signal $y(t)$ was calculated typically using a principal component regression method measured in equation (32); therefore, it was simply rewritten as a convolution theorem based on the frequency domain, as in equation (33). $Y(t)$ and $X(f)_i$ are known as elements (PSDs) obtained from the FFT calculation for the response point and reference points, respectively, whereas the unknown parameter $H(f)$ is a transfer function that was measured and analyzed using singular value decomposition (SVD), as presented in equations (34) – (43) (Noumura, K., 2011). Then, the transfer function was obtained by the product of the covariance and principal component, which was retrieved from the SVD calculation, as shown in Fig. 29. The importance of TPA as the principal component was to reduce interior noise and unrelated vibration. Finally, the summation of each variance calculated by a polynomial equation is a product of the response point.

The reference point was obtained by repeating the above procedure until the response level satisfied the target at each frequency (Noumura, K., 2011). The restructured analysis satisfied the target point based on individual observations. However, in this experiment, a combination of two locations was conducted to obtain the best contribution to the response point. Hence, the best single location derived from this highest combination using root mean square error was concluded.
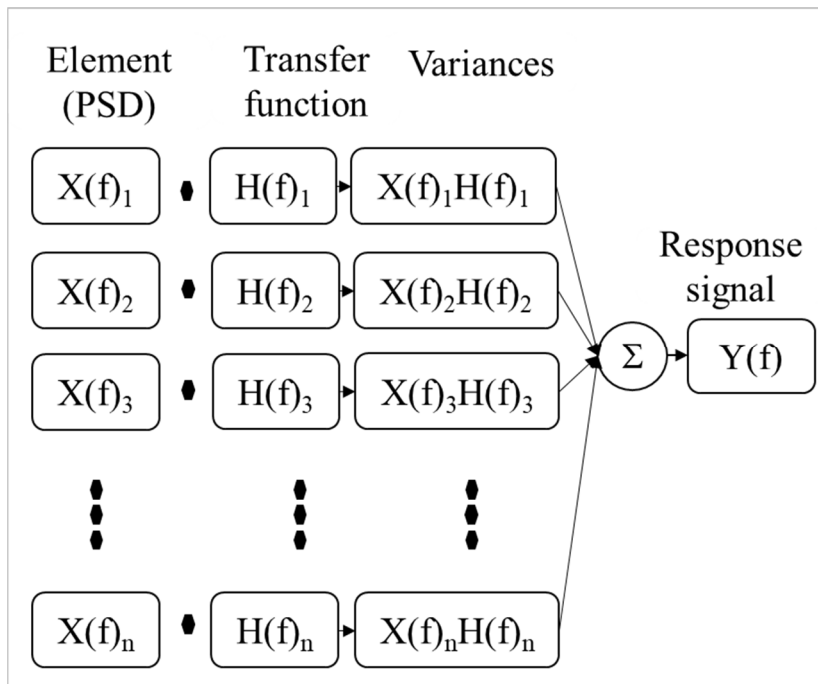
Fig. 29 Diagram of operation of transfer path analysis

$$y(t) = \sum_{i=1}^{n} x(t)_i * h(t)_i \tag{32}$$

$$Y(f) = \sum_{i=1}^{n} X(f)_i \cdot H(f)_i \tag{33}$$

$$\begin{cases} Y(f)_1 = X(f)_{11} H(f)_1 \dots + X(f)_{1n} H(f)_n \\ \quad . \\ \quad . \\ Y(f)_m = X(f)_{m1} H(f)_1 \dots + X(f)_{mn} H(f)_n \end{cases} \tag{34}$$

$$Y(f) = X(f) * H(f) \tag{35}$$

$$H(f) = [X(f)]^{-1} * Y(f) \tag{36}$$

$$X(f) = U(f) * S(f) * [V(f)]^{-1} \tag{36}$$

$$T(f) = U(f) * S(f) = X(f) * V(f) \tag{38}$$

$$Y(f) = T(f) * C(f) \tag{39}$$

$$C(f) = ([T(f)]^{-1}[T(f)])^{-1} * [T(f)]^{-1} * Y(f) \tag{40}$$

$$Y(f) = X(f) * V(f) * C(f) \tag{41}$$

$$H(f) = V(f) * C(f) \tag{42}$$

$$H(f) = V(f) * [S(f)]^{-1} * [U(f)]^{-1} * Y(f) \tag{43}$$

4.3.4 Root mean square (RMS) and root mean square error (RMSE)

In principle of TPA, the target reference points have been defined, especially from the sources of vibration. However, in research intends to identify the best reference points or highest contribution, inverse time series from the fast Fourier transform (IFFT) has been applied to measure the RMS and RMSE. The best results can be considered to reduce the number of sensors installed on the hand tractor. The equation of IFFT can be defined as in the following (43) – (44). The Inverse FFT is computed by conjugating the phase factors of the corresponding forward FFT, and the result of IFFT outputs as real values and imaginary values. In this research, the real values were used to obtain the inverse FFT.

$$Forward\ FFT \to X(m) = \sum_{n=0}^{N-1} x(n) * e^{-j2\pi nm/N} \qquad (43)$$

$$Inverse\ FFT \to x(n) = \frac{1}{N} \sum_{m=0}^{N-1} X(m) * e^{j2\pi mn/N}$$

$$= \frac{1}{N} \sum_{m=0}^{N-1} [X_{real}(m) + jX_{imag}(m)] e^{j2\pi mn/N} \#$$

$$= \frac{1}{N} \sum_{m=0}^{N-1} X_{real}(m) * e^{j2\pi mn/N} \qquad (44)$$

Where:

- N is the transform length, m is used to denote the frequency domain ordinal, and n is used to represent the time-domain ordinal

- x(n) = G_{actual} is the time-series data calculated as the actual values of the rotational angular velocity

4.4 Results and discussions

Reducing the vibration magnitude of a hand tractor is essential for achieving comfortable conditions. During a hand tractor operation, the vibration at the handgrip, which is inevitably held and driven by the operator, should be minimized to an optimum level. However, for a large structural component such as a hand tractor, the vibration elimination process should consider the whole body rather than just the handgrip (Siemens, 2014). The best selected locations with a high contribution to the handgrip can also be achieved satisfactorily.

The TPA technique was used to determine the best and highest contributions. Time series data, which were generated in a complex form from each sensor, consist of unwanted noise and inaccurate data, as presented in figure 30, which could lead to a calculation limitation to the use of the TPA method. In the mechanical analysis, the TPA, which is calculated in a time series, has more difficulty to localizing the best reference point with a high contribution; hence, the power spectrum densities obtained by the introduction of FFT at the reference points and the response point were selected and populated into the three-dimensional tensor flow matrix for the TPA analysis. The results confirm that TPA is the best application in the frequency domain (Siemens, 2014).
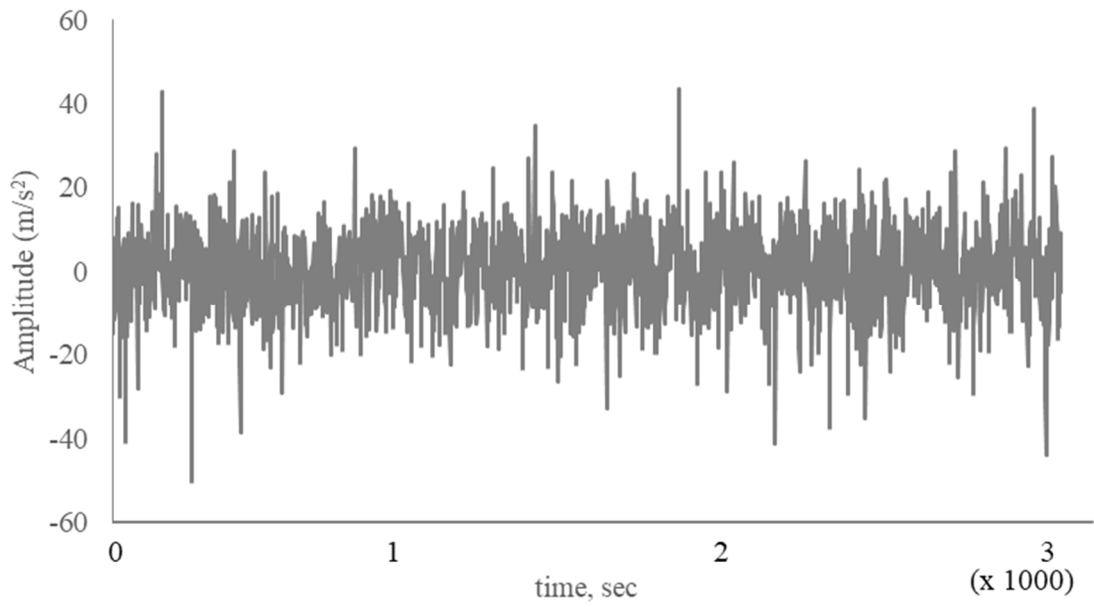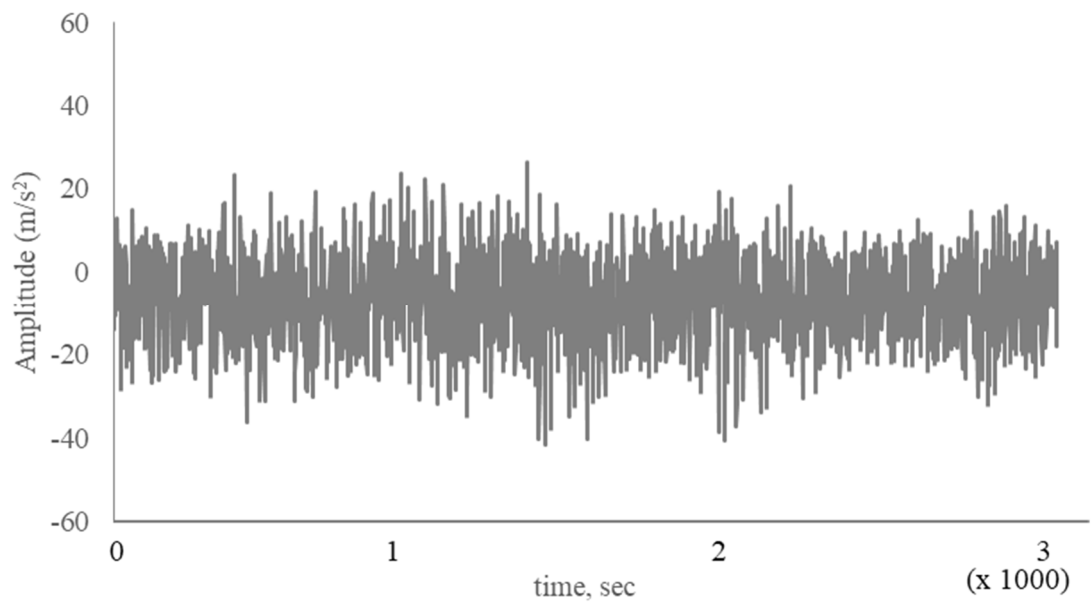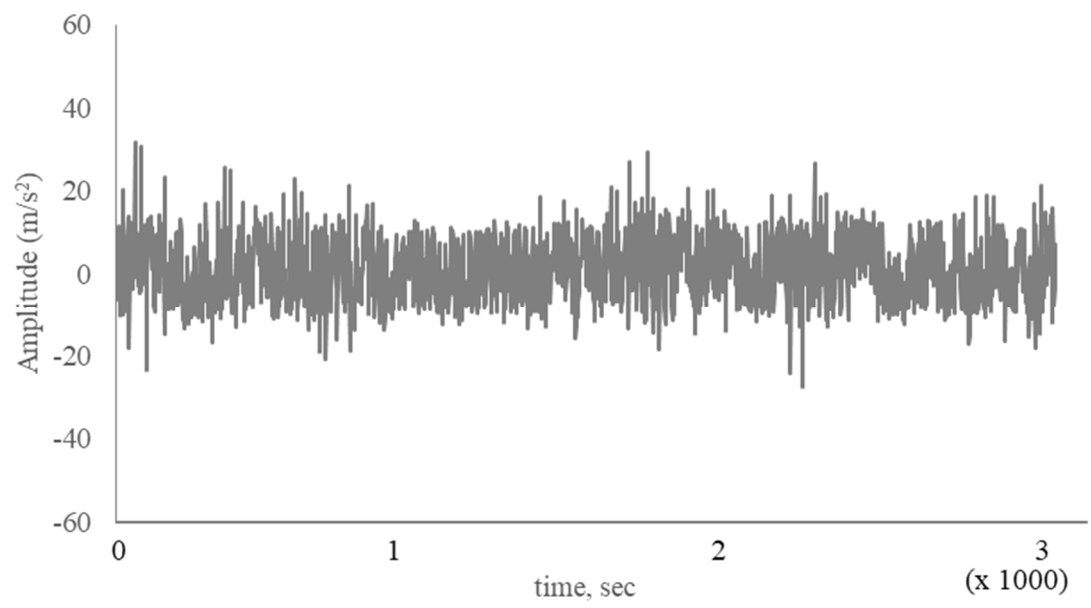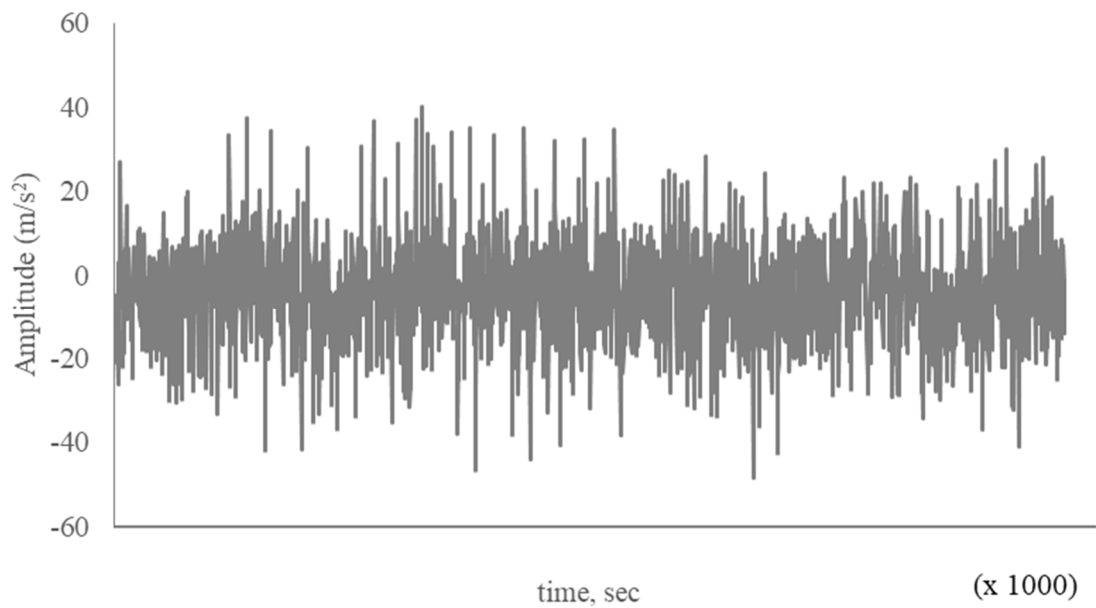
(a)

(b)

(c)

(d)

100
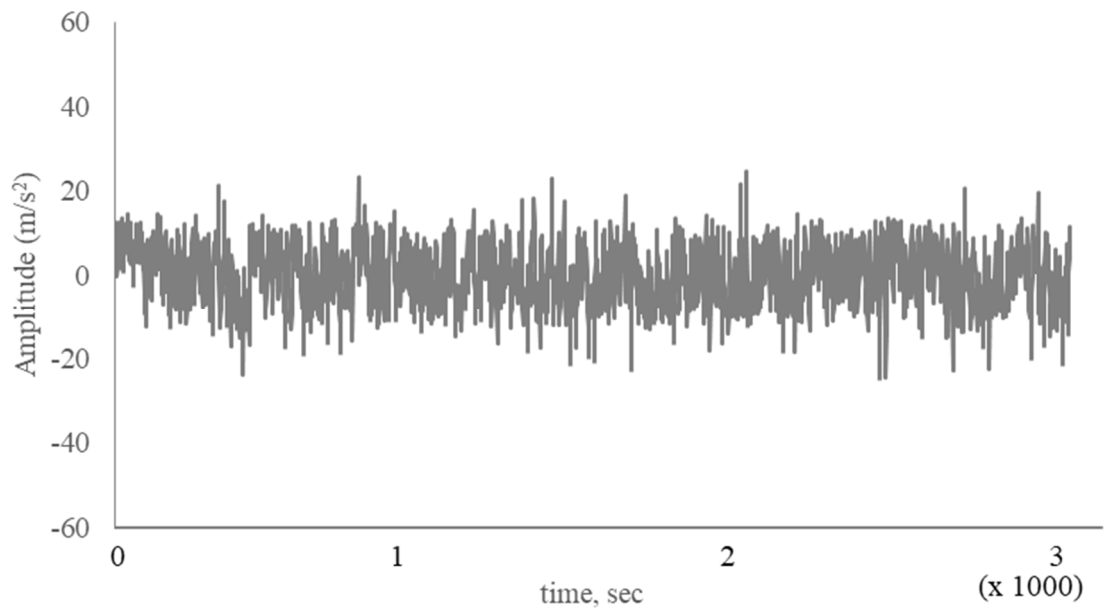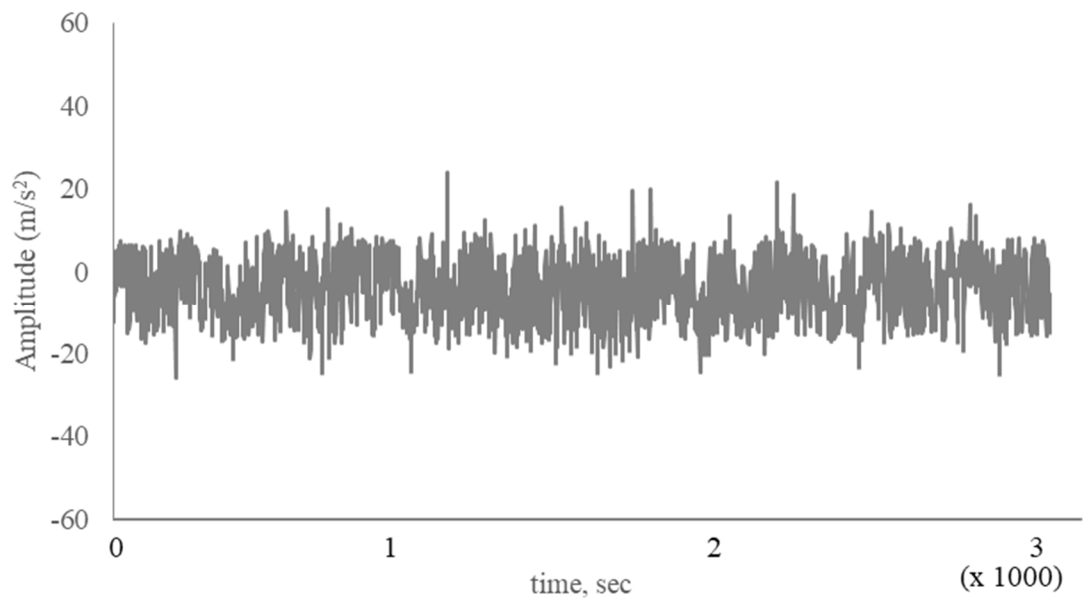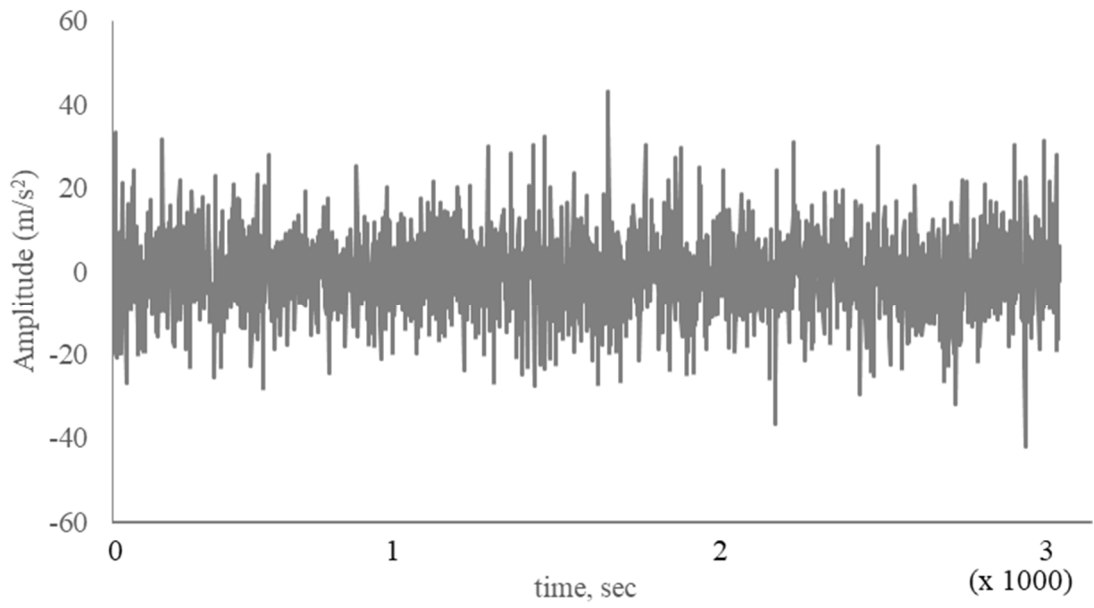
(e)

(f)

(g)

Fig. 30 Time series vibration signal at engine-right-side front (a), Time series vibration signal at engine-right-side rear (b), Time series vibration signal at engine-cover top (c), Time series vibration signal at chassis (d), Time series vibration signal at gearbox (e), Time series vibration signal at middle between handle-base and handgrip (f), Time series vibration signal at handgrip (g)

Analytically, populating the PSD as elements from the reference points and response points into the three-dimensional tensor flow for the TPA calculation, the highest and best contributions at the reference points to the response point were obtained. It can be clearly observed that TPA is a powerful tool for separating noise and actual vibration; thus, it identified the best related contribution and unrelated locations. The application of TPA showed that vibration amplitudes at EF, ER, and ET contributed significantly less to the response point. Figure 31 (a, b, c, d) presents the results of the vibration contribution from the reference points at EF, ER, and ET to the response point at the handgrip. In addition to the longitudinal, lateral, and vertical axes of the reconstructed analyses, the contribution of the results of the three locations to the response point was marginal, and the important peaks also exhibited visibly small amplitudes at predominant frequencies. At the ER, high peaks emerged at 17, 35, and 17 Hz along the longitudinal, lateral, and vertical axes, where the EF appeared at 52, 35, and 35 Hz, and the ET appeared at 20, 60, and 20 Hz, respectively. These were subsequently compared with those of the acceleration response point at the frequencies of 22, 22, and 22 Hz. Therefore, the locations of ER, EF, and ET were not considered as target points.
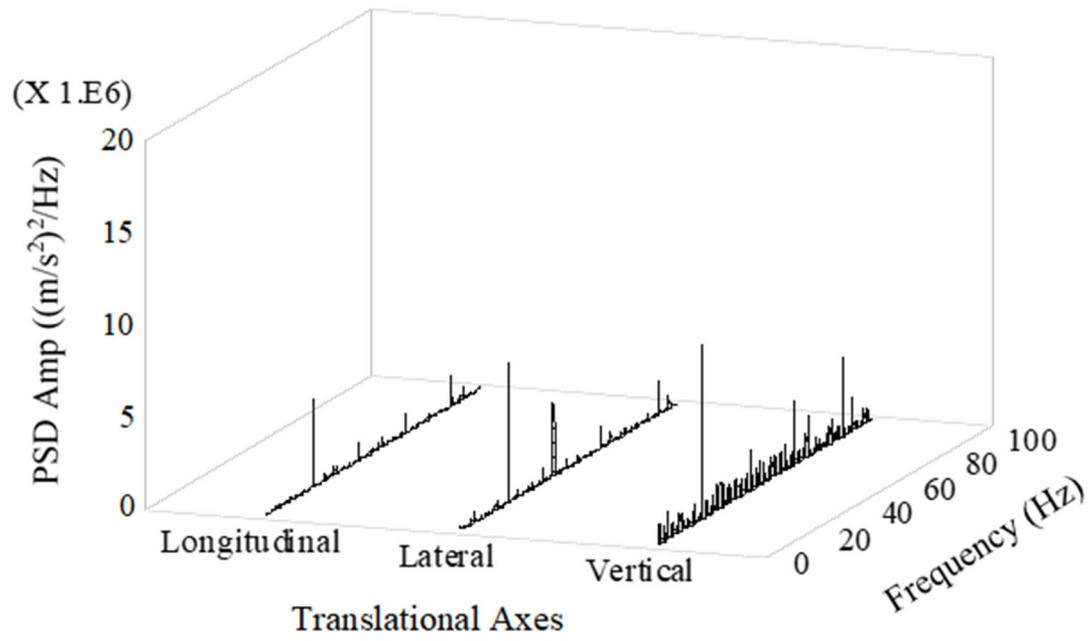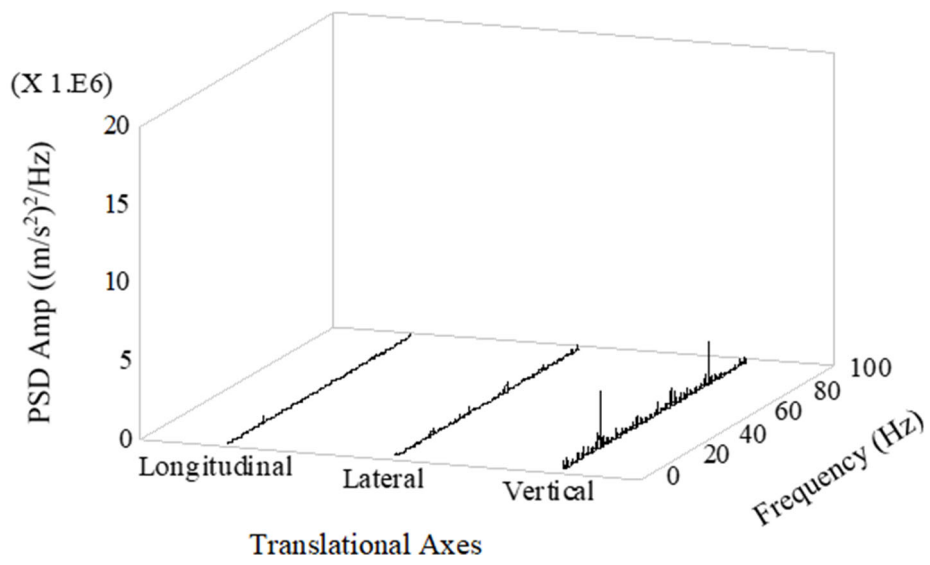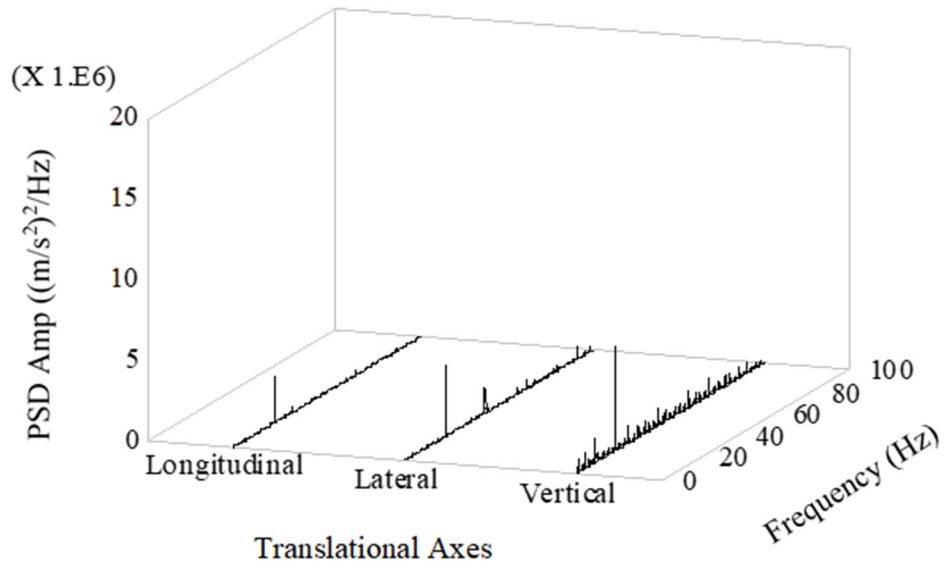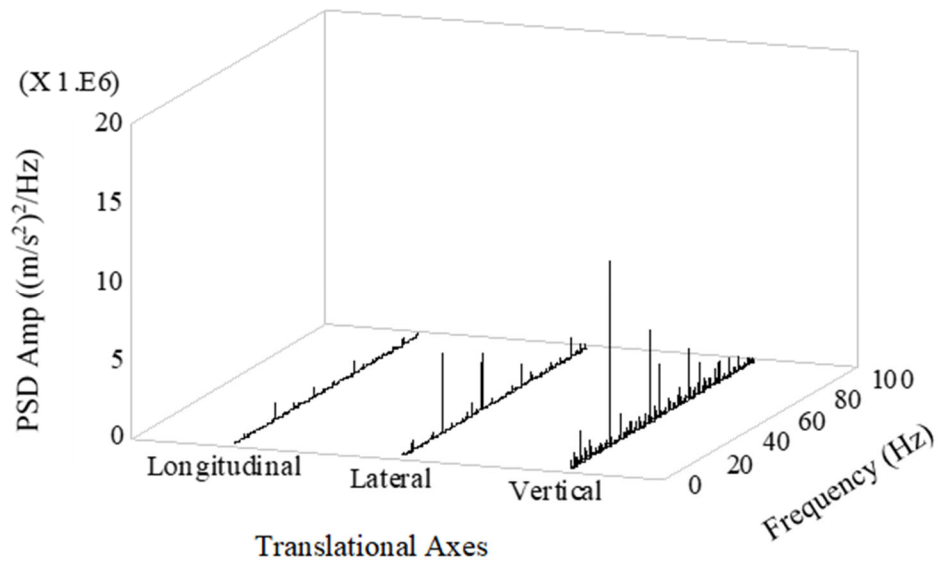
(a)
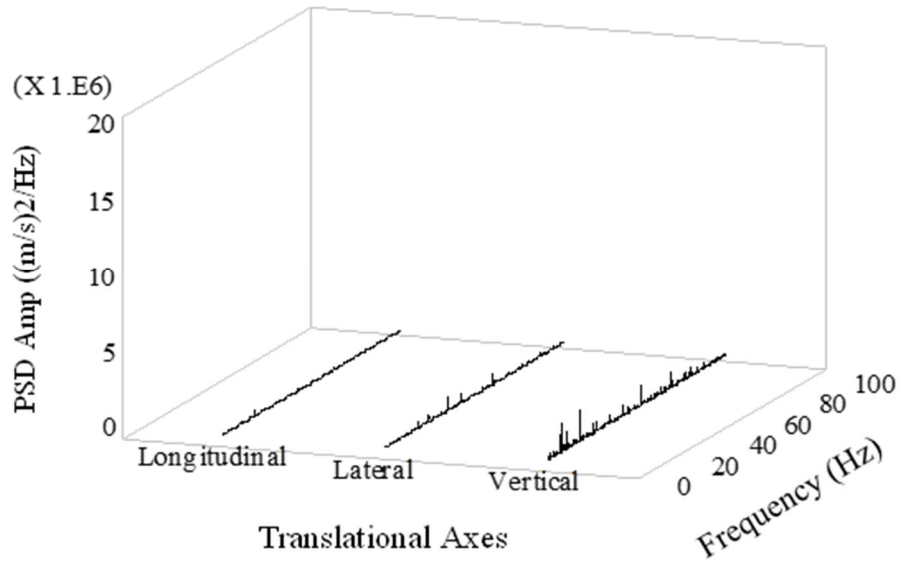
(b)
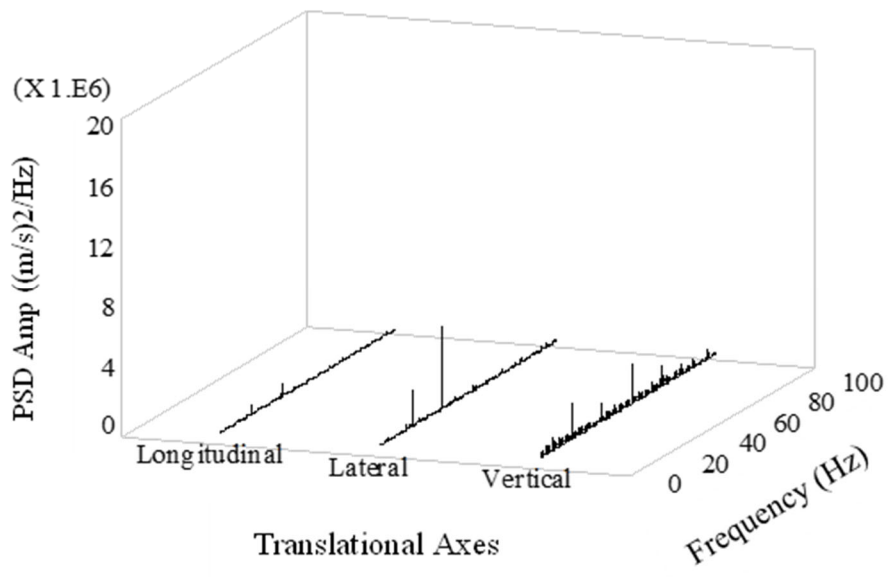
(c)

(d)

(e)

(f)

(g)

Fig. 31 A comparison of vibration behavior at each reference point using an TPA

analytical model to response point at HG: (a) Original acceleration data at response

point (HG), (b) Acceleration reconstruction data at EF, (c) Acceleration reconstruction

data at ER, (d) Acceleration reconstruction data at ET, (e) Acceleration reconstruction

data at CH, (f) Acceleration reconstruction data at GB, (g) Acceleration reconstruction

data at MH.

However, good variance contributions were observed at the CH, GB, and MH. Figure 31 (e, f, g) shows that those variances contributed largely from the reference points at identical predominant frequencies of 22, 22, and 22 Hz at the longitudinal, lateral, and vertical axes to the response point at the highest frequencies of 22, 22, and 22 Hz at the longitudinal, lateral, and vertical axes, respectively. Based on this observation, the locations of the CH, GB, and MH could be set as target points to the response point of the hand tractor. However, as recommended by YOSHIDA et al. (2018), for large structures such as vehicle bodies, a combination of multiple locations should be applied to reduce unwanted noise and inaccurate data and enhance the relationship between the input and output. Hence, a combination of two of the three locations was used exclusively.

A combination of two of the three locations was conducted in pairs. These pairs are CH-GB, GB_MH, and CH-MH, provided that these locations involve high-variance contributions to the response point, as described in the aforementioned section. The calculation process of these combinations involved multiplication of the elements of the combination, including all the individual axes and the transfer function. The response point is the sum of the variances, as shown in Fig. 29.

The results showed that, compared to the variances of the combination of GB-MH, the variances of the combination of CH-GB and CH-MH had higher contributions to the response point, as presented in Fig. 32 (a, b, c, d).
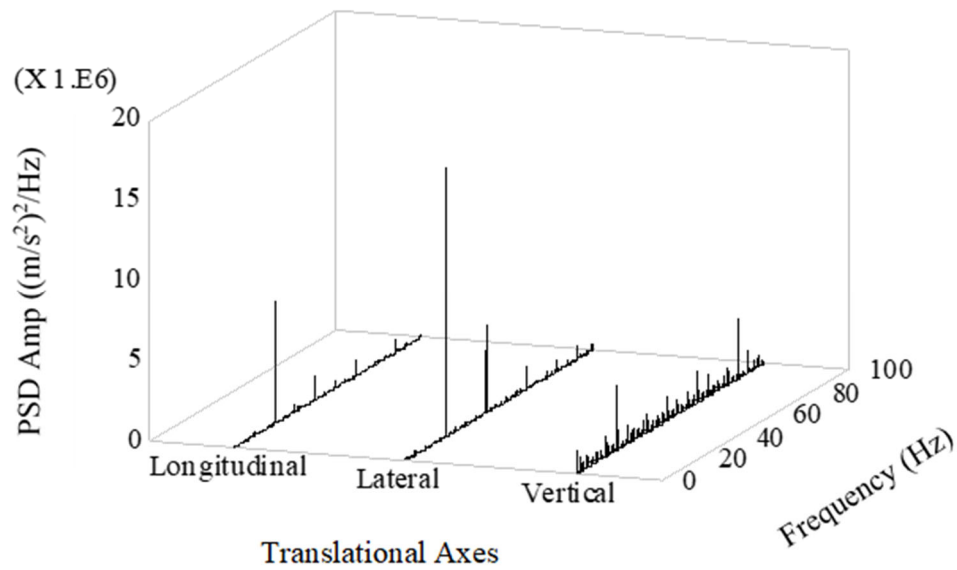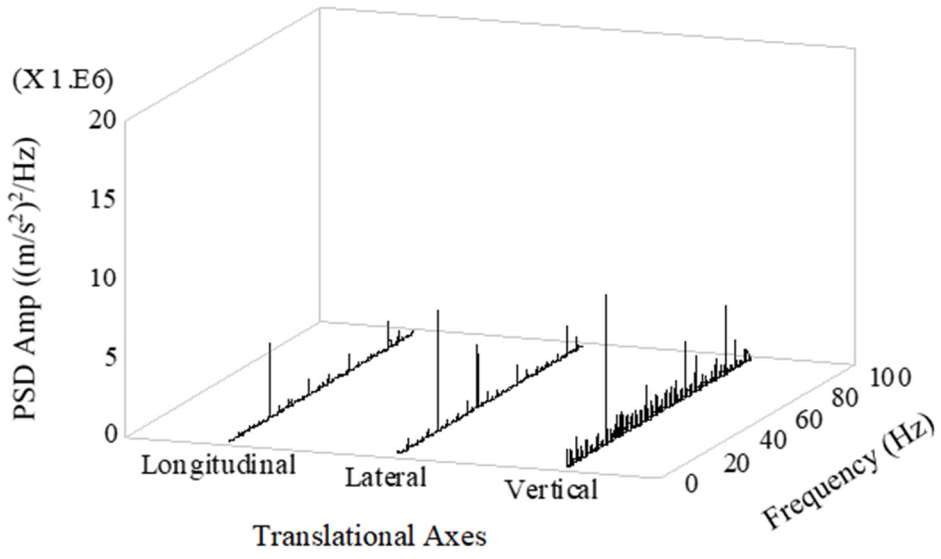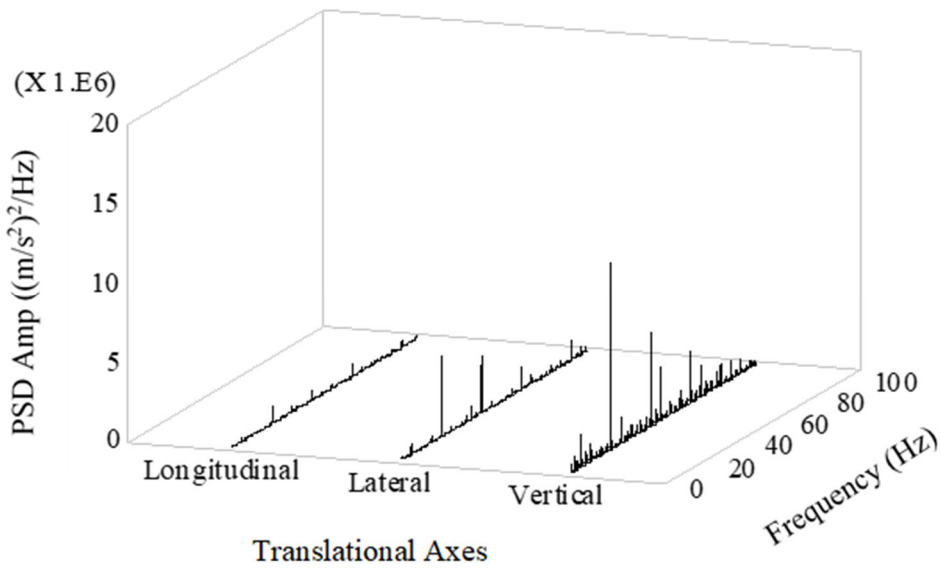
(a)

(b)
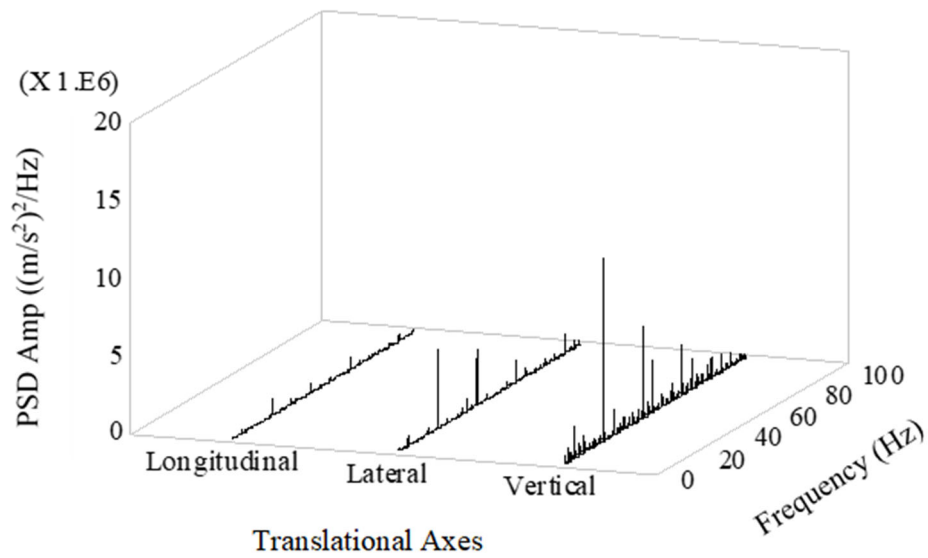
(c)

(d)

Fig. 32 A comparison of vibration behavior at two combination reference points using

an TPA analytical model to response point at HG: (a) Original acceleration data at

response point (HG), (b) Acceleration combination reconstruction points (CH-GB), (c)

Acceleration combination reconstruction points (GB-MH), (d) Acceleration

combination reconstruction points (CH-MH).

The combination of CH-GB, which contributed high variances from the reference to the response point at the predominant frequencies of 22 Hz at all axes, were also found the same tendencies at the combination of CH-MH.
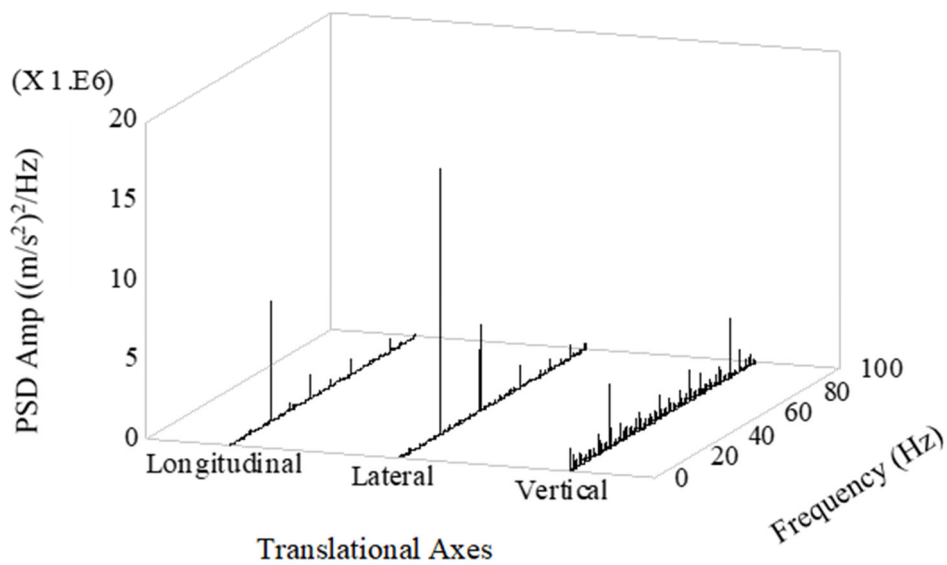
It is definitely understood that the individual variance contributions of these combinations to the response point are large; therefore, these locations could be set as target points for the response point. Nevertheless, it is recommended to consider the best contribution to reduce the number of sensors installed on the hand tractor. and that locations can be used to represent the vibration characteristics at the response point (handgrip). To develop the best reference points with a high contribution to the response point, an inverse time series obtained from an inverse FFT calculation was applied to measure the RMS and RMSE values. The RMS acceleration results are represented in Fig. 33, 34, and 35 for different engine throttles. Good patterns were satisfactorily highlighted alongside various engine throttles at the longitudinal, lateral, and vertical axes between CH-MH, response point signal (response data), and CH-GB.

Considering this, another method, that is, the RMSE method, was applied to confirm the result. As shown in Fig. 36, compared to the combination of CH and MH, the combination of CH and GB presented a very low error at all the engine throttles and axes. Hence, the combination of CH and GB is the highest reference point location to the response point. To determine the improvement part to reduce the vibration of the hand grip, the most affected reference point. Therefore, the two locations, chassis and gearbox have been conducted using RMSE method. Figure 37 showed that the reference point at the gearbox is the best reference point location, where represents the vibration characteristics to the response point, handgrip. Thus, clearly implying that the location at the gearbox is the best target point for the damper.

Fig. 33 RMS Acceleration of chassis – mid-handle, chassis – gearbox and

response point at different engine speed along longitudinal axis

Fig. 34 RMS Acceleration of chassis – mid-handle, chassis – gearbox and

response point at different engine speed along lateral axis
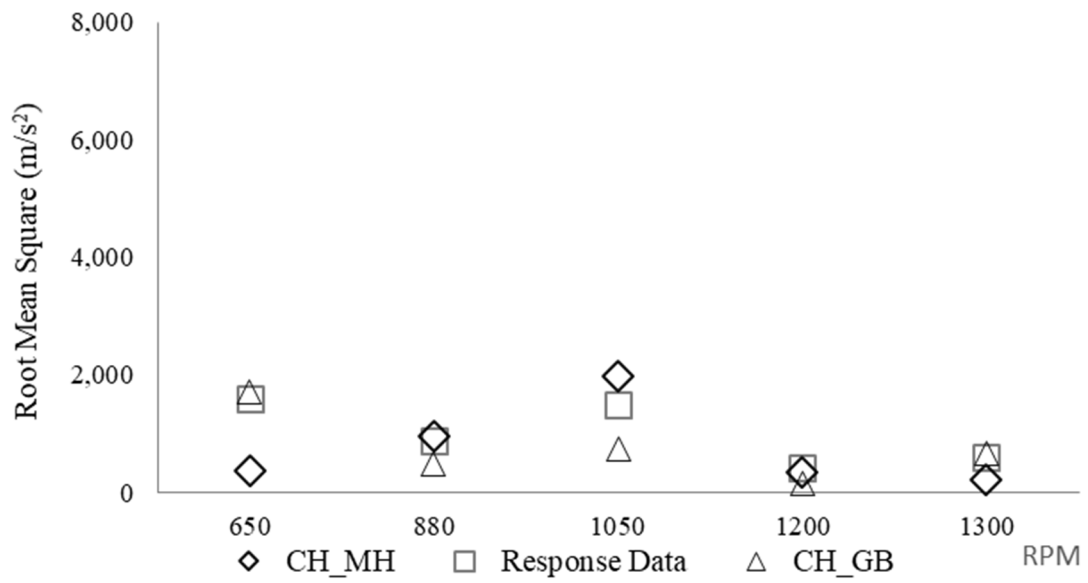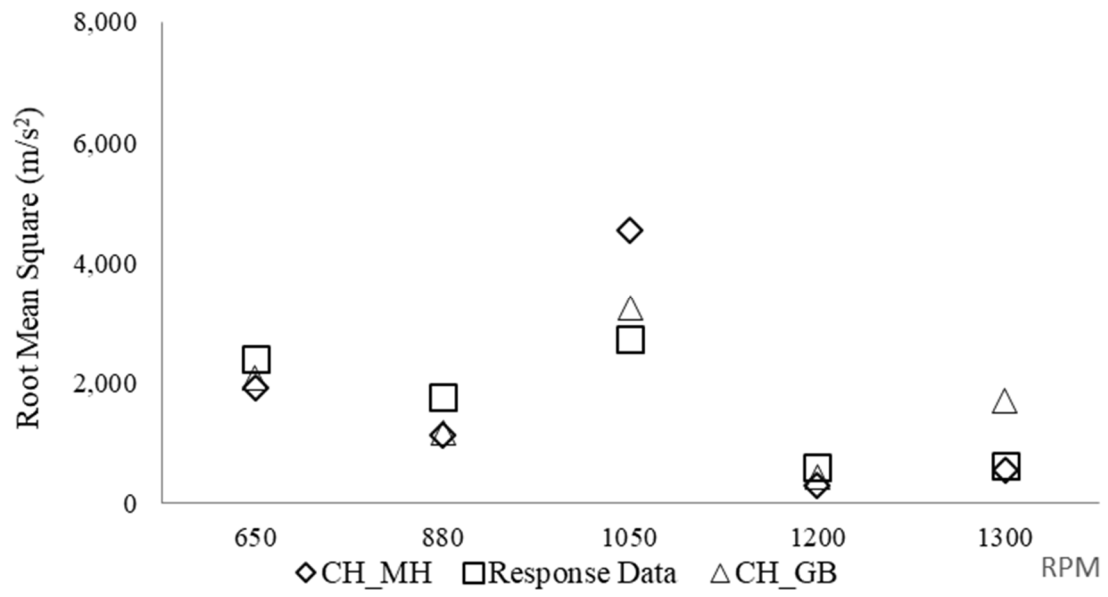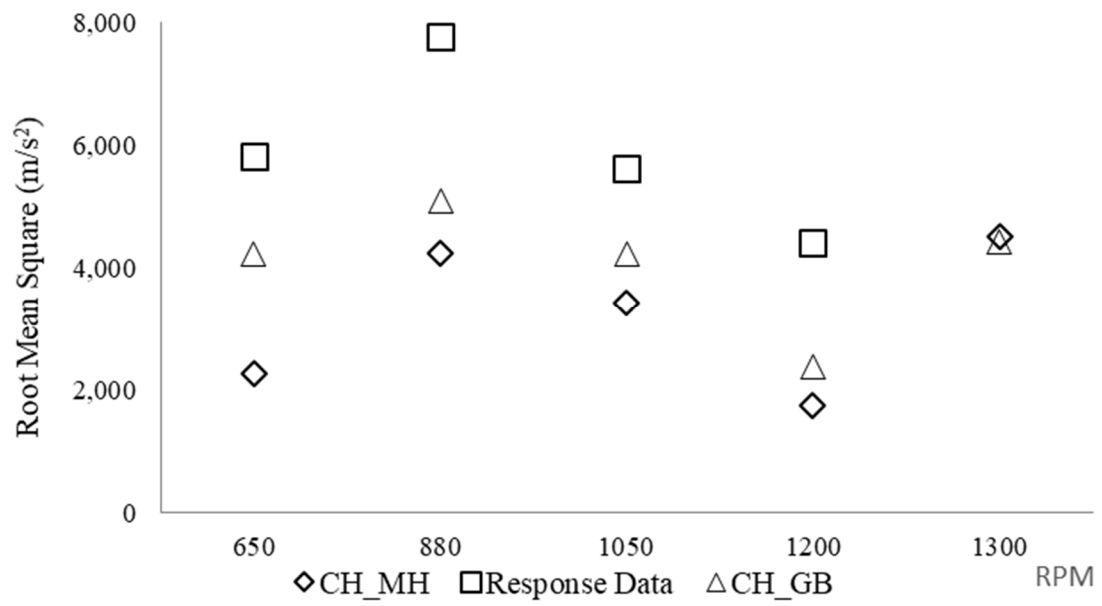
Fig. 35 RMS Acceleration of chassis – mid-handle, chassis – gearbox and

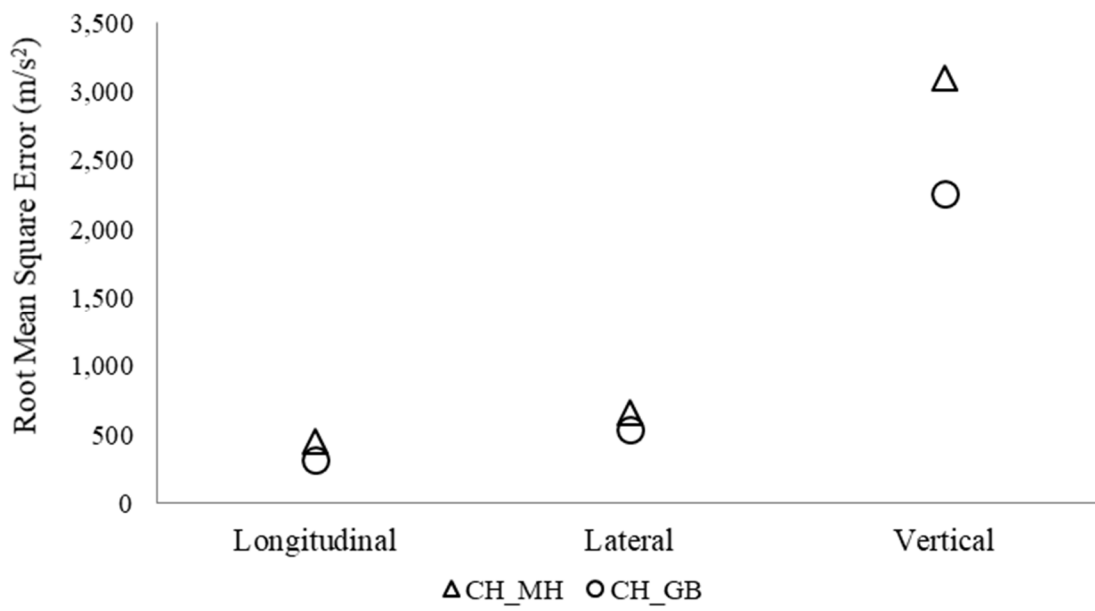response point at different engine speed along vertical axis

Fig. 36 RMSE Acceleration of chassis-mid-handle (CH_MH) and chassis-

gearbox (CH_GB) to the response data

Fig. 37 A comparation of RMSE Acceleration between

chassis and gearbox to the response data

4.5 Discussions

In the experiment, the transfer path analysis technique was used to detect the main contribution of the reference points to the response point of the hand tractor. The power spectrum densities were obtained using the time series data. Siemens (2014) confirmed that transfer path can be applied in the frequency domain. These power spectrum densities were populated into a three-dimensional tensor flow matrix for the TPA analysis. The technical TPA had high contributions at three reference points of the hand tractor: the chesses, gearbox, and mid-handle. YOSHIDA et al. (2013) concluded that TPA performed significantly well in separating the noise and actual vibration, with low and high contributions. Noumura (2011) also mentioned a high contribution from the reconstruction points to the response point when using transfer path analysis. However, the performance was then evaluated using a combination of two of the three locations, with high contributions, to improve the relationship. YOSHIDA et al. (2018) recommended that a combination of multiple reference-point signals should be utilized for a large structure, such as a vehicle body; otherwise, inaccurate data would be presented. The first two combinations of the three, CH–GB, CH – GB, and GB – MH, had a higher contribution to the response point. Thus, to obtain the best main contribution, RMS and RMSE were applied. It was concluded that, that the combination of CH – GB contributed highest variances to the response-point signal, and GB is the best target point for the damper. In a dynamic case, vibration may influence from different sources such as road condition and wheel. Chassis and gearbox where are close to wheel are susceptible to external influences. Structurally, chassis and gearbox materials are stiff and highly rigid body that do not absorb vibration well. In reverse, it highly transmits vibration to other connecting parts.

4.6 Conclusions

In this study, to identify the relationship between the reference points and the response point, seven wireless communication sensors were rigidly taped on different points of the hand tractor, mainly the EF, ER, ET, CH, GB, MH, and HG. The HG was considered as the response point, while the other six locations were regarded as reference points. The TPA technique was used analytically. In the TPA process of this experiment, the power spectrum densities obtained from the calculation of time-series data were manipulated into a three-dimensional tensor flow matrix for the analysis. This also involved embedding singular value decomposition and multiple linear regression analyses. Finally, the relationship between the reference points and the response point was obtained using a polynomial equation in the reduction loop. The calculations were manually programmed using Python.

The results showed that TPA performed significantly well in separating the unwanted signal and noise and identifying the best target reference points to the response point. For individual location performance with TPA, high contributions were found at CH, GB, and MH; however, low relationships were found at EF, ER, and ET. A combination of two of the three locations, which are CH-GB, GB-MH, and CH-MH, contributed significantly to improving the abovementioned relationship. The results showed that the combinations of chesses-gearbox and chesses-mid-handle showed a higher contribution to the response point than the combination of gearbox-mid-handle. To obtain the best reference points, the root mean square and root mean square errors from the inverse FFT were used. The results showed that the CH-GB combination contributed strongly to the response point.

Therefore, the locations, CH, and GB can be used in a compound set as the target point. Thus, to determine the improvement part to reduce the vibration of the handgrip, the most affected reference point was studied. Result presented that the location at GB is the best reference point, hence, this location can be used as a vibration damper instead of handgrip.

CHAPTER 5 SUMMARY AND CONCLUSIONS

Agriculture employs almost 80% of rural labor forces in Cambodia. It is considered to strongly support food security and as a primary source of income and GDP contributor. Agricultural tools are important for farming in Cambodia, such as draft animal forces harnessed to traditional implements. However, such traditional tools have been subsequently substituted by agricultural mechanization remarkably since 2001. The decreased number of traditional tools—draft animals from 178,941 pairs in 2009 to 560,511 pairs in 2012 is consequent to industrialization, draft animal issues, and effective agricultural mechanization. This is evident in the increase mechanization, especially hand tractors from 29,706 tools in 2001 to 151,701 tools in 2013. The incremented uses of mechanized tools meant that around 71% of the total arable land was mechanically plowed specifically by hand tractors. The extreme increase in the number of hand tractors became an attractive economic and operational alternative for small and medium farmers for land preparation and transportation. The hand tractors were hugely employed in Cambodia not only for land preparation but also transportation for small and medium farmers. The multipurpose uses of hand tractors meant that the time operation became longer and longer comparing to the uses in the developed countries that such long-time grasp on the handgrip of hand tractors would cause discomfort to operators, known as early fatigue. In this study, therefore, translational accelerations of a hand tractor under stationary mode were investigated. Vibration magnitude and dominant frequencies were observed using root mean square (RMS) and power spectrum density (PSD), and effective interventions for vibration reduction were suggested. For the measurement of vibration, seven wireless sensors were firmly tapped on different experimental locations of a hand

tractor such as front-plate right (FR), front-plate left (FL), engine top (ET), chassis (CH), gearbox (GB), mid-handle (MH), and handgrip (HG) to gain vibration transmission. Three engine revolution speeds (RPM), 1266rpm, 2110rpm, and 2658rpm were determined, indicating by a laser tachometer. An opensource Python Language was intensively and manually coded based on defined techniques—amplitude, RMS, fast-Fourier transform (FFT), PSD, and dominant frequencies. Graphical figures were visualized in 3D watermark using Statgraphics_Centurion_19.1.1 software. Results presented that the vibration magnitude was the greatest at the top of the engine along the lateral axis at low frequencies, followed by the handgrip along the vertical axis at different frequencies corresponding to the engine speed. It is showed that RMS values of the three translational accelerations at the engine top were dominated by lateral acceleration followed by longitudinal and vertical axes, subsequently, and this mention also confirmed by covariant presented in PSD results. Among the component parts of the hand tractor, the handgrip absorbs vibration directly from the engine source and transmits vibration to the operator, causing early fatigue. It is seen that the RMS values of acceleration of the handgrip were greatest along the vertical axes of 13.12 m/s^2, 15.80 m/s^2, 15.27 m/s^2 followed by the lateral axes of 8.84 m/s^2, 11.53 m/s^2, 13.16 m/s^2, and longitudinal axes of 4.79 m/s^2 ,5.60 m/s^2, 6.88 m/s^2, with respect to the three engine speeds. The result corresponded to the predominant PSDs on the vertical axis of 88 Hz, 70 Hz, 21 Hz, followed by the lateral of 44 Hz, 53 Hz, 53 Hz, and longitudinal axes of 44 Hz, 41 Hz, 21 Hz at all engine speeds. The transmission ratio at the handgrip was high on the vertical axis of 1.61, 1.15 at minimum and middle engine speeds, respectively. Nevertheless, transmission ratio was observed in low value in vertical axis of 0.69 at maximum engine speeds. The high transmission ratio in vertical axis can be also found at chassis of 0.93,

0.95, 0.70 in respect of all engine revolution speeds. The RMS of hand–arm vibration exposure was extremely higher than those stated in the health guidance zone at all engine speeds. Thus, anti-vibration measures should be introduced.

Vibration signals sourced from hand tractors are produced in a complex form; therefore, to achieve a comfortable condition, it is essential to reduce the interior vibration at the handle of the hand tractor. Transfer path analysis (TPA) technique that is well-known method to estimate the best reference points to response point of a hand tractor in a dynamic condition was employed. Six locations of the hand tractor, specifically, engine-right-side front (EF), engine-right-side rear (ER), engine-cover top (ET), chassis (CH), gearbox (GB), and middle between handle-base (MH) and handgrip (HG) were considered as reference points; whereas, handgrip was regarded as a response point. For TPA analysis, the PSDs of the seven locations were populated into a 3-dimensional matrix. Results show that with the application of TPA vibration amplitudes at EF, ER, and ET contributed significantly less to the response point at 17, 35, and 17 Hz along the longitudinal, lateral, and vertical axes, respectively. Therefore, the locations of ER, EF, and ET were not considered as target points. However, good variance contributions were observed at the CH, GB, and MH at predominant frequencies of 22, 22, and 22 Hz at the longitudinal, lateral, and vertical axes to the response point at the highest frequencies of 22, 22, and 22 Hz at the longitudinal, lateral, and vertical axes, respectively. A combination of two of the three locations was conducted in pairs. These pairs are CH-GB, GB_MH, and CH-MH, provided that these locations involve high-variance contributions to the response point. The results showed that the combination of CH-GB contributed high variances from the reference to the response point at the predominant frequencies of 22Hz at all axes. The same tendencies were also found at the combination of CH-MH.

Therefore, these locations could be set as target points for the response point. Nevertheless, it is recommended to consider the best contribution to reduce the number of sensors installed on the hand tractor. To develop the best reference points with a high contribution to the response point, an inverse time series obtained from an inverse FFT calculation was applied to measure the RMS and RMSE values. The RMS acceleration results are represented that food patterns were satisfactorily highlighted alongside various engine throttles at the longitudinal, lateral, and vertical axes between CH-MH, response point signal (response data), and CH-GB. Considering this, another method, that is, the RMSE method, was applied to confirm the result. As a result, the combination of CH and GB presented a very low error at all the engine throttles and axes. Thus, clearly implying that the combination of two locations at the CH and GB is the best target point for the damper.

BIBLIOGRAPHY

ANSI/ASA S2.70-2006 (R2016). American National Standard Guide for the Measurement and Evaluation of Human Exposure to Vibration Transmitted to the Hand. Acoustical Society of America [ASA].

Chan S., 2013. Cambodia Perspective on Rice Production and Machinery in Cambodia. Department of Agricultural Engineering Cambodia.

Charturvedi, V., Kumar, A., Singh, J.K., 2012. Power tiller: vibration magnitudes and intervention development for vibration reduction. Applied Ergonomics, 43(5), 891-901.

Chavan, V.S., Askhedkar, R., Sanap, S.B., 2013. Analysis of anti-vibration mounts for vibration isolation in diesel engine generator set. International Journal of Engineering Research and Applications (IJERA), 3(3), 1423-1428.

Cowell, P.A., 1969. Automatic control of tractor mounted implements-an implement transfer function analyser. Journal of Agricultural Engineering Research, 14 (2), 117-125.

Dewangan K.N., Tewari, V.K., 2009. Characteristics of hand-transmitted vibration of a hand tractor used in three operational modes. International Journal of Industrial Ergonomics, 39(1), 239-245.

Dewangan, K.N., Tewari, V.K., 2008. Characteristics of vibration transmission in the hand-arm system and subjective response during field operation of a hand tractor. Biosystems Engineering, 100(4), 535-546.

Erdal, K., Erkan, K., Herman, R., Wouter, S., 2013. Modeling and identification of the yaw dynamics of an autonomous tractor. 9th Asian Control Conference (ASCC)

2013, 1(6).

FAO, 2013. Mechanization for Rural Development: A review of patterns and progress from around the world. Agricultural Engineer (Mechanization and Institutions) Plant Production and Protection Division, FAO, Rome.

Francis, S.T., Ivan, E.M., Rolland, T.H., 1978. Mechanical Vibrations: Theory and Applications Second Edition. University of Colorado press, Allyn and Bacon, The United State of America.

Gialamas, T., Gravalos, I., Kateris, D., Xyradakis, P., Dimitriadis, C., 2016. Vibration analysis on driver's seat of agricultural tractors during tillage tests. Spanish Journal of Agricultural Research 14, e0210.

Heidary, B., Hassan-Beygi, R., Ghobadian, B., 2013. Investigating a power tiller vibration transmissibility using diesel-biodiesel fuel blends on stationary conditions. Journal of Mechanical Engineering and Technology 5, 19-31.

Heidary, B., Hassan-beygi, S.R., Ghobadian, B., Taghizadeh, A., 2013. Vibration analysis of a small diesel engine using diesel-biodiesel fuel blends. Agricultural Engineering International: CIGR Journal, 15(3). 117-126.

Koenigsberger, F., Tobias, S. A., 1972. Introduction, Proceedings of the Twelfth International Machine Tool and Research Conference. London and Basingstoke. Macmillan Education UK,1-1.

Marjanen, Y., 2010. Validation and improvement of the ISO 2631-1 (1997) standard method for evaluating discomfort from whole-body vibration in a multi-axis environment. Loughborough University. Dissertation.

Mehta, C. R., Shyam, M., Singh, P., Verma, R. N., 2000. Ride vibration on tractor-implement system. Applied Ergonomics, 31(3), 323-328.

Ngo, S, Chan, S., 2010. Agricultural sector financing and services for small hold farmers. MAFF and MOWRAM. Phnom Penh, Cambodia.

Noumura, K., 2006. Method of transfer path analysis for vehicle interior sound with no excitation experiment. F2006D183, Proceedings of FISITA World Automotive Congress, Yokohama, Japan.

OpenDevelopment Cambodia. 2015. Agriculture and fishing. https://opendevelopmentcambodia.net/topics/agriculture-and-fishing/. Cambodia. Accessed August, 5, 2020.

Salokhe, V. M., Majumdar, B., Islam, M. S., 1995. Vibration characteristics of a power tiller. Journal of Terramechanics, 32(4), 181-197.

Sam, B., Kathirvel, K., 2006. Vibration characteristic walking and riding type power tillers. Biosystem Engineering, 95(4), 517–528.

Sayed, M. E., Habashy, S., Adawy, M. E., 2012. Evaluation of whole-body-vibration exposure to Cairo Subway (Metro) Passengers. International Journal of Computer Applications, 55(8), 7-15.

Siemens PLM Software, 2014. Advanced transfer path analysis techniques.

Singh T.V., Kumar R.M., B.C. Viraktamath., 2011. Selective Mechanization in Rice Cultivation for Energy Saving and Enhancing Profitability. Rice Knowledge Management Portal (RKMP). India.

Stikeleather, L.F., 1991. Seat vibration and ride comfort. ASAE in Human Factors-a series of quality instructional teaching modules. Module 6, 22-22.

Taghizadeh, A., Hashjin, T. T., Ghobadian, B., Nikbakht, A. M., 2007. Evaluation of vibration in Power Tiller on the asphalt surface. Proceedings of the International Agricultural Engineering Conference. Bangkok, Thailand, (CD-ROM).

Tiwari, P.S., Gite, L.P., 2006. Evaluation of work-rest schedules during operation of a rotary power tiller. International Journal of Industrial Ergonomics, 36, 203-210.

Yibin, Y., Libin, Z., Fang, X., Meidui, D., 1998. Vibratory characteristics and hand-transmitted vibration reduction of walking tractor. Transactions of the ASAE, 41(4), 917-922.

YOSHIDA J., YAMASHITA D., 2013. Target level setting method for the reference signal of operational TPA. Journal of System Design and Dynamics, 7(4), 317-327.

YOSHIDA J., MAJIMA R., ISEMURA J., 2018. Obtaining method of high contributing whole body principal component mode by separated measurements. Mechanical Engineering Letters, 4, 18-00290.